



DeepWind Deliverable

Grant Agreement number: 256769

Project title: Future Deep Sea Wind Turbine Technologies

Deliverable No.: D5.2

Deliverable title: Spar-type floating support structure and mooring system configuration

Deliverable status: closed

Name of lead beneficiary: MAT

Nature of deliverable: R

Dissemination level: PU

Due date from Annex 1: M42

Actual submission date: M48

Quality check approval by:

Petter A. Berthelsen

date:

24/9-14



CONTENT

PART 1 (MARINTEK)

Conceptual design of floater and mooring system for the DeepWind concept.
Technical report MT2014 A-115

PART 2 (DTU)

Addendum – Time Domain Simulations.

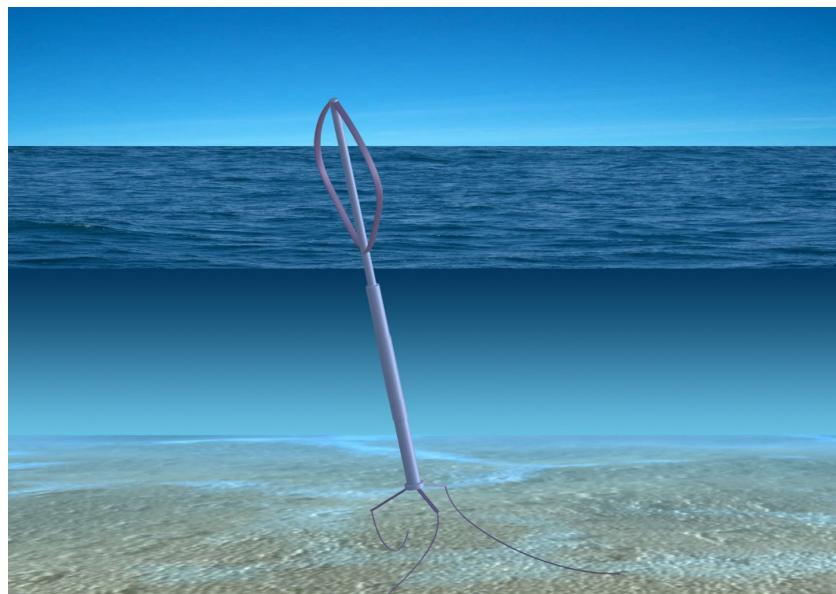
Report

Conceptual design of floater and mooring system for the DeepWind concept

Deliverable D5.2

Author(s)

Petter Andreas Berthelsen



Norsk Marinteknisk
Forskningsinstitutt AS
Norwegian Marine Technology
Research Institute

Address:
P.O. Box 4125 Valentinlyst
NO-7450 Trondheim NORWAY

Telephone: +47 4641500
Telefax: +47 73510034

marintek@marintek.sintef.no
www.marintek.sintef.no
Enterprise / VAT No.:
NO 937 357 370 MVA

Report

Conceptual design of floater and mooring system for the DeepWind concept

Deliverable D5.2



KEYWORDS:

Motion analysis
Floating production
Mooring analysis

VERSION 0	DATE 3rd September 2014
AUTHOR(S) Petter Andreas Berthelsen	
CLIENT(S) EU DeepWind	CLIENT'S REFERENCE D5.2
PROJECT NO 302000201	NUMBER OF PAGES/APPENDICES 42 / 3

ABSTRACT

This report presents the conceptual design of a floating support structure and mooring system for the DeepWind concept - a 5 MW vertical axis offshore wind turbine. The DeepWind concept consists of a Darrieus rotor mounted on a spar buoy support structure. The conceptual design is carried out in an iterative process, involving the different subcomponents. The present work is part of the second design iteration and the objective is to find a feasible floating support structure and mooring system for the DeepWind concept.

PROJECT MANAGER
Petter Andreas Berthelsen

SIGNATURE
Petter A. Berthelsen

CHECKED BY
Ivar Fylling

SIGNATURE
Ivar Fylling

APPROVED BY
Øyvind Hellan

SIGNATURE
Øyvind Hellan

REPORT NO
MT2014 A-155

ISBN

CLASSIFICATION
Unrestricted

CLASSIFICATION THIS PAGE
Unrestricted



Document History

VERSION	DATE	VERSION DESCRIPTION
0	3rd September 2014	Final version



Table of Contents

1	INTRODUCTION	5
1.1	Objectives and scope of work	5
1.2	Background	5
2	DESIGN CONSIDERATION	7
2.1	Floating support structure	7
2.2	Mooring system	7
2.2.1	Basic design considerations	8
2.2.2	Material selection	9
2.2.3	Footprints	10
2.3	Load conditions	10
2.4	Special consideration for a vertical axis wind turbine	10
3	DESIGN APPROACH	12
3.1	Optimization method	12
3.1.1	Mathematical formulation	13
3.1.2	Cost function	14
3.1.3	Constraints	14
3.1.4	Optimization variables	15
3.2	Analysis methods	15
3.2.1	Vessel motion	15
3.2.2	Mooring	17
3.2.3	Hydrodynamic coefficients	18
3.2.4	Aerodynamic loads	19
3.2.5	Optimization algorithm	20
3.3	Program structure	20
4	ROTOR BLADES AND GENERATOR DESIGN	23
4.1	Rotor blades	23
4.1.1	Aerodynamic loads	23
4.2	Generator	23
5	CONCEPTUAL DESIGN OF FLOATER AND MOORING SYSTEM	26
5.1	STEP 1 - Spar buoy dimensions	26
5.1.1	Input parameters	26
5.1.2	Spar dimensions	27
5.1.3	Radiation and diffraction analysis	29
5.2	STEP 2 - Mooring optimization	30
5.2.1	Environmental description	30
5.2.2	Design requirements	31
5.2.3	Design parameters	31
5.2.4	Input parameters	32
5.2.5	Load coefficients	33
5.3	Results and discussion	34
5.3.1	Results from optimization	34
5.3.2	Line break simulations	37
6	CONCLUDING REMARKS	39



REFERENCES	41
A WAMIT RESULTS - CASE 1 WITH 3 LINES	A-1
B ADDITIONAL PLOTS	B-1
B.1 Line characteristics	B-1
B.2 Restoring properties of mooring system	B-7
B.3 Line profiles	B-24
C ADDITIONAL TABLES	C-1
C.1 Line data	C-1
C.2 Restoring properties of mooring system	C-4
C.2.1 Case 1, 3 lines	C-4
C.2.2 Case 2, 3 lines	C-7
C.2.3 Case 3, 3 lines	C-7
C.2.4 Case 1, 6 lines	C-7
C.2.5 Case 2, 6 lines	C-7
C.2.6 Case 3, 6 lines	C-7



1 INTRODUCTION

1.1 Objectives and scope of work

This report has been worked out by MARINTEK, as part of the EU FP7 - ENERGY - 2010 - FET project DeepWind - Future Deep Sea Wind Turbine Technologies. The overall objective of this project is to explore the technologies needed for development of a new and simple floating offshore concept with a vertical axis rotor mounted on a rotating floating support structure. This document fulfils MARINTEK's contribution to deliverable D5.2 in WP5 - Mooring, floating and torque absorption systems. The objective of WP5 is to identify a feasible floating support structure and cost-optimized mooring system configuration for the floating support structure of a vertical-axis wind turbine.

The scope of the present work is to specify a feasible mooring system configurations and floater size. The report also includes a short introduction to mooring systems and some basic design considerations, including description of the methodology behind WINDOPT. A spar type floating support structure and mooring system is optimized with respect to design requirements and aerodynamic and hydrodynamic loads on the floating vertical axis wind turbine. The design is based on revised input from rotor and generator design (second iteration).

Due to limitations in the handling of mooring system stiffness contribution to motion transfer functions in the applied version of WINDOPT, the work had to be carried out in two steps:

1. Establish the main dimension of a spar buoy with sufficient support capacity and stability that can serve as a floating support structure for the DeepWind concept.

The main dimensions of the spar buoy is obtained from a simple optimization approach (as described in ref. [1]), where the design variables comprise the spar buoy geometry and ballasting. The approach used herein is somewhat simplified where only static stability and restrictions on natural periods have been considered. The floater design serve as input to the mooring optimization in the next step.

2. Establish a set of cost optimized mooring system for the DeepWind concept.

The optimization tool WINDOPT [2] is used to select a feasible mooring system. This program utilizes efficient design tools for analysis of mooring system forces and vessel motions, and combines this with a gradient search method for solution of non-linear optimization problems with arbitrary constraints.

1.2 Background

The interest for floating offshore wind turbines has increased the recent years. Limited access to shallow water areas in some key regions has driven the focus towards deeper water. While bottom-mounted offshore wind turbines are limited to water depths of approximately 30 ~ 50 meters, floating concepts will allow installation in deeper water. This will allow deployment of offshore wind farms further offshore in areas with stronger and steadier wind, and with less visual impact. The potential is believed to be large, provided that cost can be brought down to an acceptable level.

Most of the research and concept development have so far been based on traditional horizontal axis wind turbine (HAWT) technology. E.g. a full scale floating HAWT mounted on a spar buoy has been deployed off the south-west coast of Norway by Statoil in the Hywind project [3] in 2009. Principal Power deployed their first full scale pilot of their semisubmersible concept WindFloat off the coast of Aguçadoura, Portugal [4]. Other examples of floating HAWT-concepts that are currently being developed are e.g. SWAY [5], BlueH [6], WindSea [7], the hybrid SPAR-Concept [8] and Fukushima MIRAI [9].



Figure 1.1: Artistic illustration of the DeepWind concept.

The EU DeepWind project is based on the idea that technical improvement in offshore wind energy is necessary, which calls for dedicated technology development rather than using existing land based solutions. DeepWind is based on a spar type floater concept with an innovative offshore vertical axis wind turbine. A Darrieus type rotor design is used. An illustration of the concept is given in Figure 1.1, and a general overview is given in [10] and the references therein. The DeepWind concept differs from traditional spar-type concepts since the entire structure is rotating. The power is generated by a generator placed at the bottom of the structure which is held in position by the mooring system. An essential difference between vertical axis- and horizontal axis turbines is the difference in magnitude of the torque, being inversely proportional with the rotor speed, and that the torque of the HAWT is balanced by gravity forces, while the much larger torque of the VAWT must be balanced by the mooring system.

The mooring lines for the DeepWind concept must be designed so that it can withstand the large yaw moment from the rotating turbine. This requires a considerable stiffness in yaw. The floating support structure must have sufficient roll and pitch stiffness in order to resist the large aerodynamic loads on the wind turbine, but at the same time the system needs to be compliant enough to avoid resonant motions induced by the first order wave loads. Other important aspects such as the Magnus effect and frictional losses due to the rotating structure is not considered at present. The Magnus effect for a vertical axis wind turbine is further discussed in [11].



2 DESIGN CONSIDERATION

Design principles for an overall conceptual design of a floating VAWT are discussed in [12]. The present work considers only the design of the floating support structure and the mooring lines.

2.1 Floating support structure

The spar is a deep draught vertical circular cylinder with buoyancy chambers at the upper part and a heavier section at the lower end for stabilization. The draught is usually deep enough to limit vertical wave forces such that the vertical motions of the spar buoy are rather small. A stable spar buoy design requires that the mass centre is located below the centre of buoyancy, ensuring that the floater stays upright with low roll and pitch motion. The upper part of the spar buoy is narrowed such that a small cross-sectional diameter is obtained in the wave zone, which limits the wave loads on the structure, and gives a vertical resonance period well above the energetic wave period range. The spar concept is commonly used in the offshore oil and gas industry as deep water production platforms, and it has shown to be a promising solution also for floating offshore wind turbines due to its favourable motion behaviour.

The selection of hull shape and size depends on functional requirements, and the following basic design requirements should be considered for a floating wind turbine:

- Natural periods in heave and roll/pitch should be larger than the dominating wave periods to avoid resonant motion response.
- Sufficient buoyancy to carry specified payload and weight of the mooring system.
- Sufficient vertical stiffness for variable vertical load.
- Sufficient stiffness in roll and pitch to avoid excessive tilting of turbine axis due to environmental loads.
- Acceleration should be limited to avoid damage to machinery components.

The natural periods in heave and roll/pitch should be carefully selected to ensure that effects like Mathieu instability is unlikely to occur or can be controllable [13].

The specifications of design requirements may be different for operating and survival conditions, and for damage conditions. The design of the floating platform depends on the rotor design (both weight distribution and aerodynamic loads), and changes will alter the shape and size of the spar hull.

2.2 Mooring system

A soft mooring system is used to maintain the position of a floating structure while exposed to environmental loads from wind, waves and current. The restoring forces provided by the mooring system increases with the platform offset and balances the environmental loads. This restoring stiffness is generally too small to influence the wave frequency motion significantly [14], but soft mooring systems are vulnerable to slow-drift motions of the platform. This low-frequency response caused by higher order wave forces may lead to large peak tensions in the lines.

A comprehensive guide to mooring design can be found in [15]. Mooring systems are often classified as either catenary or taut systems. A catenary system provides horizontal compliancy mainly through geometric effects, and the stiffness is governed by the shape and the submerged weight of the mooring lines. Catenary systems are commonly sized such that there is no uplift at the anchor. This allows for using drag embedment anchors (depending on sea-bed conditions) since there will be small or no vertical loads at the anchor. For taut systems the compliancy



is mainly elastic. Taut systems require anchors that can withstand a significant vertical force component, e.g. pile and suction anchors. These type of anchors are more costly to install than drag embedment anchors.

2.2.1 Basic design considerations

Basic design requirements for mooring systems are:

- The extreme tension in the mooring lines should be less than the breaking strength (scaled by a safety factor)
- Sufficient fatigue life
- Sufficient horizontal stiffness to limit floater offset
- Sufficiently compliant (soft) system to avoid resonant motion induced by first order wave forces
- Adequate static horizontal pretension to provide sufficient yaw stiffness
- Redundancy

Mooring line tension

The design standards, such as DNV-OS-E301 [16] and ISO 19901-7 [17], requires that dynamic analysis is performed to ensure that the extreme tension in the mooring lines does not exceed the line breaking strength. The design equation for extreme tension with partial safety factors is defined as

$$S_c - T_{c,\text{mean}}\gamma_{c,\text{mean}} - T_{c,\text{dyn}}\gamma_{c,\text{dyn}} \geq 0 \quad (2.1)$$

where $T_{c,\text{mean}}$ and $T_{c,\text{dyn}}$ are the characteristic mean and dynamic tension and S_c is the line capacity. The partial safety factors, $\gamma_{c,\text{mean}}$ and $\gamma_{c,\text{dyn}}$, are specified in the standards and depend on the type of analysis performed and the consequence class defined for the mooring system. DNV [13] recommends that the mooring system is designed to high safety class due to the possible severe consequences for adjacent wind turbines if a floater is disengaged from its station keeping system. In addition it is common to perform fatigue analysis for assessment of the lifetime of the mooring system.

One basic design consideration is that the wave frequency motions of the structure, in freely floating condition, must not cause unacceptable tension in the mooring lines. This puts a constraint on acceptable stiffness, as the mooring lines have to be sufficiently compliant (soft).

Horizontal floater motions

The mooring system for a floating offshore wind turbine must be designed such that the floater offset, combined with motions, will not damage the power cable. Further, the offset must be limited so as to avoid collision with nearby installations both for intact and damaged mooring systems (mooring line failure).

A mooring system provides horizontal restoring forces and the corresponding horizontal stiffness is especially important for two things:

- The horizontal mooring stiffness determines the horizontal offset of the floating unit. A stiff mooring system gives smaller offsets than a soft system under the same static environmental forces.



- The horizontal mooring stiffness together with the total mass (structural mass + hydrodynamic added mass) determines the natural periods in surge, sway and yaw. It is important to design the system soft enough, such that these natural periods are large enough to avoid resonant motions induced by first order wave forces. On the other hand, soft systems are vulnerable for so-called slow drift motions, caused by second order wave forces. Surge natural periods for large volume moored structures are typically in the range 100 - 200 s. The natural periods of the other modes of motion (heave, roll and pitch) are mainly governed by hydrostatic properties of the floating unit.

Redundancy

The mooring system should have redundancy, i.e. still provide acceptable offset and line tension after one line breakage, both during transient and after new equilibrium is established. For oil and gas installations it is common to have mooring lines in clusters of 2-4 lines. The tension is then distributed over several lines, giving lower tension in each individual lines. Redundancy is obtained in case of a line break, which is important to avoid large offsets which may be harmful to risers and other cables. Hywind is equipped with 3 mooring lines, evenly spread at 120°. Large offsets will occur in case one of the mooring lines breaks, and this will possibly lead to breakage of the power cable. There are no structures nearby Hywind and thus there is no risk of collision. For a floating wind farm, the number of mooring lines and possible clustering will need to be addressed.

2.2.2 Material selection

Mooring lines are usually made from chain, steel wire rope or synthetic fibre rope, or combinations of these. Typically, chain provides weight and catenary effects, while steel wire or fibre ropes provides elasticity for taut systems. For optimal performance, combination of chain and wire is often used for a wide range of water depths [15]. In addition, buoys and clump weights can also be used to alter the horizontal stiffness and vertical mooring force.

Chain is the most common mooring line material. It is more robust than wire rope with respect to wear and tear. This is especially relevant for the touchdown point of the mooring line on the seabed, where there obviously is wear of the mooring line due to seabed contact. Another aspect at the touchdown point is to avoid bending stresses which may be fatal for wire rope. The connection from the mooring lines to the floating unit is often a system with fairleads and winches. The pretension of the mooring system can then be changed by adjusting the mooring line length with the winches. For such systems it is preferable to have chain in the upper mooring line segment, again to avoid bending stresses in wire rope. However, wire winches for steel wire mooring have also been applied. As a disadvantage, the winches need a relatively large deck space and introduce a relatively large deck weight. Chain is also easier to handle during installation. A disadvantage of chain is that the cost per unit length is higher than for wire rope, but a wire line has to be longer than a chain line to obtain the same compliancy. Also, chain has less fatigue capacity than steel wire.

Fibre rope is an alternative to steel wire and chain material. Synthetic fibre ropes have superior strength to weight ratios, and have the potential to become more important as an alternative choice. The fibre ropes are particularly attractive for deep water installations due to the light weight. However, other properties, such as high elasticity and the capability of absorbing dynamic motions through line extension without causing excessive dynamic tension [14], make fibre ropes highly relevant also for floating wind turbines in shallower water. A disadvantage with fibre ropes is that axial compression and hysteric heating needs to be avoided. Also, a considerable change in axial stiffness after installation will require fibre ropes to be re-tensioned. There is today only limited experience with synthetic fibre ropes in real conditions, and this often leads to over-conservative designs with large safety factors.

2.2.3 Footprints

Mooring systems have large "footprints" as mooring lines tend to be quite long (several times the water depth). When planning a wind farm consisting of several floating wind turbines one needs to make sure that the mooring systems for the different turbines do not come in conflict with each other.

2.3 Load conditions

The final design of floater and mooring system depends on the external load conditions considered. In this work, external loads are limited to environmental loads due to wind, waves and current. According to design standards (e.g. IEC 61400-3 [18]), it is common to subdivide external conditions into normal and extreme categories:

- Normal conditions – recurrent structural loading conditions
- Extreme conditions – rare events

Normal conditions are in particular important for fatigue life analysis. Long-term environmental description, such as H_s - T_p and wave direction distribution, is needed for these analysis. This scatter diagram contains information about probability of occurrence and is highly dependent on site location.

Extreme conditions consist of potentially critical combinations of wind, waves and current. In the absence of information of joint probability distribution of extreme waves, wind and current, a conservative combination of the extreme conditions may be found acceptable. For offshore oil and gas installations in Norwegian waters, it is according to DNV-OS-E301 [16] common practice to base the design condition on a return period of 100 years for wind and waves, combined with 10 years return period for current. IEC 61400-3 [18] recommends 50 year return period for waves and wind, combined with 10 years return period for current.

2.4 Special consideration for a vertical axis wind turbine

In order to convert energy, the generator need to be restrained from rotating with the turbine shaft. The restoring moment from the mooring lines must therefore be sufficient to balance the yaw moment caused by the rotating turbine. The linearized restoring moment M_{yaw} can be written as

$$M_{yaw} = K_{66}\alpha_{yaw},$$

where α_{yaw} is the yaw angular offset and K_{66} is the linear yaw stiffness. For a concentric mooring system, i.e. the mooring lines are spread in a radial pattern, the linear yaw stiffness K_{66} is given as

$$K_{66} = \sum_{i=1}^{N_{lines}} R_{f,i} T_{H,i},$$

where N_{lines} is the number of lines, $R_{f,i}$ is the fairlead radius as defined in Figure 2.1, and $T_{H,i}$ is the horizontal pretension of the i th mooring line.

A minimum yaw stiffness can be ensured by large horizontal pretension combined with a large fairlead radius. But extending the fairleads with torque arms far beyond the spar hull may introduce additional structural problems. This can be avoided by using a so-called crowfoot delta-line connection instead; however, delta lines have not been considered in the present work. Further, a high line tension is usually unfavorable with respect to fatigue, and a better solution to maintain a certain yaw stiffness may be to use a large number of mooring lines if each mooring line can be made relatively cheap.

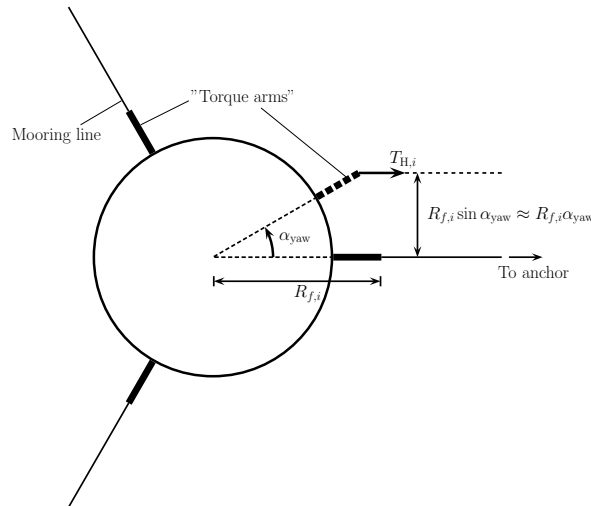


Figure 2.1: An overview of a buoy with a concentric mooring system. The figure illustrates the restoring moment created by the mooring lines.

Another concern is the yaw natural frequency. The mooring system is compliant in yaw, and there will be two rigid-body eigen modes for the yaw system. These yaw modes are to some extent governed by the generator stiffness [19]. A stiff generator gives a low frequency mode that consist of the spar and the stator yawing as a rigid body about the mooring, and a high frequency mode where the stator oscillates about the generator spring. A compliant generator gives a low frequency mode where the spar oscillates about the generator spring, and the high frequency mode is the stator oscillating about the moorings. Svendsen and Merz [19] investigated the dynamic effect of the generator stiffness, and concluded that a compliant generator is required. A stiff generator gives a poorly damped low frequency mode, and also the control system notch filter at 2P is not very effective. For a compliant generator the low frequency mode is well-damped and the 2P notch filter is effective. This works well unless the stator-mooring system has a resonance frequency that coincides with the 2P frequency, in which the stator will tend to oscillate [20]. Such oscillation may have an undesirable effect on the mooring lines.



3 DESIGN APPROACH

The present work is carried out in two steps:

Step 1 Establish the main dimension of a spar buoy with sufficient support capacity and stability that can serve as a floating support structure for the DeepWind concept.

Step 2 Establish a set of cost optimized mooring system for the DeepWind concept.

In step 1, the main dimensions of the spar buoy are obtained from a simple optimization approach. The spar geometry and ballasting have been optimized such that functional design requirements for static stability and natural periods are satisfied. The analysis methodology is described in DeepWind deliverable D5.1 [1] where spar dimensions were obtained for initial rotor blade and generator design (first design iteration). In this report, the spar dimensions are revised to account for recent changes in the rotor and generator design (second iteration). The static effect of wind load is the only external load included in the analysis. However, the floater design serve as input to the mooring optimization in step 2 where dynamic responses due to wind and wave loads are accounted for.

The optimization tool WINDOPT [2] is used to select a set of feasible mooring systems in step 2. WINDOPT utilizes efficient design tools for analysis of mooring system forces and vessel motions, and combines this with a gradient search method for solution of non-linear optimization problems with arbitrary constraints. The program can be used for simultaneous optimization of the floating spar buoy and mooring system; however, in the present work only the features for optimizing the mooring lines have been used. The geometry of the spar buoy obtained in step 1 remains unchanged in the optimization, but changes to the floater motion transfer functions due to changes of the mooring system is accounted for and also ballast is adjusted to compensate for the weight of the mooring lines. These changes are done in an outer loop calculation. A simple illustration of the calculation flow is given in Figure 3.1.

The reason for updating the motion transfer function outside of WINDOPT is that the current version of WINDOPT does not include the mooring stiffness when calculating the floater motion transfer functions. Due to the fairly large distance between the floaters mass centre and the fairleads it becomes important to include the horizontal mooring stiffness in order to get the correct eigen periods in pitch and roll. The hydrodynamic coefficients are obtained using WAMIT [21].

Descriptions of the optimization and analysis methods for step 2 are given below. The procedure for step 1 is outlined in ref. [1].

3.1 Optimization method

WINDOPT attempts to find the cheapest solution that satisfies a set of design requirements. The cost minimization is based on a nonlinear optimization approach with arbitrary constraints. WINDOPT is an extension of the mooring and riser optimization tool MOOROPT [22, 23], and consists of the following three tools:

NLPQL A general purpose program for optimization of nonlinear functions subjected to arbitrary constraints [24].

MIMOSA A standard mooring analysis program [25] used for the static and dynamic response analyses, both vessel motions and line tensions, required for the optimization.

WAMOF3 A hydrodynamic analysis tool for calculating hydrodynamic coefficients required as input to MIMOSA.

Note that in the present work the hydrodynamic coefficients are obtained using WAMIT instead of WAMOF.

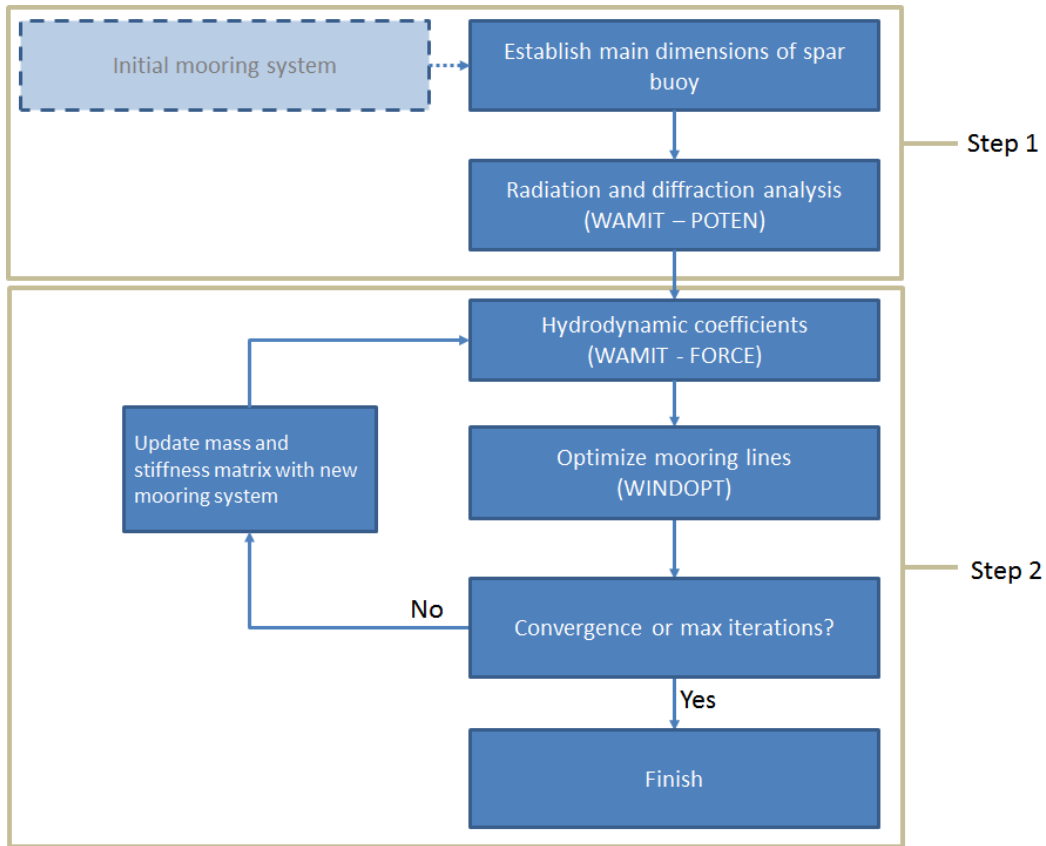


Figure 3.1: Calculation flow chart.

3.1.1 Mathematical formulation

The optimization program needs a model that specifies the measure or function to minimize (cost function), optimization variables (design parameters), and constraints (design requirements). Mathematically, the optimization problem is formulated as follows:

$$\begin{aligned} \min F(\mathbf{X}) \\ \mathbf{X} \in \mathbb{R}^n : \quad & g^j(\mathbf{X}) \geq 0, \quad j = 1, \dots, m, \\ & \mathbf{X}_L \leq \mathbf{X} \leq \mathbf{X}_U. \end{aligned}$$

where F denotes the cost function, \mathbf{X} denotes the design variables, g denotes the design constraints, n is the number of design variables, m is the number of constraints, and \mathbf{X}_L and \mathbf{X}_U denotes lower and upper bounds, respectively, applied to the design variables.

NLPQL uses a sequential unconstrained minimization technique (SUMT). This is based on separating the constraint functions by penalty functions to provide a continuous search 'surface'. This method has proved to be efficient for the mooring optimization problem. The search algorithm in NLPQL requires calculations of the partial derivatives of the objective function and the constraints with respect to all variables. Finite difference approximations have to be used since analytical derivatives are not available for the constraints. The constraint functions may be strongly nonlinear; therefore, two-sided differences are used in order to reduce the inaccuracy of the numerical approximations that may lead to poor convergence behavior. This means that for every function and gradient evaluation, the number of system analysis is $2N_{\text{var}} + 1$, where N_{var} is the number of optimization variables.

3.1.2 Cost function

The cost function to be minimized is the material cost of the mooring lines, i.e.

$$F = F_{\text{moor}}.$$

The cost function can be written as

$$F_{\text{moor}} = \sum_{i=1}^{N_{\text{lines}}} \sum_{j=1}^{N_{\text{seg},i}} C_{i,j}, m_{i,j}, l_{i,j},$$

where the subscripts i, j denotes the j th line segment of the i th mooring line and C is the cost per unit mass of the line segment, m is the mass per unit length, and l is the length of the line segment.

3.1.3 Constraints

The design constraints are formulated as a set of functions g required to be non-negative in the search algorithm. The following spar design constraints are applied:

- Upper and lower bounds on heave period, $T_{3,L} \leq T_3 \leq T_{3,U}$:
 $g^{v1} = (T_{3,U} - T_3)/T_{3,U}$
 $g^{v2} = (T_3 - T_{3,L})/T_{3,L}$
- Upper and lower bounds on pitch period, $T_{5,L} \leq T_5 \leq T_{5,U}$:
 $g^{v3} = (T_{5,U} - T_5)/T_{5,U}$
 $g^{v4} = (T_5 - T_{5,L})/T_{5,L}$
- Upper bound on tower inclination angle, i.e. φ_{max} should be smaller than φ_{lim} :
 $g^{v5} = (\varphi_{\text{lim}} - \varphi_{\text{max}}) / \varphi_{\text{lim}}$
- Upper bound on horizontal acceleration at generator level, i.e. $a_{\text{nac,max}}$ should be smaller than $a_{\text{nac,lim}}$:
 $g^{v6} = (a_{\text{nac,lim}} - a_{\text{nac,max}})/a_{\text{nac,lim}}$

The following constraints are applied to the mooring system:

- Maximum horizontal floater offset XHOR:
 $g^{l7} = (\text{XHOR}_{\text{lim}} - \text{XHOR}_{\text{max}})/\text{XHOR}_{\text{lim}}$
- Minimum safety factors for maximum tension F in mooring line segment:
 $g^{l1} = (F_{\text{B}} - F_{\text{max,mean}} \cdot \gamma_{\text{mean}}^{(1)} - F_{\text{max,dyn}} \cdot \gamma_{\text{dyn}}^{(1)})/F_{\text{B}}$
- Maximum slope angle from horizontal at anchor:
 $g^{l4} = (\text{Slope}_{\text{lim}}^{(4)} - \text{Slope}_{\text{max}})/\text{Slope}_{\text{lim}}$
- Minimum static horizontal pretension F_{hor} limit (intended for minimum yaw stiffness requirement):
 $g^{l8} = (F_{\text{hor}} - F_{\text{hor,lim}})/F_{\text{hor,lim}}$

The subscripts dyn denotes dynamic analysis, stat denotes static analysis, lim denotes the limiting constraint value, and max and min denote the maximum and minimum calculated value, respectively. The safety factors are denoted γ , and F_{B} is the line break strength.



3.1.4 Optimization variables

Only continuous variables can be considered as optimization variables since a gradient search method is used. This means that the composition of the mooring lines (the number of lines, line segments, and buoys) must be fixed and specified as input.

The mooring system may consist of one or more line types, each specified by a line characteristic. The lines may lay out in symmetrical or arbitrary pattern. Three groups of optimization variables can be selected for the mooring lines:

1. Line variables
 - i) Line direction
 - ii) Pretension or distance to anchor
2. Segment variables
 - i) Segment length
 - ii) Segment diameter
3. Buoy variables; Net submerged weight

The segment and buoy variables have direct influence on the objective function, but the line variables have only indirectly influence through constraints. If the mooring line diameter is changed, then the other cross section data, such as submerged weight, break strength and mass, are modified accordingly.

3.2 Analysis methods

The mooring analysis software MIMOSA [25] is used for the inner loop static and dynamic response analysis. This tool uses efficient frequency-domain techniques to calculate wave frequency and low frequency rigid-body vessel motions in 6 degrees of freedom. The mooring line responses are obtained by either a quasi-static analysis or a simplified dynamic analysis. Morison-type drag forces for mooring line dynamics are also included in the simplified dynamic model.

3.2.1 Vessel motion

The complete vessel motion response analysis can be separated into three sub problems when applying the frequency domain technique. The three separated response problems are:

- The mean steady drift response (static analysis)
- The wave frequency (WF) response
- The slow drift low frequency (LF) response

Each response problem are described below.



Static analysis

Static equilibrium position is obtained when positioning forces and moments balance static loads from the environment. MIMOSA calculates the static position by solving the following equation numerically:

$$\mathbf{F}_{mo}(\mathbf{X}) + \mathbf{F}_{hy}(\mathbf{X}) + \bar{\mathbf{F}}_{cu}(\mathbf{X}) + \bar{\mathbf{F}}_{wi}(\mathbf{X}) + \bar{\mathbf{F}}_{wa}(\mathbf{X}) = 0, \tag{3.1}$$

where

\mathbf{F}_{mo} – mooring forces

\mathbf{F}_{hy} – hydrostatic and gravitational restoring forces

$\bar{\mathbf{F}}_{cu}$ – current loads

$\bar{\mathbf{F}}_{wi}$ – static wind loads

$\bar{\mathbf{F}}_{wa}$ – mean wave drift forces

and \mathbf{X} is the position and orientation vector. The 6-component vectors \mathbf{F} are generalized load vectors that contain both force and moment components. Equation (3.1) is nonlinear and may have more than one equilibrium position.

Wave frequency motion

MIMOSA computes the first order wave frequency (WF) motion using the wave spectrum, $S_{\zeta}^{WF}(\omega)$, and the linearized transfer functions, $H_i^{WF}(\omega)$, from wave to vessel motion for all 6 degrees of freedom. The WF response spectrum for each mode of motion becomes

$$S_{X_i}^{WF}(\omega) = |H_i^{WF}(\omega)|^2 S_{\zeta}^{WF}(\omega), \quad \text{for } i = 1, \dots, 6.$$

The standard deviation of the responses are given as

$$\begin{aligned} \sigma_{X_i}^{WF} &= \sqrt{\int_0^{\infty} S_{X_i}^{WF}(\omega) d\omega}, \\ \sigma_{v_i}^{WF} &= \sqrt{\int_0^{\infty} \omega^2 S_{X_i}^{WF}(\omega) d\omega}, \\ \sigma_{a_i}^{WF} &= \sqrt{\int_0^{\infty} \omega^4 S_{X_i}^{WF}(\omega) d\omega}, \end{aligned}$$

for position, velocity and acceleration, respectively.

The significant response is derived from the Rayleigh distribution as the mean value of the one-third largest peaks of motion and is given as

$$X_{sign,i}^{WF} = 2\sigma_{X_i}^{WF},$$

and the maximum is given as the expected largest value:

$$X_{max,i}^{WF} = \sqrt{2}\sigma_{X_i}^{WF} \left(\sqrt{\log N_i^{WF}} + \frac{0.2886}{\sqrt{\log N_i^{WF}}} \right), \tag{3.2}$$

where N_i^{WF} is the mean number of zero up-crossing of the response. It is here assumed that the response is a narrow-banded Gaussian process, so that the peaks are Rayleigh distributed.

LF motion

The low frequency motion is computed in frequency domain from the following equation:

$$(\mathbf{M} + \mathbf{A}_0)\ddot{\mathbf{X}}^{LF} + \mathbf{C}\dot{\mathbf{X}}^{LF} + \mathbf{K}\mathbf{X}^{LF} = \mathbf{F}^{LF}.$$

Here \mathbf{X}^{LF} and \mathbf{F}^{LF} are the LF position response and load vectors, respectively. \mathbf{M} is the mass matrix and \mathbf{A}_0 is the zero frequency added mass matrix. The damping matrix \mathbf{C} is obtained by stochastic linearization of the damping model with respect to the vessel's velocities. The stiffness matrix \mathbf{K} is calculated by linearization of the nonlinear mooring restoring forces.

The power spectral density matrix for the LF response is

$$S_X^{LF}(\omega) = \mathbf{H}^{LF}(\omega)S_F^{LF}(\omega)\mathbf{H}^{LF}(\omega), \quad (3.3)$$

where S_F^{LF} is the power spectral density matrix of LF wave forces and wind forces, and the matrix transfer function is given by

$$\mathbf{H}^{LF}(\omega) = [-\omega^2(\mathbf{M} + \mathbf{A}_0) + j\omega\mathbf{C} + \mathbf{K}]^{-1}, \quad j = \sqrt{-1}.$$

The covariance matrix of the LF position is obtained by integrating the power spectra in Eq. (3.3). The significant values of the LF motion responses, $X_{sign,i}^{LF}$, are given as twice the corresponding standard deviations.

The LF wave loads are not Gaussian and special consideration is needed for calculation of the extreme response values. MIMOSA uses Stansberg's method [26] to estimate the extreme LF wave response, $X_{max,wa,i}^{LF}$. The extreme value of the wind-induced part of the response, $X_{max,wi,i}^{LF}$, is Gaussian and can be estimated separately using Eq. (3.2). The combined extreme value from wind and LF waves is then calculated as

$$X_{max,i}^{LF} = \sqrt{(X_{max,wa,i}^{LF})^2 + (X_{max,wi,i}^{LF})^2}.$$

WF+LF motion

MIMOSA use a heuristic method, based on model tests and simulation studies, to calculate combined WF and LF extreme values. The combined WF and LF motion is given by

$$X_{max}^{tot} = \max(X_{max}^{WF} + X_{sign}^{LF}, X_{sign}^{WF} + X_{max}^{LF}).$$

3.2.2 Mooring

In the present work, MIMOSA uses the catenary (CAT) method to solve for the mooring line configuration. It is here assumed that the lines are formed as catenaries and can be modelled by the catenary equations. For a single mooring line, the mathematical problem is given by a two-point boundary value problem and must be solved numerically.

The CAT method obtains the line configuration by a "shooting method"; the boundary conditions at one end is iterated in order to satisfy the specified boundary conditions at the other end. For each iteration, the ordinary differential equations are solved as an initial value problem. The resulting cable configuration is two-dimensional, i.e. the mooring line is assumed to be located in a vertical plane. The consequence of this is that the horizontal projection of the mooring line will always be a straight line to the anchor, i.e. the effect of transverse friction on the sea bottom is neglected so the line will rotate freely about the anchor.

**LF tension**

The variation in line tension calculation caused by the LF vessel motion is calculated quasi-statically. This means that the line geometry and tension along the line are functions of the top tension analysis only, and that line inertia and damping forces acting on the line are not taken into account. For quasi-static analysis, a two-dimensional table is created of the line characteristics as a function of fairlead position relative to the location of the anchor. For any position of the floater the total tension and direction is found from interpolation on the line characteristic table.

WF tension

The line tension arising from the vessel's WF motion are calculated using the Simplified Analytical Model [27]. This model accounts for dynamic effects such as velocity and acceleration of the line. The method is based on the following assumptions:

- Only the tangential component of the top end motion is assumed to have any effect on the dynamic tension.
- The shape of the dynamic motion due to a tangential excitation is assumed to be equal to the change in static line geometry.
- Mass forces on the line are neglected.
- The elastic elongation of the line is determined quasi-statically.

The line's dynamic behaviour is modelled in an approximate manner by a single-DOF second order transfer function where only the upper end motion in the most important direction is considered. The model is very fast and suitable for frequency domain analysis.

3.2.3 Hydrodynamic coefficients

The spar buoy motion transfer function and wave drift force coefficients are required as input to MIMOSA. Hydrodynamic coefficients are found by using the software WAMIT [21], which is a three dimensional frequency domain panel code for diffraction analysis. WAMIT is used to provide wave to motion transfer functions (RAOs) as well as mean wave drift coefficients. The coefficients depend on wave direction and frequency.

WAMIT is run in two steps:

POTEN solves for the radiation and diffraction velocity potentials (and source strengths) on the body surface for the specified modes, frequencies and wave headings.

FORCE computes global quantities including the hydrodynamic coefficients, motions, and first and second-order forces.

POTEN depends only on the geometry of the floater and is run one time only, prior to the mooring optimization. FORCE depends on floater mass and stiffness properties and is therefore re-run for every outer loop iteration where changes of mooring system properties are accounted for.

3.2.4 Aerodynamic loads

The large variation of wind load on the vertical axis wind turbine is mainly due to the rotation of the rotor which continually changes the position of the blades relative to the wind. The excitation frequency is associated with the rotor blade passing frequency, which is $2P$ for a two bladed turbine. In order to have a reasonable model of the wind turbine in MIMOSA the wind spectrum can be 'tuned' to represent the aerodynamic load fluctuations of the rotor [2].

The wind loads are assumed to be proportional to the wind velocity squared:

$$F_i = C_i U(t)^2, \quad (3.4)$$

where the subscript i denotes the i th mode of motion, C_i is the wind load coefficient and $U(t)$ the wind velocity. The wind can be decomposed into a mean wind velocity \bar{U} and a gust velocity $u'(t)$ such that

$$U(t) = \bar{U} + u'(t).$$

Ignoring terms of order u'^2 , then Equation (3.4) can be decomposed into a mean load \bar{F}_i and a fluctuating component $F'_i(t)$ where

$$\bar{F}_i = C_i \bar{U}^2 \quad (3.5)$$

and

$$F'_i(t) = 2C_i \bar{U} u'(t).$$

The wind load coefficients for the rotor blades are chosen to give the correct mean aerodynamic load. In order to have a model that represent the fluctuating load, the gust velocity must be tuned accordingly.

The power spectrum of the fluctuating wind load can be related to the gust velocity spectrum S^{wi} by

$$S_{F_i}^{wi}(f) = (2C_i \bar{U})^2 S^{wi}(f),$$

where f is the gust frequency. Further, the mean square value of the fluctuating load can be written as

$$\sigma_{F_i}^2 = 4C_i^2 \bar{U}^2 \int_0^{\infty} S^{wi}(f) df = 4C_i^2 \bar{U}^2 \sigma_{wi}^2, \quad (3.6)$$

where σ_{wi} is the standard deviation of the wind gust.

In the present work the Davenport wind spectrum is used. The Davenport spectrum is given by

$$S^{wi}(f) = \frac{4\kappa L^2 f}{\left[1 + \left(\frac{Lf}{U_{10}}\right)^2\right]^{4/3}},$$

where U_{10} is the mean wind speed at 10 m height above mean sea level, κ is a surface roughness coefficient, and L is a length scale.

The standard deviation of the wind gust is proportional to the mean wind speed and is given by [28]

$$\sigma_{wi} = \sqrt{6\kappa} U_{10}.$$

Combining this expression with Equation (3.6) gives the 'tuned' value for κ which will give the targeted load fluctuation, i.e.

$$\kappa = \frac{\sigma_{F,i}^2}{6(2C_i U_{10}^2)^2},$$

where the wind load coefficient is obtained from Equation (3.5),

$$C_i = \frac{\bar{F}}{U_{10}^2},$$

in order to ensure correct mean wind load.

Further, the length scale L can be adjusted such that the peak of the wind spectrum coincides with the 2P frequency, as illustrated in Figure 3.2.

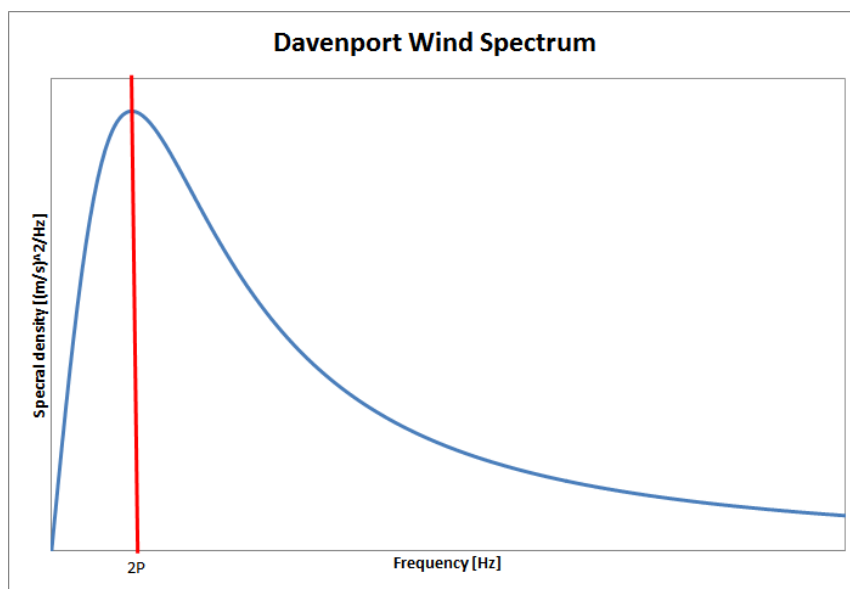


Figure 3.2: Davenport wind spectrum.

3.2.5 Optimization algorithm

NLPQL uses a sequential unconstrained minimization technique (SUMT). This is based on multiplying the constraint functions by penalty functions to provide a continuous search 'surface' with a steep negative gradient in 'un-acceptable' regions of the design space. The search algorithm in NLPQL requires calculations of the partial derivatives of the objective function and the constraints with respect to all variables. Finite difference approximations have to be used since analytical derivatives are not available for the constraints. The constraint functions may be strongly nonlinear; therefore, two-sided differences are used in order to reduce the inaccuracy of the numerical approximations that may lead to poor convergence behavior. This means that for every function and gradient evaluation, the number of system analysis is $2N_{\text{var}} + 1$, where N_{var} is the number of optimization variables.

3.3 Program structure

Input data to WINDOPT are specifications of:



- Payload, including rotor data
- Initial hull shape
- Initial mooring system
- Material cost and design requirements
- Design variables including variation ranges to be considered

Output data include:

- Optimized mooring specification
- Printout of initial and final system performance
- Key data from optimization algorithm

The main steps of the program flow are outlined below:

1. Specify optimization variables \mathbf{X} (including ranges), constraints, material cost data and payload.
2. Read spar buoy specification and initial mooring.
3. Run MIMOSA for initial system to obtain initial responses.
4. Start optimization algorithm
 - i) Function evaluation:
 - Run MIMOSA for extreme conditions.
 - Calculate values of objective functions and constraints.
 - ii) Gradient evaluation:

Same procedure as Function evaluation, carried out for a positive and negative increment of each variable.
 - iii) Check convergence and constraints. If satisfactory or maximum iteration reached then stop, else search for improved solution \mathbf{X} and return to step i).
5. Analysis completed.

The sequence of MIMOSA analyses for extreme response calculations are repeated N_{case} times, where each case is repeated for N_{env} different environments. The system data is modified for every case, e.g. changing rotor drag coefficient, etc. Then, for all cases and every environment MIMOSA calculates the following:

- Mean vessel position and inclination.
- Maximum and minimum line tension.
- WF Vessel motion for generator acceleration.
- WF+LF Vessel motion for dynamic pitch angle.



An optimization run may terminate because an optimum has been found, the maximum number of iterations have been reached, or it is impossible to find an improved solution. If maximum number of iterations have been reached, the optimization can be restarted using the last solution as a starting point to see if further improvement can be obtained by more iterations. If it is not possible to find an improved solution, the gradient calculation may not yield a profitable search direction or the variable range may be blocking the search direction. In that case, the variable specifications and/or the initial conditions should be changed before attempting a new optimization run.

It should be noted that the gradient search tries to find improved solutions in the vicinity of the initial data. Therefore, it may be useful to run the optimization with different initial data or variable ranges. If the optimization is terminated with negative constraint values (unacceptable conditions), the results should be carefully checked in order to decide whether it is acceptable, or to find out which parameters to modify to improve the results.

4 ROTOR BLADES AND GENERATOR DESIGN

The design of the rotor blades, rotor blade shaft, and generator is carried out in other work packages in the DeepWind project. The following sections summarize key parameters of the rotor and generator design that have been used as input in the present work.

4.1 Rotor blades

The rotor design used as input is the final iteration of the DeepWind 5MW design as given by [29]. A schematic illustration with the main dimensions of the turbine is presented in Figure 4.1 and the key parameters are specified in Table 4.1. Note that the rotor blade shaft consist only of the section between the lower and upper part of the rotor blades.

Table 4.1: Key parameters of the 5MW rotor blades and tower shaft

Description	Unit	Value
Rotor blade (1 blade):		
Mass	t	48.03
Center of mass (above SWL)	m	81.74
Radius of gyration, horizontal axis (blade COG)	m	51.55
Radius of gyration, vertical axis (main axis)	m	40.38
Rotor blade shaft:		
Mass	t	354.7
Center of mass (above SWL)	m	76.47
Radius of gyration, horizontal axis	m	40.64
Radius of gyration, vertical axis	m	2.87
Performance data:		
Rated power	MW	5
Rated rotational speed	RPM	6.11
Rated wind speed	m/s	14
Cut in wind speed	m/s	4
Cut out wind speed	m/s	25

4.1.1 Aerodynamic loads

The relationship between the aerodynamic loads and the wind speed are shown in Figure 4.2. The plots show the mean value, maximum value and standard deviation. The aerodynamic loads are obtained from HAWC2 simulations [29, 30] with no turbulence in the incoming wind and no wave loads on the floater.

The pressure point of the wind load is approximately 38.7 m above the still water level.

4.2 Generator

The generator configuration selected is nominated A3 [31]. The generator is placed inside a housing which also contains solid ballast. The dimensions of the housing and the amount of ballast have been selected to make the generator box (generator and housing) neutrally buoyant in water.

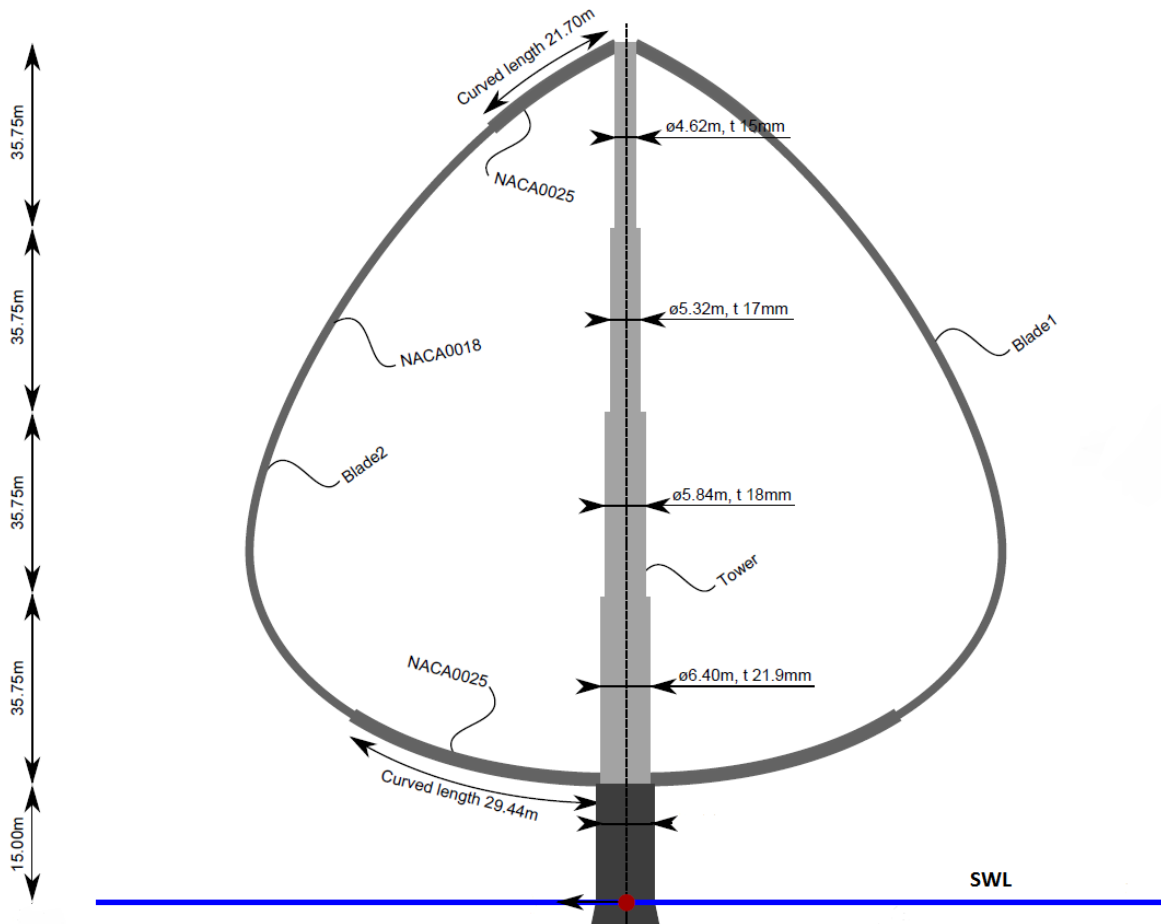


Figure 4.1: Schematic illustration of the rotor blades and rotor shaft (from ref. [29]).

The given dimensions and mass properties are summarized in Table 4.2. It is assumed that the centre of gravity is at the centre of the generator box and that there is a uniform mass distribution along the vertical axis.

Table 4.2: Mass properties and dimensions of the generator box

Description	Unit	Generator only	Generator box
Height	m	13	13
Diameter	m	7.1	7.4
Mass	t	380	573.6
I_{55}	tm^2	-	$1.04 \cdot 10^4$
I_{66}	tm^2	1315	3872

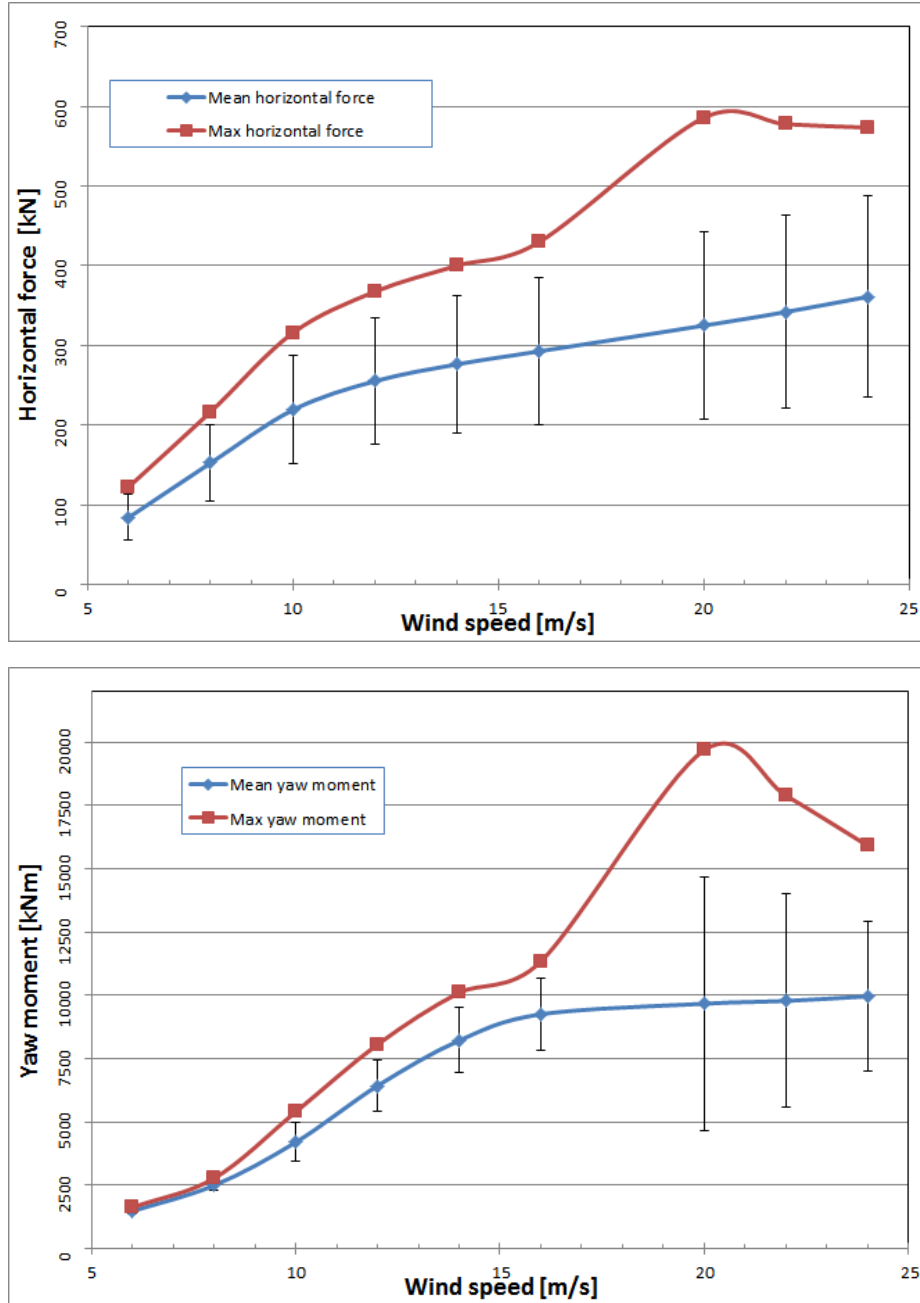


Figure 4.2: Relationship between wind speed and aerodynamic loads for the 5MW vertical axis wind turbine.

5 CONCEPTUAL DESIGN OF FLOATER AND MOORING SYSTEM

5.1 STEP 1 - Spar buoy dimensions

The analysis procedure used to determine the spar dimensions is described in DeepWind deliverable D5.1 [1].

A simple optimization approach is followed, where the spar geometry and ballasting have been optimized such that functional design requirements are satisfied. In step 1 the functional requirements are limited to static stability and natural periods. A reasonable guestimate for mooring system properties (e.g. weight and horizontal stiffness) have been used in the analysis in order to obtain an initial spar configuration.

The geometry of the spar is used as input to Step 2, where it remains unchanged throughout the mooring system optimization. However, in order to account for changes in the mooring system, relationships between the floater mass properties and the vertical load from the mooring lines are established. These relationships together with mooring stiffness properties are used in Step 2 to update the floater mass and motion characteristic for the motion analysis in the mooring system optimization.

5.1.1 Input parameters

Constraints

The following constraints are applied for defining the spar dimensions:

Upper and lower bounds on the natural periods in heave and pitch:

$$\begin{aligned} T_{n3,l} &\leq T_{n3} \leq T_{n3,u} \\ T_{n5,l} &\leq T_{n5} \leq T_{n5,u} \end{aligned}$$

Upper bound on static inclination angle:

$$\phi \leq \phi_{\max}$$

Upper bound on spar buoy draught:

$$T \leq T_{\max}$$

The design limits are summarized in Table 5.8. The natural periods and the static inclination angles are calculated as described in Chapter 3 in ref [1].

Table 5.1: Design constraint values.

Parameter	unit	Case 1
$T_{n3,l}$	[s]	23.0
$T_{n3,u}$	[s]	26.0
$T_{n5,l}$	[s]	26.0
$T_{n5,u}$	[s]	35.0
ϕ_{\max}	[deg]	10.0
T_{\max}	[m]	108.0



Material selection

The spar hull is made of steel with density 7850 kg/m^3 . The ballast material is un-compact, water saturated Olivine with density 2600 kg/m^3 .

The cost of material is:

$$q_{\text{steel}} = 3750 \text{ Euro/t,}$$

$$q_{\text{ballast}} = 50 \text{ Euro/t.}$$

Wind force

The maximum static horizontal wind force is given in Table 5.2. As a conservative estimate the maximum value from Figure 4.2 is used in the analysis.

Table 5.2: Maximum horizontal wind force.

Description	Parameter	unit	Value
Max horizontal force	F_{wind}	[kN]	600
Point of attack (above SWL)	H_{wind}	[m]	38.70

Payload

The payload is assumed to be fixed and comprise of rotor tower, rotor blades, generator, and the mooring lines. Input data for the rotor tower and blades are given by Table 4.1 in Chapter 4, and the generator data can be found in Table 4.2. The initial values for the mooring system are summarized in Table 5.3.

Table 5.3: Mooring line forces.

Description	Parameter	unit	Value
Vertical force	$F_{z,m}$	[kN]	-1500
Stiffness surge	$K_{11,m}$	[kN/m]	250

5.1.2 Spar dimensions

Figure 5.1 illustrates the spar geometry and the resulting dimensions are summarized in Table 5.4. Relationship between the vertical load from the mooring lines and key parameters of the spar buoy are summarized in Table 5.5.

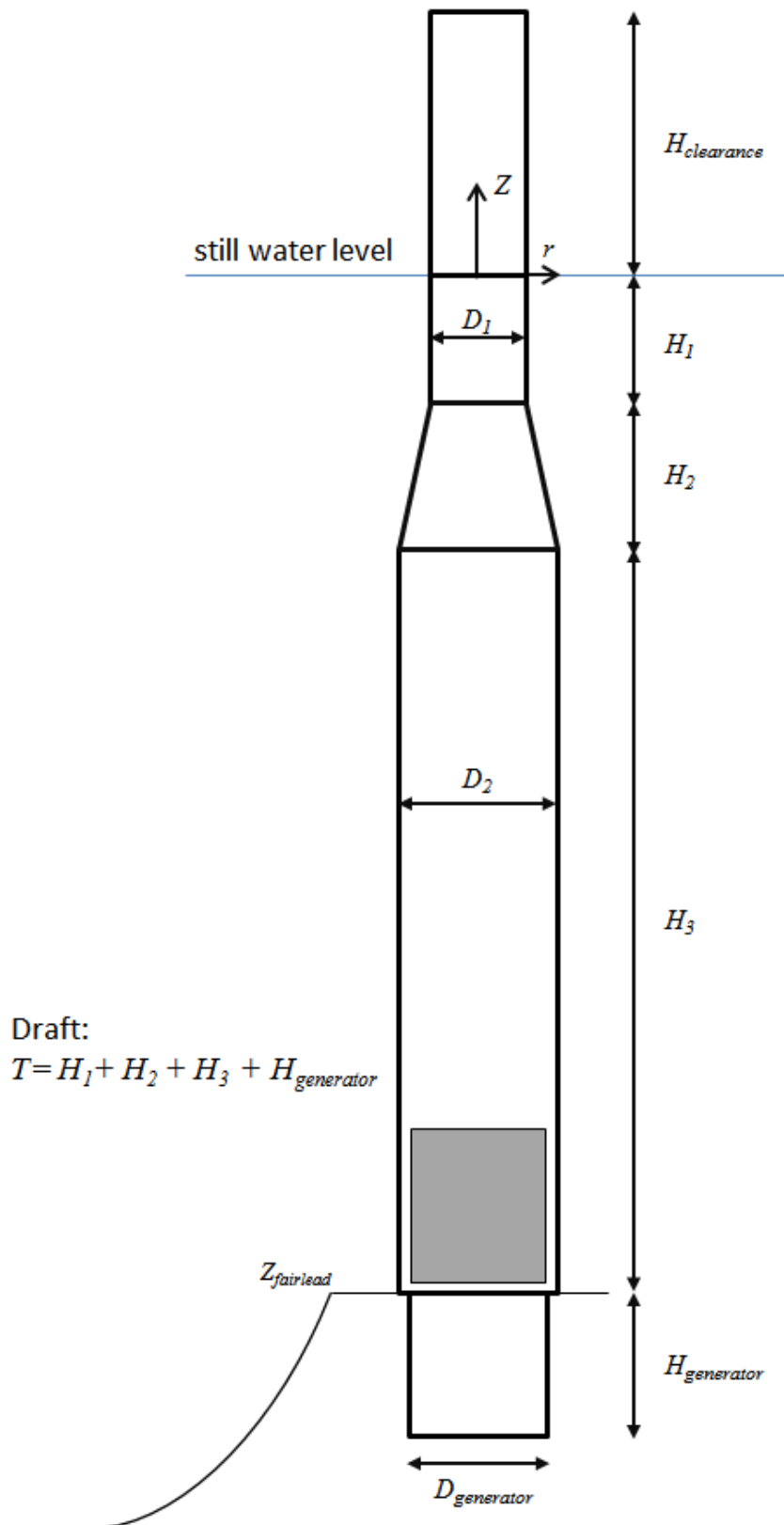


Figure 5.1: A simple illustration of the main dimensions describing the spar buoy, including definition of coordinate system.

Table 5.4: Spar hull geometry obtained from the optimization.

Description	Parameter	unit	Value
Spar hull geometry			
Wall thickness	τ	[mm]	50
Height clearance section	$H_{\text{clearance}}$	[m]	15.0
Height upper section	H_1	[m]	5.0
Height tapered section	H_2	[m]	10.0
Height main section	H_3	[m]	80.0
Height generator	$H_{\text{generator}}$	[m]	13
Draught	T	[m]	108.0
Upper diameter	D_1	[m]	6.8
Main diameter	D_2	[m]	8.0
Generator box diameter	$D_{\text{generator}}$	[m]	7.4
Displaced Volume	V	[m ³]	5193.0
Centre of buoyancy	Z_B	[m]	-54.46
Water plane area	A_w	[m ²]	36.32
Displacement	Δ	[t]	5322.8
Position fairlead	Z_{fairlead}	[m]	-95.0

 Table 5.5: Relationship between the vertical load from the mooring lines ($F_{z,m}$) and spar parameters.

Description	Parameter	unit	Expression
Centre of gravity (COG)	Z_G	[m]	$1.0714 \cdot 10^{-8} F_{z,m}^2 - 1.2870 \cdot 10^{-4} F_{z,m} - 62.762$
Total mass [†]	M_{Spar}	[t]	$0.1019 F_{z,m} + 5322.8$
Inertia about COG	I_{44}, I_{55}	[t·m ²]	$-6.4286 \cdot 10^{-3} F_{z,m}^2 + 491.36 F_{z,m} + 3.4489 \cdot 10^7$
Total spar cost		[kEuro]	$4055.9 + 0.05(M_{\text{Spar}} - 5118.91)$

[†] Total mass includes spar mass (steel hull and ballast), generator, rotor blades and rotor tower, excluding weight of mooring system.

5.1.3 Radiation and diffraction analysis

Radiation and diffraction velocity potentials are obtained from WAMIT analysis using the POTEN function. An illustration of the panel model of the floater for the WAMIT analysis is shown in Appendix A (see Figure A.1).



5.2 STEP 2 - Mooring optimization

Two different types of mooring system configurations are considered:

- 3 line chain system. The lines are evenly spread at 120°.
- 6 line chain system. The lines are evenly spread at 60°.

For both configurations, the linearized yaw stiffness is varied to obtain a set of different designs. The yaw stiffness is changed by:

- Changing the fairlead radius, i.e. radial distance to centre of floater (Torque arms)
- Changing the minimum horizontal tension of mooring lines

A matrix of the different optimization cases are shown in Table 5.6

Table 5.6: Optimization cases.

	Fairlead radius R_f [m]	Horizontal pretension T_H [kN]		
		Case 1 $K_{66} = 19200$ kNm/rad	Case 2 $K_{66} = 28800$ kNm/rad	Case 3 $K_{66} = 40800$ kNm/rad
3 Lines	8.0	800	1200	1700
	10.0	640	960	1360
	14.0	457	686	971
6 Lines	8.0	400	600	850
	10.0	320	480	680
	14.0	229	343	486

5.2.1 Environmental description

The Hywind test site off the west coast of Norway has been selected as a relevant site for evaluation of the DeepWind concept [12]. The critical environmental conditions selected for the extreme analysis are summarized in Table 5.7 and outlined below. Fatigue analysis has not been included in the present analysis.

Table 5.7: Environmental conditions. The wind speed is the 1 hour mean wind speed at 10 m above sea level, the current speed is the maximum surface current.

Wind speed: 24 m/s
Waves: $H_s=14$ m, $T_p=16$ s
Current: 0.7 m/s

Water depth

The water depth at selected location is 220 m.



Waves

The JONSWAP spectrum is used to describe the waves. The most critical wave condition selected for the current location is 14 m significant wave height at 16 s peak period, which is estimated from the 100-year extreme condition in [32].

Current

The tidal current is 0.2 m/s and the maximum wind driven current is taken as 0.5 m/s. This gives the total surface current speed equal to 0.7 m/s. The current profile is defined according to [33]. The wind driven current is reduced linearly to zero at 50 m water depth, while a simple power law is used to model the tidal current profile.

Wind

Wind speed of 24 m/s is selected because that is the wind speed with maximum mean wind loads provided from the aerodynamic analysis [29] summarized in Section 4.1.1. Wind is modelled as a constant wind where a varying speed component with zero mean (gust) is added to the constant component using the Davenport spectrum.

The wind spectrum parameters, κ and L , are tuned according to the description in Section 3.2.4 to mimic the actual wind load fluctuations. See Section 5.2.5 for selection of parameters. In addition, the more common value for the length scale ($L = 1200$ m) is also included in the analysis in order to capture effects from the variations of the wind gust.

Environmental direction

In the present analysis, collinear weather direction is assumed, i.e. wind, waves and current are acting in the same direction. This is believed to be the most conservative choice of combinations of weather direction. E.g. for the DeepWind concept, the mooring lines fairleads are below the point of attack of the current force such that wind and current traveling in the same direction will give the largest pitch angles.

5.2.2 Design requirements

The design constraints are summarized in Table 5.8. The minimum safety factors are chosen according to DNV-OS-E301 [16] for consequence class 2 where the constraint is implemented as given by Eq. (2.1) where F_B is the line breaking strength. A zero slope angle at the anchor is enforced to avoid vertical loads on the anchor. This will allow for drag anchors to be used.

5.2.3 Design parameters

For the optimization of the mooring lines, the following design variables are selected:

- Segment length
- Segment diameter
- Pretension at fairlead

The vertical position of the fairlead follows the position of the bottom section of the spar buoy.

Table 5.8: Design constraint values (design limits).

Constraint	Design limit	Constraint	Design Limit
Heave T_3 , min:	23.0 s	Offset, max:	50.0 m
Heave T_3 , max:	26.0 s	Safety factors:	
Pitch T_5 , min:	26.0 s	$\gamma_{c,mean}$	1.40
Pitch T_5 , max:	35.0 s	$\gamma_{c,dyn}$	2.10
Heel angle, max:	15.0 deg	Slope angle:	0.0 deg
Generator accel, max:	2.5 m/s ²	Horizontal pretension:	
		T_H , see Table 5.6	

5.2.4 Input parameters

Rotor and generator

The present work is based on the final design of the rotor blades and generator as presented in Chapter 4. The rotor blades, including the turbine tower shaft above sea level, and the generator is assumed to remain unchanged throughout the present optimization analysis. Key parameters of the rotor and generator are summarized in Tables 4.1 and 4.2.

Mooring chain material

The material properties for the chain are summarized in Table 5.9. The property values are based on R4 quality studless chain with a nominal diameter of 80 mm. In the optimization run, the minimum break load and weight in water are updated as follows:

$$\begin{aligned} \text{MBL} &= \text{MBL}_0(d^2/d_0^2), \\ ww &= ww_0(d^2/d_0^2), \end{aligned}$$

where d is the diameter of the mooring line and the subscript 0 denotes the initial values.

Table 5.9: Initial mooring line material properties.

Description	unit	Chain
Nominal diameter, d_{nom}	m	0.08
Minimum Break Load, MBL	kN	6594
Mass/length	kg/m	128
Submerged weight, ww	kN/m	1.092
Elastic modulus, E	kN/m ²	$5.73 \cdot 10^7$
Cost/mass	Euro/t	2875



5.2.5 Load coefficients

Aerodynamic load coefficients

The wind load coefficients for the rotor blades are chosen to give the correct mean aerodynamic load. The load coefficients are summarized in Table 5.10.

Further, the wind spectrum is tuned according to the description in Section 3.2.4 to represent the actual wind load fluctuations of the rotor, i.e. standard deviation and peak load frequency. The following values were selected for the surface roughness coefficient κ and length scale L :

$$\kappa = 0.00509 \text{ and } L = 92\text{m.}$$

Table 5.10 shows the target and estimated loads for the rotor. Only one set of wind spectrum parameters can be adjusted per environment. To be conservative, κ is chosen to give exact match for the horizontal force fluctuation since this provides a conservative estimate for the yaw moment fluctuation. The length scale L was selected to obtain a peak load close to the rotor blade passing frequency $2P$ (~ 0.10 Hz).

Table 5.10: Aerodynamic load coefficients for $U_{10} = 24.0$ m/s. The table also compares the estimated load fluctuations with results from HAWC2 [30].

Description	Load Coefficient	Calculated with HAWC2 [29]		Estimated with Davenport spectrum	
		\bar{F}	σ_F	\bar{F}	σ_F
Horizontal force	0.6270	361.16 kN	126.24 kN	361.16 kN	126.23 kN
Yaw moment	17.2998	9964.71 kNm	2954.75 kNm	9964.71 kNm	3482.81 kNm

Hydrodynamic load coefficients

Hydrodynamic coefficients such as motion transfer functions (RAOs) and second-order wave forces are calculated using the FORCE function in WAMIT. Transfer functions and mean wave drift coefficients for Case 1 with 3 mooring lines can be found in Appendix A.

Current forces are estimated using Morison’s equation with a drag coefficient C_D equal to 0.7.



5.3 Results and discussion

5.3.1 Results from optimization

Table 5.11 and 5.12 show feasible designs that satisfy the design constraints in Table 5.8. Additional plots and tables of the resulting mooring line properties are provided in Appendix B and C for reference. In order to ensure that WINDOPT found a feasible solution, several optimization runs with different initial pretensions were carried out. For most cases, the optimal solution converged to the same mooring properties; however, WINDOPT failed to find any feasible solution for Case 1 with 6 lines and $R_f = 8.0$ m.

The results show that for the given conditions there is no major difference in cost for the various configurations. The mooring lines become cheaper as the fairlead radius is increased. This is as expected since the required pretension decreases for larger radial distances to the fairlead, and thus chains with smaller diameters can be used. Increasing the yaw stiffness provides a more costly mooring system as the line pretension is increased.

The cost difference between a 3-line and 6-line configuration is relatively small (less than 20 % for mooring line cost). The reason for this is that the 6-line system needs much smaller chain diameters which compensates the cost for the additional lines. The main difference between the 3- and the 6-line system with respect to design is that the line tension is much lower for a 6 line configuration, which can be considered profitable regarding fatigue damage for the mooring lines and for the torque arms. Further, a 6-line system has redundancy and will not pose any threat to neighboring installations in case of a line failure. On the other hand, the installation time for 6 lines will be longer providing additional cost not accounted for in the present results. Also, a 6-line mooring system requires twice as many anchors as a 3 line system. However, each anchor can be smaller in size due to less load per line and the unit price is therefore expected to be lower.

Note that the natural periods provided in Tables 5.11 - 5.12 are based on an eigenvalue analysis of the linearized system matrix of the spar platform in mean position (exposed to environmental loads). The natural periods in surge decreases for increased yaw stiffness. The yaw natural periods are based on the stator-mooring system (i.e. the stator oscillating about the moorings) which has a much higher resonance frequency (shorter periods) than the 2P oscillation from the rotor rotation.

Note also that the cost of anchors and cost of installation work is not included explicitly in the cost function that is minimized.



Table 5.11: Final results for optimized spar buoy and mooring lines. 3 mooring lines.

Parameter	Unit	Case 1			Case 2			Case 3		
		8.0	10.0	14.0	8.0	10.0	14.0	8.0	10.0	14.0
Fairlead radius R_f	m	8.0	10.0	14.0	8.0	10.0	14.0	8.0	10.0	14.0
Chain length	m	864.83	778.90	752.03	1138.10	978.41	824.82	1519.80	1271.60	1003.40
Chain diameter	mm	76	73	65	84	79	73	89	86	79
Distance to anchor	m	843	756	727	1119	958	803	1504	1254	984
Min hor. pretension	kN	801	643	457	1202	962	687	1701	1362	974
Fairlead Z_{FL}	m	-95.00	-95.00	-95.00	-95.00	-95.00	-95.00	-95.00	-95.00	-95.00
Total mass [†]	t	5182.1	5201.8	5230.8	5133.3	5162.6	5197.4	5085.3	5117.2	5162.4
Mass centre [†]	m	-62.56	-62.59	-62.64	-62.49	-62.53	-62.59	-62.40	-62.46	-62.53
Inertia about SWL I_{55}	tm ²	3.380e+07	3.390e+07	3.404e+07	3.355e+07	3.370e+07	3.387e+07	3.331e+07	3.347e+07	3.370e+07
Surge T_1 , min	s	70.7	74.9	75.4	63.7	67.4	76.4	56.8	60.7	67.3
Surge T_1 , max	s	71.5	75.9	76.3	63.9	67.6	79.6	56.8	60.9	67.5
Heave T_3 , min	s	23.8	23.9	24.1	23.6	23.7	23.9	23.4	23.5	23.8
Heave T_3 , max	s	23.8	23.9	24.1	23.6	23.7	23.9	23.4	23.5	23.8
Pitch T_5 , min	s	26.2	26.3	28.2	26.1	26.2	26.5	25.9	26.0	26.3
Pitch T_5 , max	s	26.2	26.3	28.2	26.1	26.2	26.5	25.9	26.0	26.3
Yaw T_6 , min	s	1.7	1.5	1.4	1.6	1.5	1.3	1.6	1.5	1.3
Yaw T_6 , max	s	1.7	1.5	1.4	1.6	1.5	1.3	1.6	1.5	1.3
Heel angle, max	deg	10.4	10.4	10.6	10.9	10.8	10.7	11.4	11.1	10.8
Generator accel., Surge	m/s ²	0.63	0.60	0.54	0.74	0.70	0.64	0.83	0.79	0.71
Generator accel., Sway	m/s ²	0.29	0.27	0.23	0.22	0.20	0.18	0.17	0.16	0.15
Generator accel., Heave	m/s ²	0.30	0.30	0.29	0.31	0.30	0.30	0.31	0.31	0.30
Offset, max	m	26.9	27.6	29.1	25.3	25.9	27.0	24.3	24.7	25.5
Min safety factor [‡]	[-]	1.85	1.91	1.91	1.88	1.89	1.91	1.84	1.87	1.89
Spar buoy cost	kEuro	4059.1	4060.0	4061.5	4056.6	4058.1	4059.8	4054.2	4055.8	4058.1
Mooring line cost	kEuro	861.9	710.3	551.8	1392.1	1061.2	759.3	2088.1	1621.0	1079.1
Total cost	kEuro	4921.0	4770.4	4613.3	5448.7	5119.3	4819.1	6142.3	5676.8	5137.2

[†] Mass and mass centre includes mass of steel hull, ballast, generator and top rotor structure.

[‡] Minimum safety factor is here given as the line capacity divided by the maximum total tension.

Table 5.12: Final results for optimized spar buoy and mooring lines. 6 mooring lines.

Parameter	Unit	Case 1		Case 2			Case 3		
Fairlead radius R_f	m	10.0	14.0	8.0	10.0	14.0	8.0	10.0	14.0
Chain length	m	1008.10	799.90	1076.10	924.73	999.86	1381.70	1188.70	948.96
Chain diameter	mm	49	48	59	57	49	61	60	57
Distance to anchor	m	987	774	1058	904	979	1367	1171	929
Min hor. pretension	kN	321	229	601	481	342	849	681	486
Fairlead Z_{FL}	m	-95.00	-95.00	-95.00	-95.00	-95.00	-95.00	-95.00	-95.00
Total mass [†]	t	5208.5	5227.0	5134.3	5159.7	5203.0	5094.5	5119.1	5159.3
Mass centre [†]	m	-62.60	-62.63	-62.49	-62.53	-62.60	-62.42	-62.46	-62.53
Inertia about SWL I_{55}	tm ²	3.393e+07	3.402e+07	3.356e+07	3.369e+07	3.390e+07	3.336e+07	3.348e+07	3.368e+07
Surge T_1 , min	s	68.8	68.6	62.1	64.1	65.9	57.5	61.3	63.6
Surge T_1 , max	s	69.1	68.8	62.1	64.3	66.5	57.6	61.6	63.9
Heave T_3 , min	s	24.0	24.1	23.6	23.7	24.0	23.5	23.5	23.7
Heave T_3 , max	s	24.0	24.1	23.6	23.7	24.0	23.5	23.5	23.7
Pitch T_5 , min	s	29.9	29.4	26.0	25.9	29.3	25.9	26.0	26.1
Pitch T_5 , max	s	29.9	29.4	26.0	25.9	29.3	25.9	26.0	26.1
Yaw T_6 , min	s	1.8	1.5	1.6	1.4	1.4	1.6	1.4	1.3
Yaw T_6 , max	s	1.8	1.5	1.6	1.4	1.4	1.6	1.4	1.3
Heel angle, max	deg	10.6	10.7	10.7	10.8	11.0	10.8	10.8	10.8
Generator accel., Surge	m/s ²	0.51	0.49	0.64	0.62	0.55	0.71	0.68	0.63
Generator accel., Sway	m/s ²	0.25	0.23	0.22	0.21	0.18	0.17	0.16	0.15
Generator accel., Heave	m/s ²	0.30	0.30	0.31	0.30	0.30	0.31	0.31	0.30
Offset, max	m	28.5	30.2	25.6	26.3	27.9	24.5	25.0	26.0
Min safety factor [‡]	[-]	1.90	1.88	1.88	1.89	1.89	1.78	1.87	1.89
Spar buoy cost	kEuro	4060.4	4061.3	4056.7	4057.9	4060.1	4054.7	4055.9	4057.9
Mooring line cost	kEuro	826.4	630.0	1302.6	1036.4	846.1	1759.2	1487.0	1059.8
Total cost	kEuro	4886.7	4691.3	5359.2	5094.4	4906.2	5813.8	5542.9	5117.7

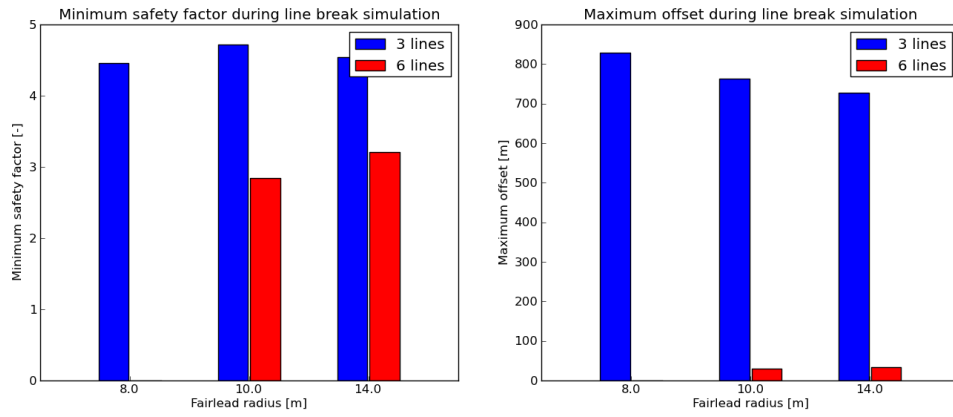
[†] Mass and mass centre includes mass of steel hull, ballast, generator and top rotor structure.

[‡] Minimum safety factor is here given as the line capacity divided by the maximum total tension.

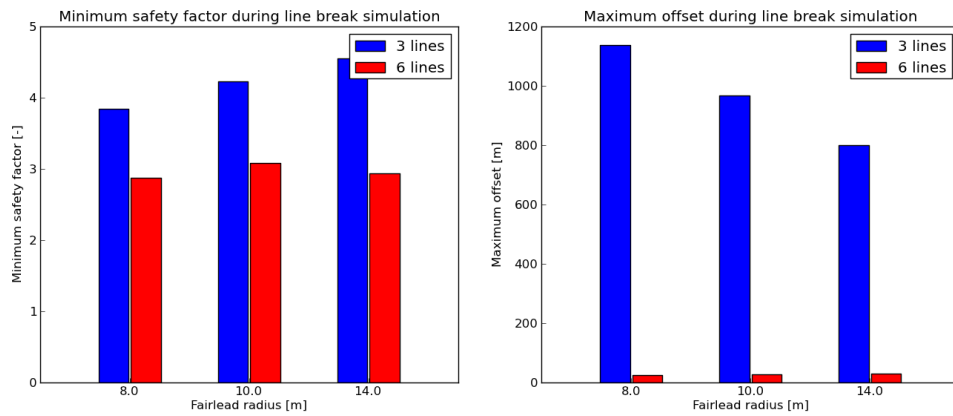


5.3.2 Line break simulations

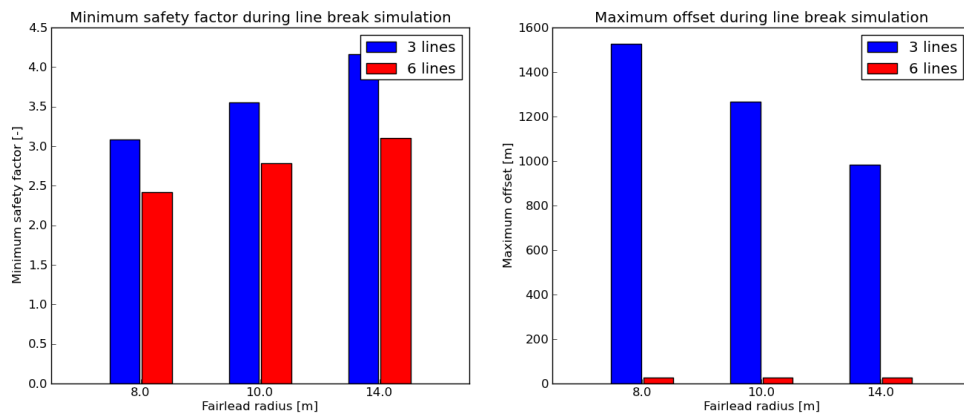
Due to possible nearby structures it is necessary to perform transient analysis of mooring line failure. In MIMOSA this is done by starting from equilibrium condition with static environmental forces and then break the most loaded mooring line. The maximum horizontal offset and the minimum safety factor can then be obtained. Figure 5.2 shows results from transient line break simulations for both the 3-line and the 6-line chain systems. Large drift-off is obtained for the 3-line system, which may not be acceptable as this may lead to possible conflict with adjacent wind turbines in an offshore wind park. DNV-OS-E301 [16] recommends to increase the safety factor by a factor of 1.2 for non-redundant systems. The reason for higher safety factors after break in the 3-line system than in the 6-line system is that only the two leeward lines with 120 deg spacing remain in the 3-line system, while the 6-line system still has an up-wind line with fairly high load.



(a) Case 1



(b) Case 2



(c) Case 3

Figure 5.2: Minimum safety factor and maximum offset during line break simulations.



6 CONCLUDING REMARKS

The conceptual design of a floating support structure and mooring system for the 5MW vertical axis DeepWind concept has been presented. The work has been carried out as the solution of an optimization problem where the optimization procedure tries to find a cheaper solution while satisfying a set of design requirements. However, it should be emphasized that the gradient search method tries to find improved solutions in the vicinity of the initial data, and due to the complex shape of the constraint functions and inaccuracies of the numerical search algorithm the search may converge to local optima that are inferior to the best solution. On the other hand, the main focus of the study is the feasibility of the concept rather than finding an optimal solution. The results are intended to be used for further design iterations, including other sub-components, which will eventually result in a better integrated design.

The mooring system design requires some special attention due to the large yaw moment caused by the rotating turbine. A minimum yaw stiffness is required in order to balance the wind induced yaw moment. The yaw stiffness is determined by the fairlead radius, the horizontal component of pretension and the number of mooring lines. To avoid too high loads on the mooring lines and fairlead connection, one possibility is to use a mooring configuration consisting of several mooring lines. The present results indicate that the cost for the additional lines for a 6-line configuration compared to a 3-line system is only marginal. The reason for this is that the 6 lines require smaller chain diameters due to less load per line. Low line tension is also positive with respect to fatigue. One important difference between the 3- and the 6-line system with respect to design is that the 6-line system has redundancy and will not pose any threat to neighbouring wind turbines in case of a line failure. DNV-OS-E301 [16] recommends an increase in safety factors for non-redundant systems.

Note that additional cost for anchors and installation has not been included in the comparison. Such installation costs depend on several parameters, including:

- the complexity of the installation
- possible weather windows
- the daily rate for the installation vessels, which depends heavily on the demand
- distance to shore
- type of anchors to be installed

Pre-installed mooring system is preferable, and may cut down installation cost. Development of new vessels, custom made for installation of offshore wind turbines, may lead to reduced installation costs compared to today's costs.

The choice of anchor will depend on the seabed properties and the loading direction. Vertical forces on the anchor are allowed for pile and suction anchors, but not for drag embedded anchors [34]. Pile or suction anchors are probably more suitable if one would like nearby wind turbines to share anchors. However, pile and suction anchors are more costly to install than drag anchors. Another anchor type which may be relevant is the so-called torpedo anchor, see e.g. [35]. This anchor type is relatively new, can be loaded in any direction and seems promising with respect to reduced installation costs.

Only extreme load conditions have been considered in the present analysis. Fatigue damage has not been included in the optimization process. The stiffer the mooring system is, the more vulnerable it will be to fatigue damage. This follows from basic fatigue analysis, where the damage rate for a narrow banded (tension or stress) process can be expressed as

$$D_{\text{NB}} = \frac{\nu_0 T}{K} \left(2\sqrt{2}\sigma\right)^m \Gamma\left(\frac{m}{2} + 1\right),$$



where ν_0 is the mean up-crossing of the stress process, σ is the standard deviation of the stress, T is the duration of the sea state, $\Gamma(\cdot)$ is the Gamma function, K and m are fatigue properties of the material. A stiff mooring system will give higher wave frequency (WF) loads, σ_{WF} , and higher low frequency loads, σ_{LF} , and will contribute to a larger damage rate. A mooring system should therefore not be too stiff, as this will adversely affect the fatigue life. On the contrary, it should not be too soft in order to avoid excessive horizontal offsets. Large offset will increase the cost of the power cable. Fatigue should be addressed in a later design iteration, but will require a complete scatter diagram being available providing the joint distribution of waves, wind and current, including the frequency of occurrence.

The present design is based on a simplified aerodynamic load model where the wind spectrum has been tuned to mimic the actual aerodynamic load fluctuations. However, the present approach models the floater as a single rigid-body and does not account for the correct dynamical effects from the rotating turbine. More accurate analysis involving sophisticated aero- and hydroelastic models are recommended for final verification of the integrated system.

It should also be pointed out that the present design is based on the input provided as summarized in Chapter 4. Any changes or corrections to the input data from other work packages (e.g. modifications to the rotor and generator design, changes to aerodynamic loads) may alter the present size and dimensions of the floater and mooring system.



References

- [1] MARINTEK, “Floating spar buoy for the DeepWind concept - Deliverable D5.1,” 2014. Report no. MT2014-A-008.
- [2] I. J. Fylling and P. A. Berthelsen, “WINDOPT – an optimization tool for floating support structures for deep water wind turbines,” in *Proceedings of OMAE*, (Rotterdam, The Netherlands), June 19–24 2011.
- [3] Statoil, Norway, *Hywind facts sheet*, 2009. www.statoil.com/no/TechnologyInnovation/NewEnergy/RenewablePowerProduction/Offshore/Hywind/Downloads/Hywind%20Fact%20sheet.pdf.
- [4] Principle Power, *First WindFloat Successfully Deployed Offshore - press release*, 2011. http://www.principlepowerinc.com/news/press_PPI_WF_deployment.html.
- [5] SWAY AS. www.sway.no.
- [6] <http://www.bluegroup.com/>.
- [7] WindSea AS. www.windsea.no.
- [8] T. Utsunomiya, H. Matsukuma, S. Minoura, K. Ko, H. Hamamura, O. Kobayashi, I. Sato, Y. Nomoto, and K. Yasui, “On sea experiment of a hybrid spar for floating offshore wind turbine using a 1/10 scale model,” in *Proceedings of OMAE*, (Shanghai, China), June 6–11 2010.
- [9] “Japan: Experimental offshore floating wind farm project,” 2013. <http://www.offshorewind.biz/2013/10/11/japan-experimental-offshore-floating-wind-farm-project-2/>.
- [10] U. S. Paulsen, T. F. Pedersen, H. A. Madsen, K. Enevoldsen, P. H. Nielsen, J. Hattel, L. Zanne, L. Battisti, A. Brighenti, M. Lacaze, V. Lim, J. W. Heinen, P. A. Berthelsen, S. Carstensen, E.-J. de Ridder, G. van Bussel, and G. Tescione, “DeepWind – an innovative wind turbine concept for offshore,” in *EWEA2011*, (Brussels, Belgium), March 14–17 2011.
- [11] S. Carstensen, X. Madviwalla, L. Vita, and U. S. Paulsen, “Lift of a rotating circular cylinder in unsteady flows,” in *Proceedings of ISOPE*, (Rhodes, Greece), June 17–22 2012.
- [12] L. Vita, U. S. Paulsen, P. H. Nielsen, P. A. Berthelsen, and S. Carstensen, “Design and aero-elastic simulation of a 5MW floating vertical axis wind turbine,” in *Proceedings of OMAE*, (Rio de Janeiro, Brazil), June 10–15 2012.
- [13] K. O. Ronold, E. Landet, V. L. Hansen, , E. L. R. Jørgensen, M. Godvik, and A. L. H. Hopstad, “Guideline for offshore floating wind turbine structures,” in *Proceedings of OMAE*, (Shanghai, China), June 6–11 2010.
- [14] S. Chakrabarti, ed., *Handbook of Offshore Engineering*, vol. 2. Elsevier Ltd., 2005.
- [15] N. Baltrop, ed., *Floating structures: a guide for design and analysis*, vol. 2. Centre for Marine Technology and Petroleum Technology, CMPT, 1998.
- [16] Det Norske Veritas, *Offshore Standard: Position Mooring. DNV-OS-E301*, October 2010. www.dnv.com.
- [17] ISO, “Petroleum and natural gas industries - Specific requirements for offshore structures - Part 7: Station-keeping systems for floating offshore structures and mobile offshore units,” 2005. ISO 19901-7:2005.
- [18] International Electrotechnical Commission, *Wind turbines – Part 3: Design requirements for offshore wind turbines. IEC 61400-3*, 1.0 ed., February 2009.



- [19] H. G. Svendsen and K. O. Merz, "Description of rotor control concepts," Technical report, DeepWind deliverable D4.2, SINTEF Energy, March 2013. Version 1.0.
- [20] U. S. Paulsen, H. A. Madsen, K. Kragh, P. H. Nielsen, I. Baran, J. Hattel, E. Ritchie, K. Leban, H. Svendsen, and P. A. Berthelsen, "Deepwind - from idea to 5 MW concept," in *EERA DeepWind'2014, 11th Deep Sea Offshore Wind R&D Conference*, (Trondheim, Norway), January 22–24 2014.
- [21] WAMIT, *User Manual*. Massachusetts Institute of Technology, Cambridge, MA, USA, 1995. Rev. 5.3/5.3s.
- [22] I. J. Fylling, "Automated optimization of deepwater mooring system design," in *Proceedings of OMAE*, (Yokohama, Japan), April 14–17 1997.
- [23] I. J. Fylling and G. Kleiven, "Integrated optimized design of riser and mooring system for floating production vessels," in *Proceedings of OMAE*, (New Orleans, USA), February 14–16 2000.
- [24] K. Schittkowski, "NLPQL: A FORTRAN subroutine solving constrained non-linear programming problems," *Annals of Operation Research*, vol. 5, no. 2, pp. 485–500, 1985.
- [25] MARINTEK, Trondheim, Norway, *MIMOSA User's Documentation*. www.marintek.sintef.no/software.
- [26] C. T. Stansberg, "Prediction of extreme slow-drift amplitudes," in *Proceedings of OMAE*, (New Orleans, USA), February 14–17 2000.
- [27] K. Larsen and P. C. Sandvik, "Efficient methods for the calculation of dynamic mooring line tension," in *Proceedings of the First European Offshore Mechanics Symposium*, (Trondheim, Norway), August 20–22 1990.
- [28] W. Gawronski, "Three models of wind-gust disturbances for the analysis of antenna pointing accuracy," *IPN Progress report 42-149*, 202.
- [29] K. A. Kragh, H. A. Madsen, and D. R. S. Verelst, "2nd iteration design loads for the DeepWind 5MW turbine," technical report, DTU Wind Energy, 16 April 2014. Draft version.
- [30] DTU Wind, "Internal communication, LoadsForFloaterDesign_sim_id_5MW35.ods." E-mail, May 22, 2014.
- [31] DeepWind research partners, "Internal communication." Web meeting, May 1, 2014.
- [32] Norwegian Technology Standards Institution, *NORSOK Standard N-003, Action and action effects*, February 1999. Rev 1., www.nts.no/norsok.
- [33] Det Norske Veritas, *Recommended Practice: Environmental conditions and environmental loads. DNV-RP-C205*, October 2010. www.dnv.com.
- [34] Sjøfartdirektoratet, "Forskrift om posisjonering og ankringssystemer på flyttbare innretninger," 2009. RSR 14-2009.
- [35] Deep Sea Anchors. <http://www.deepseaanchors.com>, Cited: 24th September 2014.

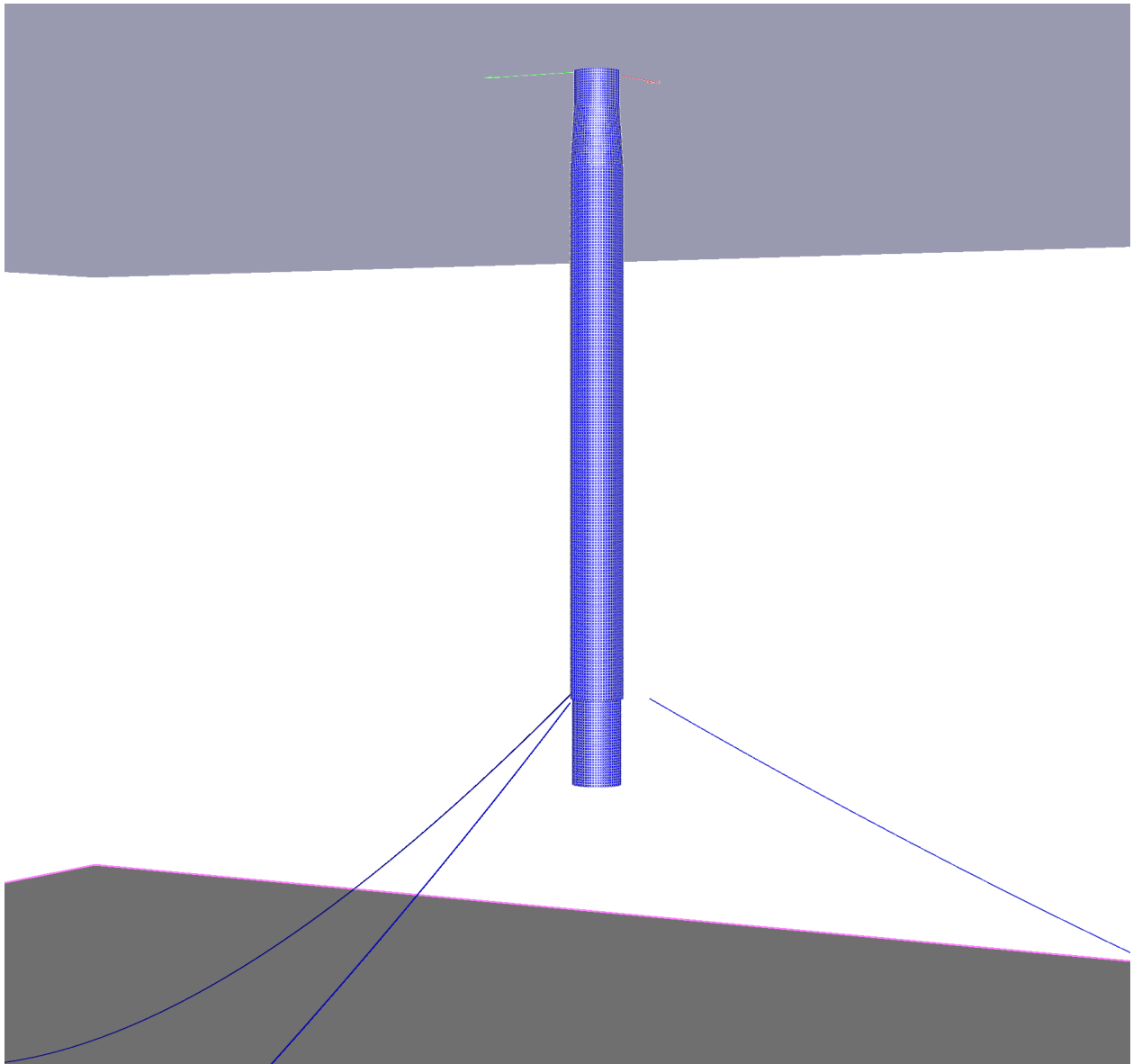
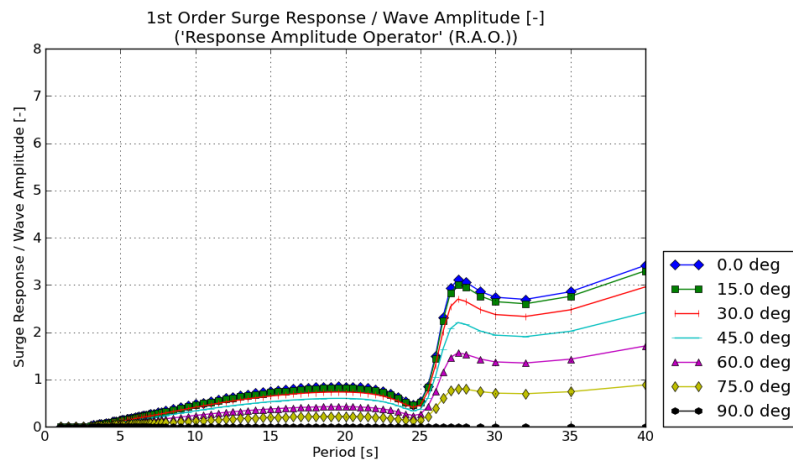
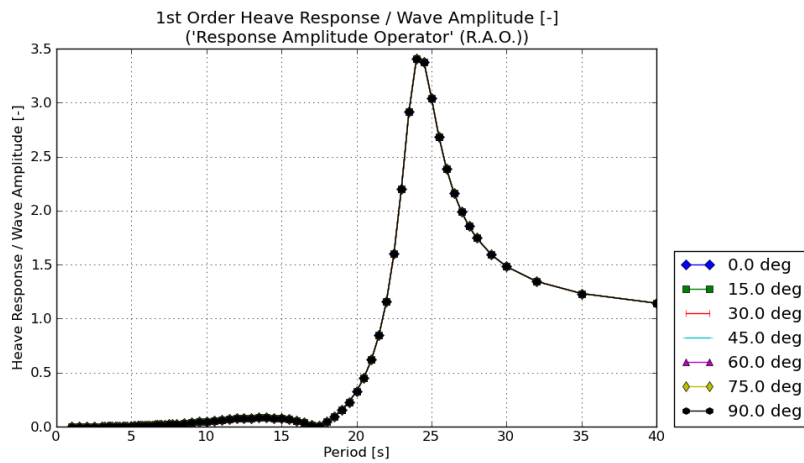
A WAMIT RESULTS - CASE 1 WITH 3 LINES

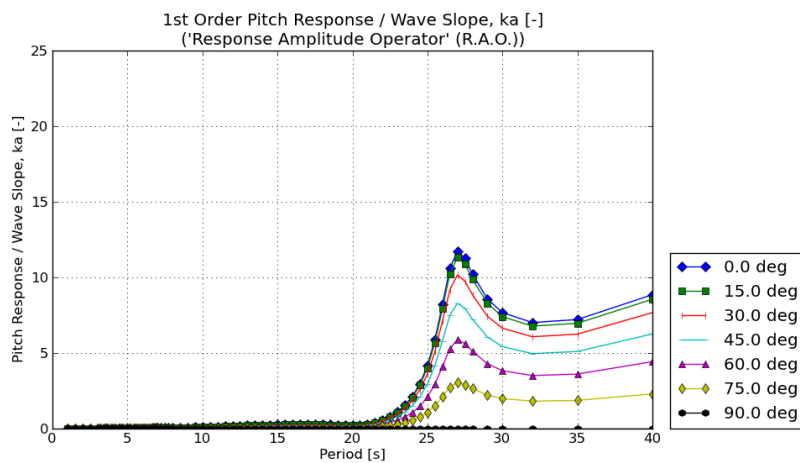
Figure A.1: A snapshot of the panel model with a 3 line mooring system. Two planes of symmetry with total of 4530 panels.



(a) Surge

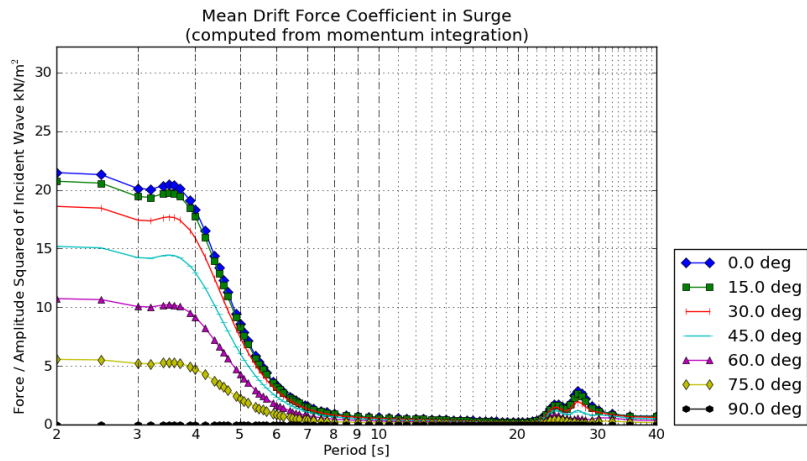


(b) Heave

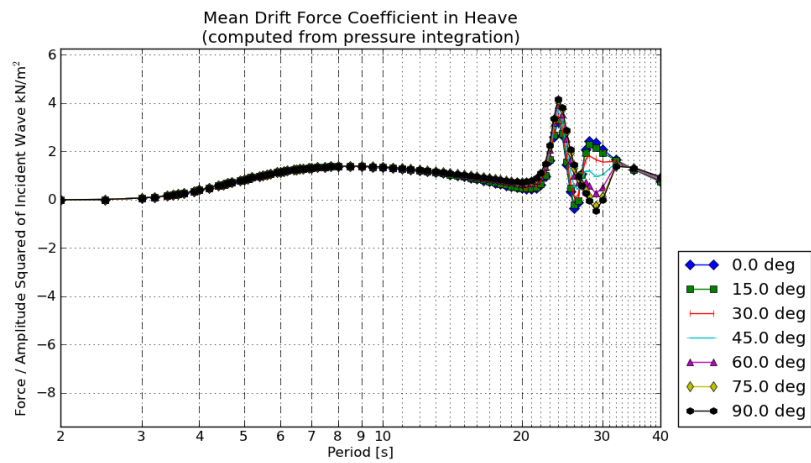


(c) Pitch

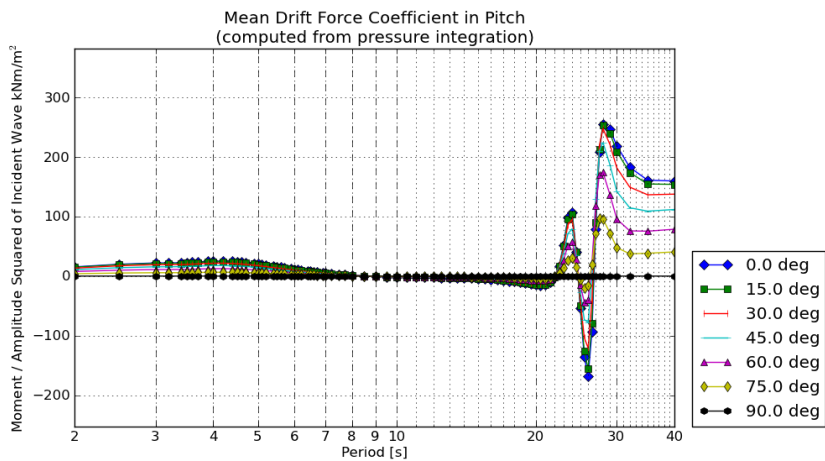
Figure A.2: Wave to motion transfer functions from WAMIT for surge, heave and pitch.



(a) Surge



(b) Heave

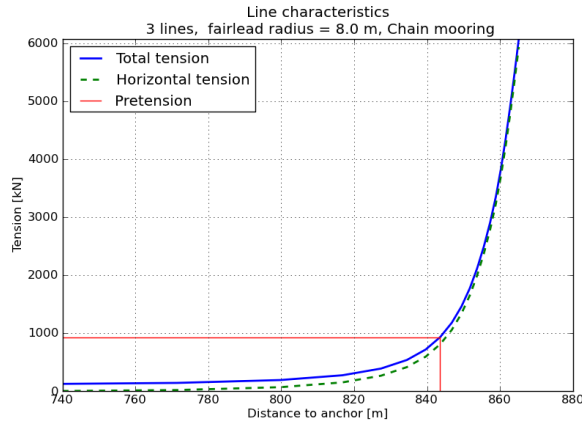


(c) Pitch

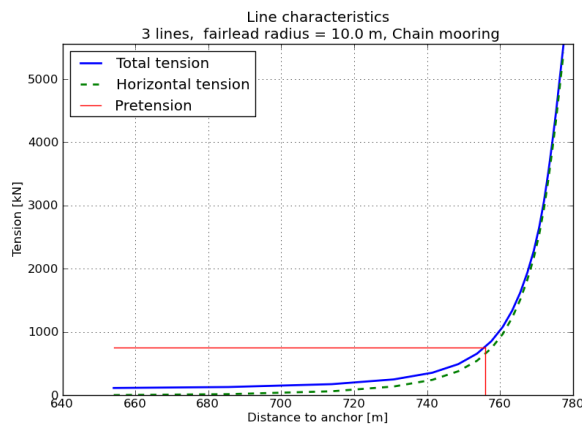
Figure A.3: Mean wave drift coefficients from WAMIT for surge, heave and pitch.

B ADDITIONAL PLOTS

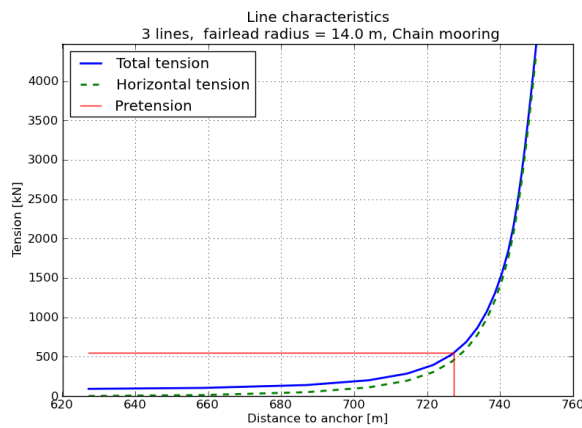
B.1 Line characteristics



(a) Fairlead radius, $R_f = 8.0$ m

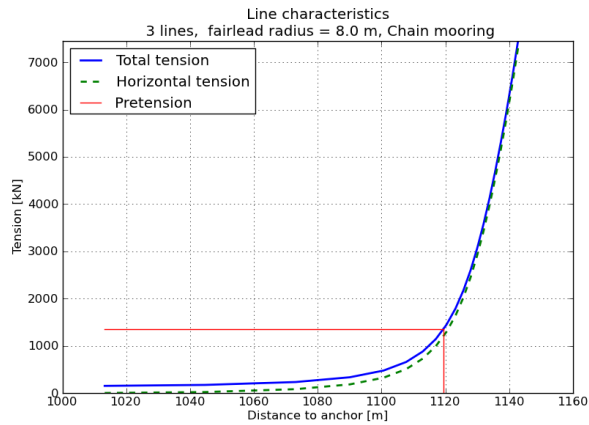


(b) Fairlead radius, $R_f = 10.0$ m

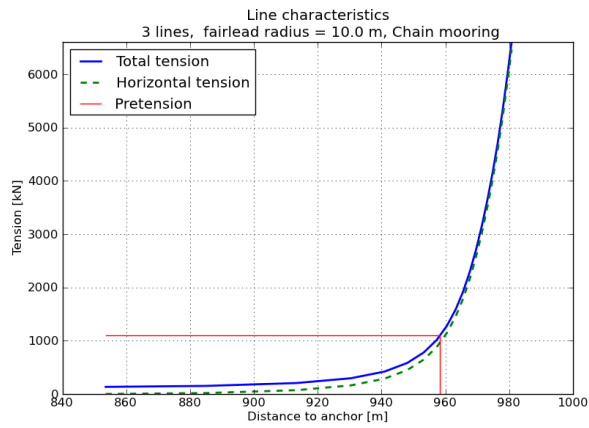


(c) Fairlead radius, $R_f = 14.0$ m

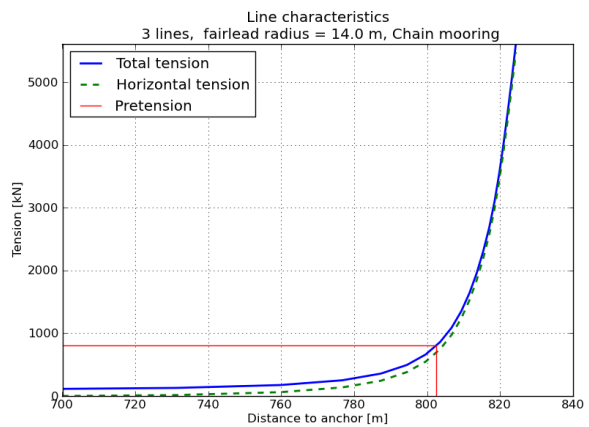
Figure B.1: Case 1; Line characteristics for 3 line system.



(a) Fairlead radius, $R_f = 8.0$ m

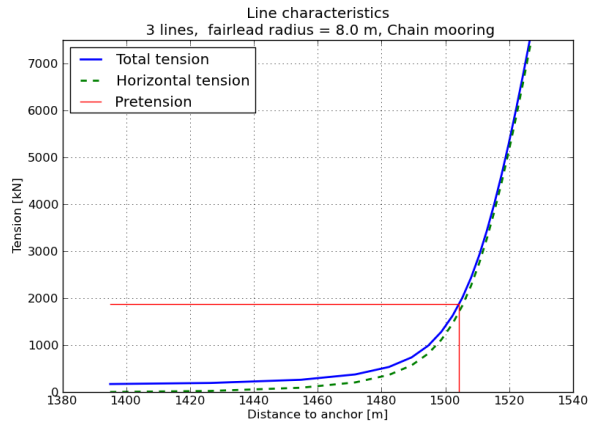


(b) Fairlead radius, $R_f = 10.0$ m

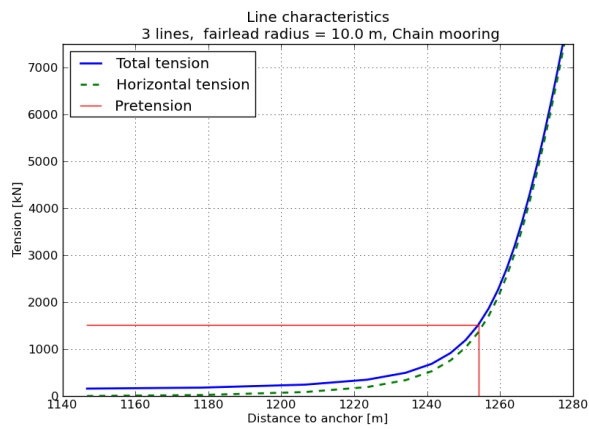


(c) Fairlead radius, $R_f = 14.0$ m

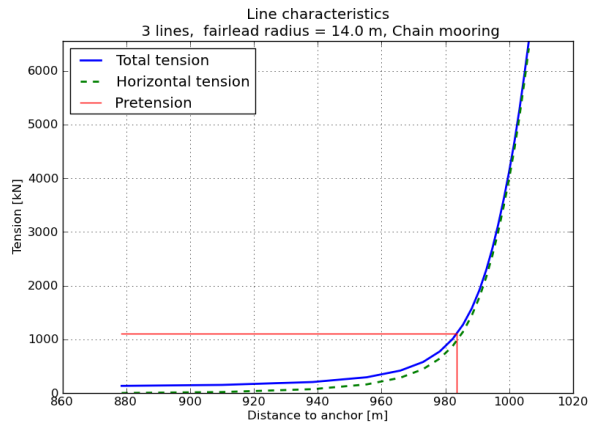
Figure B.2: Case 2; Line characteristics for 3 line system.



(a) Fairlead radius, $R_f = 8.0$ m

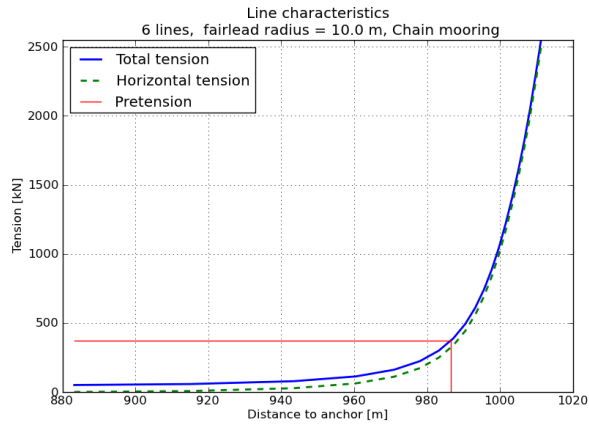


(b) Fairlead radius, $R_f = 10.0$ m

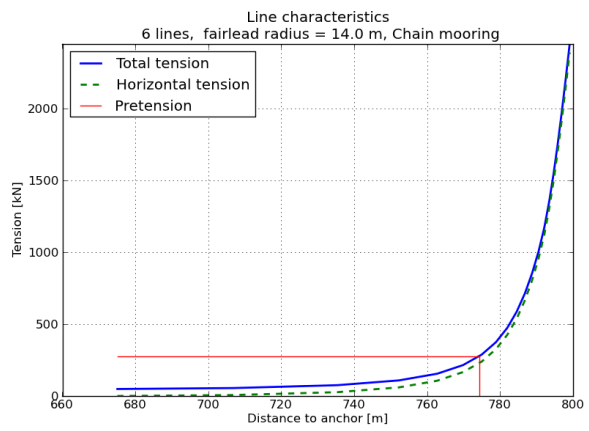


(c) Fairlead radius, $R_f = 14.0$ m

Figure B.3: Case 3; Line characteristics for 3 line system.

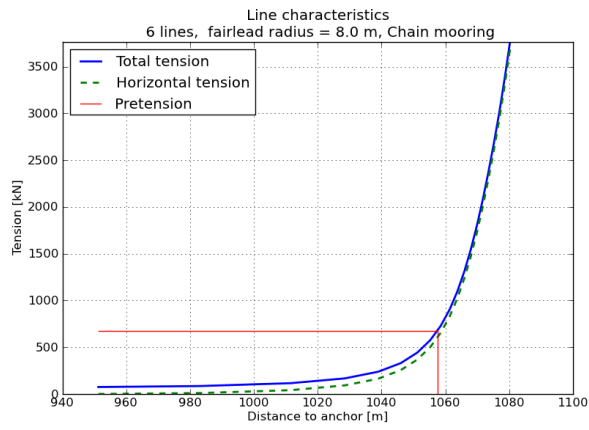


(a) Fairlead radius, $R_f = 10.0$ m

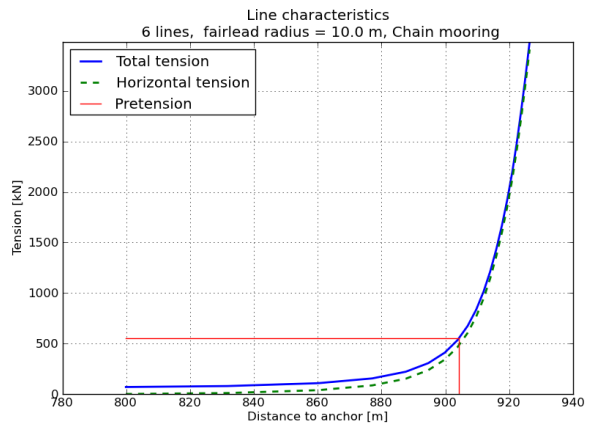


(b) Fairlead radius, $R_f = 14.0$ m

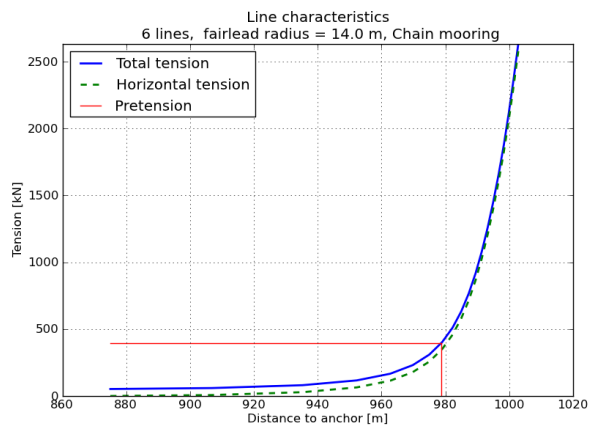
Figure B.4: Case 1; Line characteristics for 6 line system.



(a) Fairlead radius, $R_f = 8.0$ m

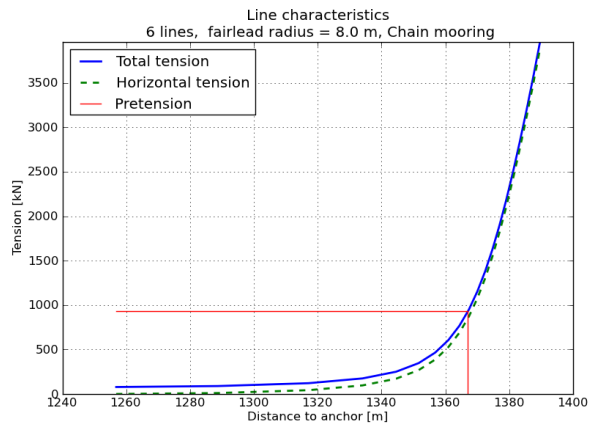


(b) Fairlead radius, $R_f = 10.0$ m

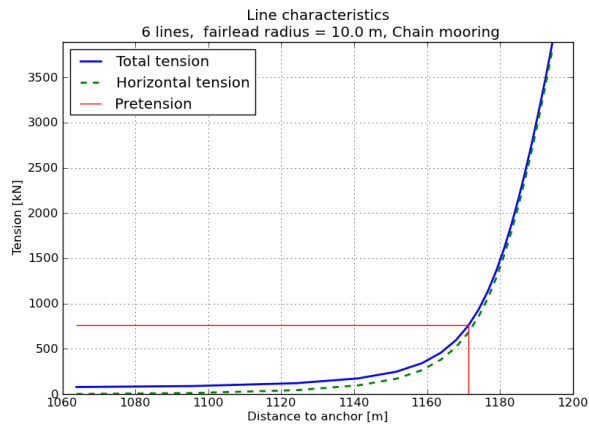


(c) Fairlead radius, $R_f = 14.0$ m

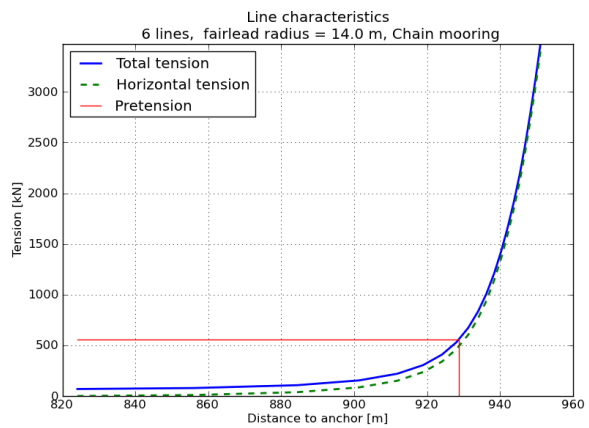
Figure B.5: Case 2; Line characteristics for 6 line system.



(a) Fairlead radius, $R_f = 8.0$ m



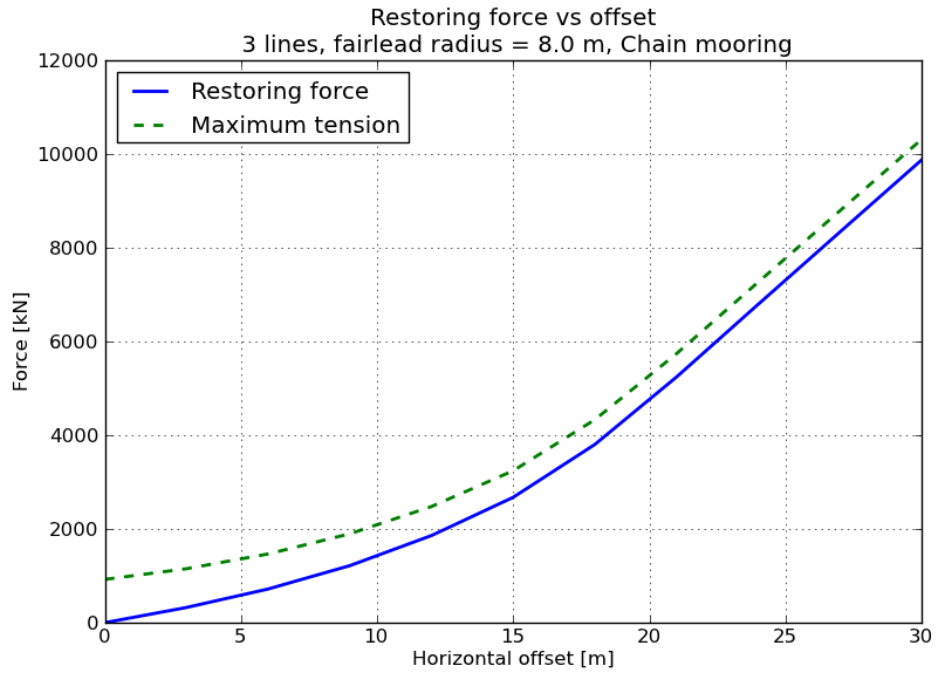
(b) Fairlead radius, $R_f = 10.0$ m



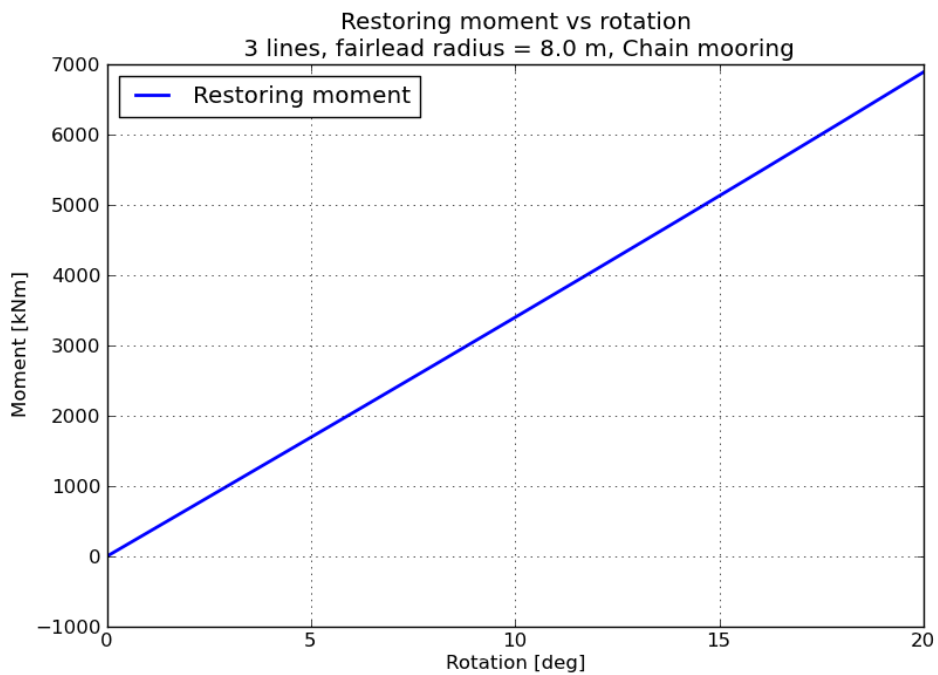
(c) Fairlead radius, $R_f = 14.0$ m

Figure B.6: Case 3; Line characteristics for 6 line system.

B.2 Restoring properties of mooring system

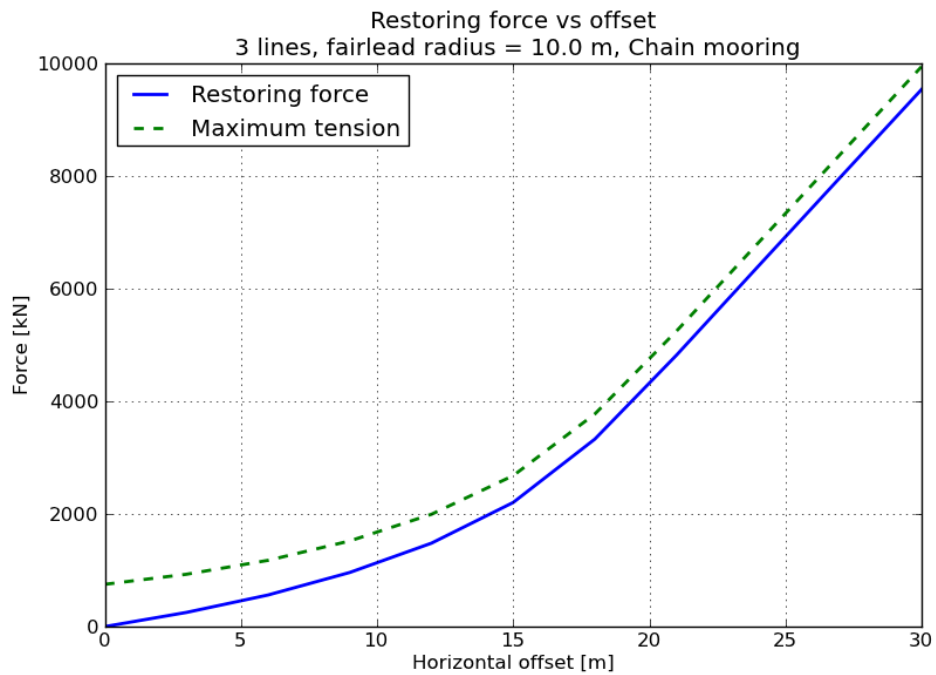


(a) Restoring force

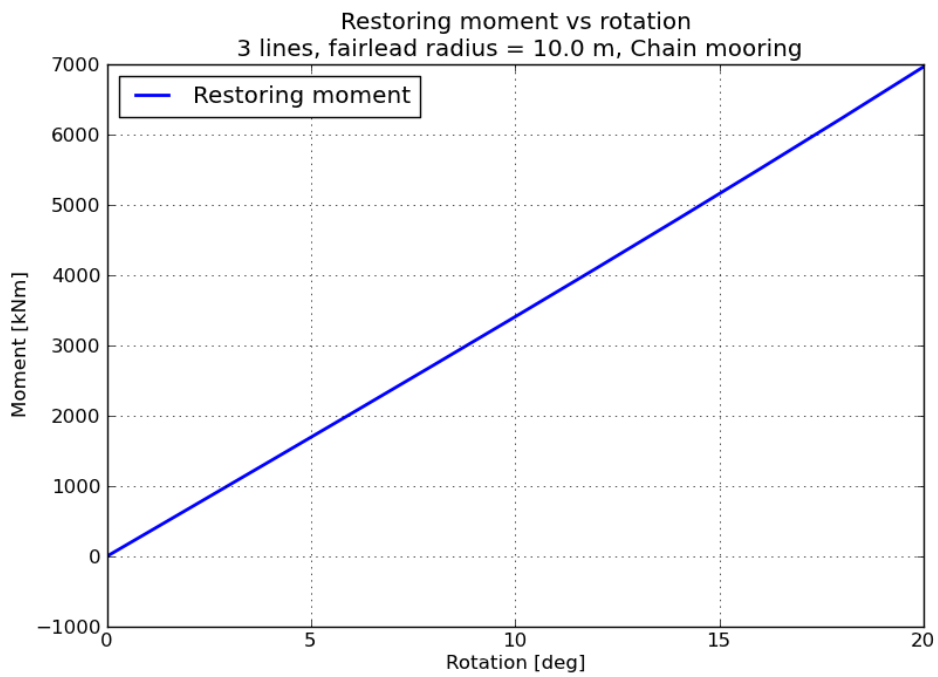


(b) Restoring moment

Figure B.7: Mooring system restoring properties for 3 line system; Case 1; fairlead radius, $R_f = 8.0$ m

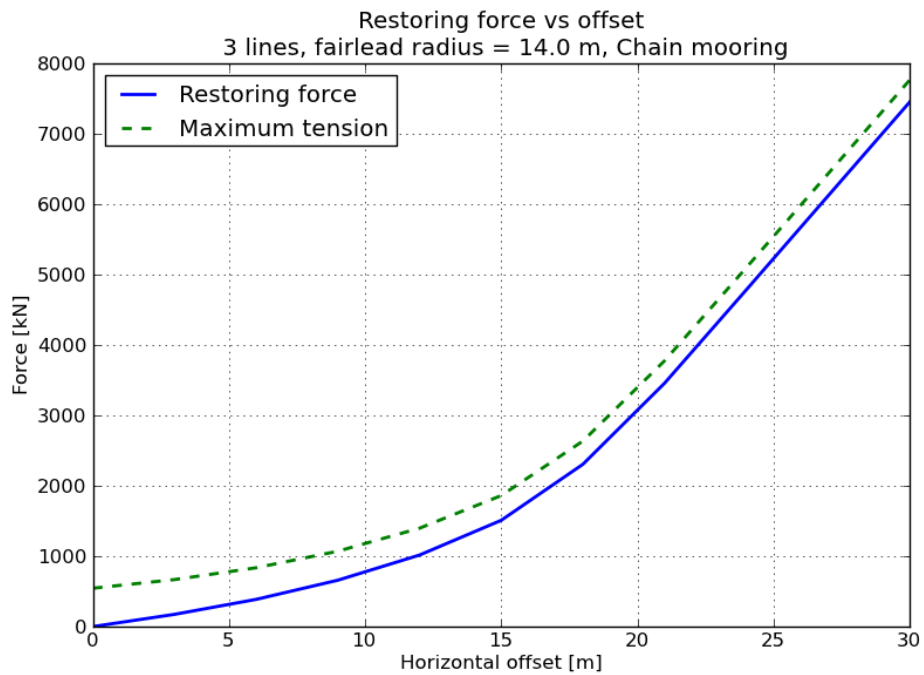


(a) Restoring force

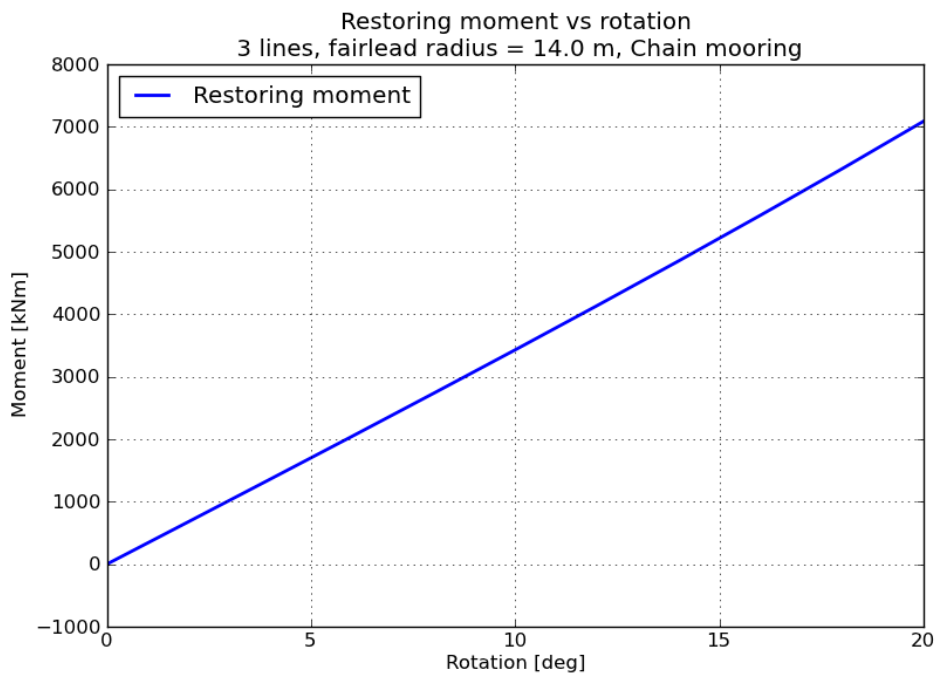


(b) Restoring moment

Figure B.8: Mooring system restoring properties for 3 line system; Case 1; fairlead radius, $R_f = 10.0$ m

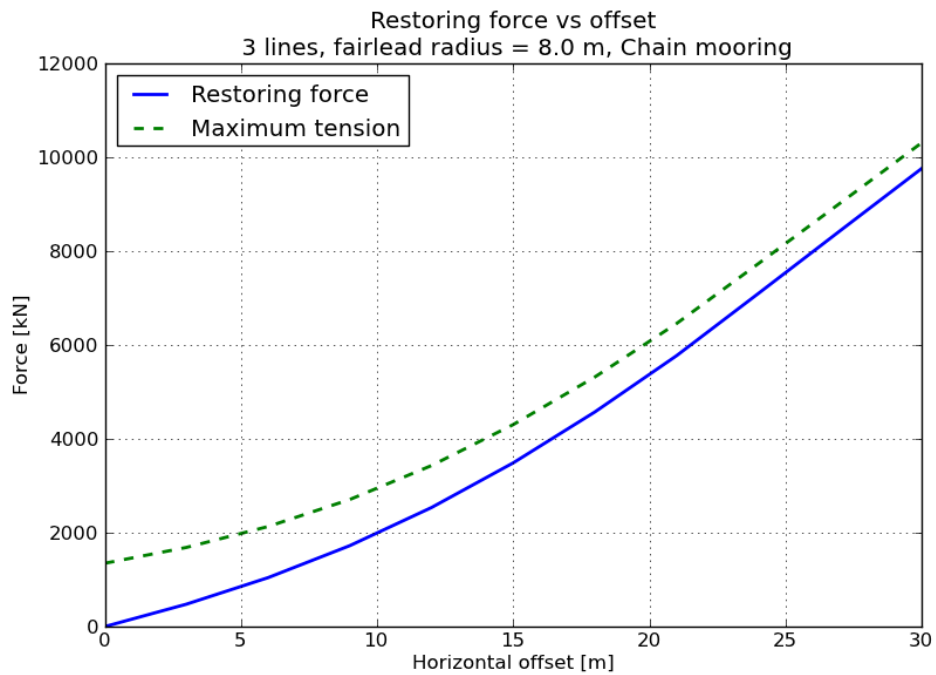


(a) Restoring force

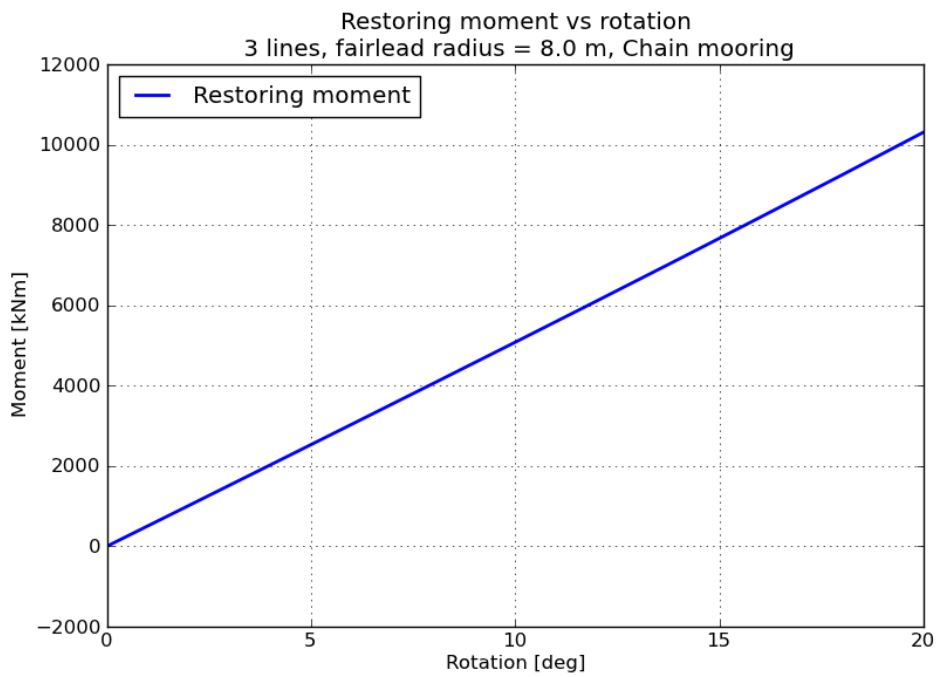


(b) Restoring moment

Figure B.9: Mooring system restoring properties for 3 line system; Case 1; fairlead radius, $R_f = 14.0$ m

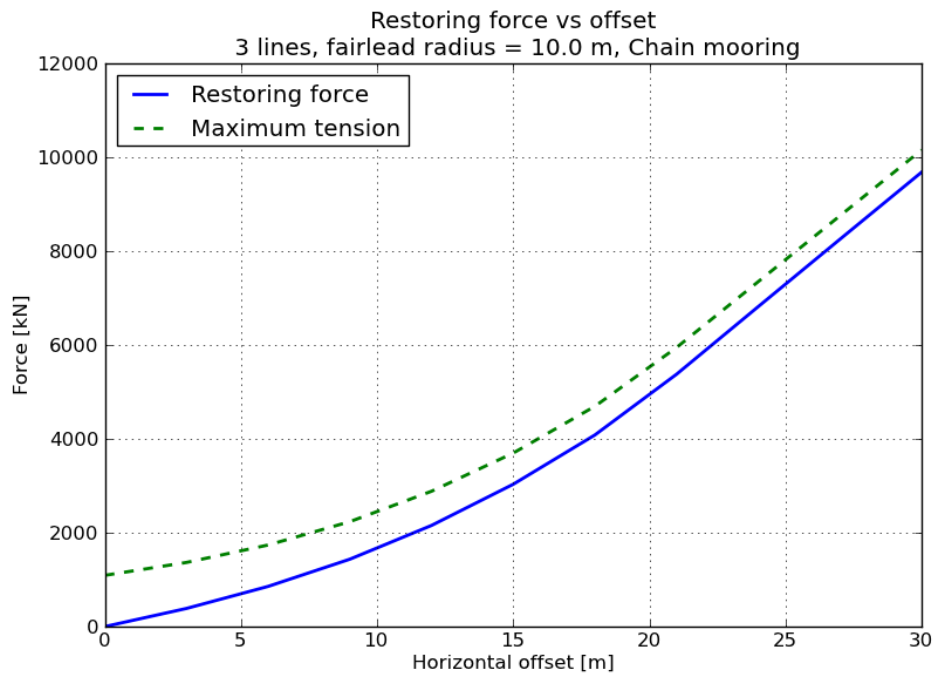


(a) Restoring force

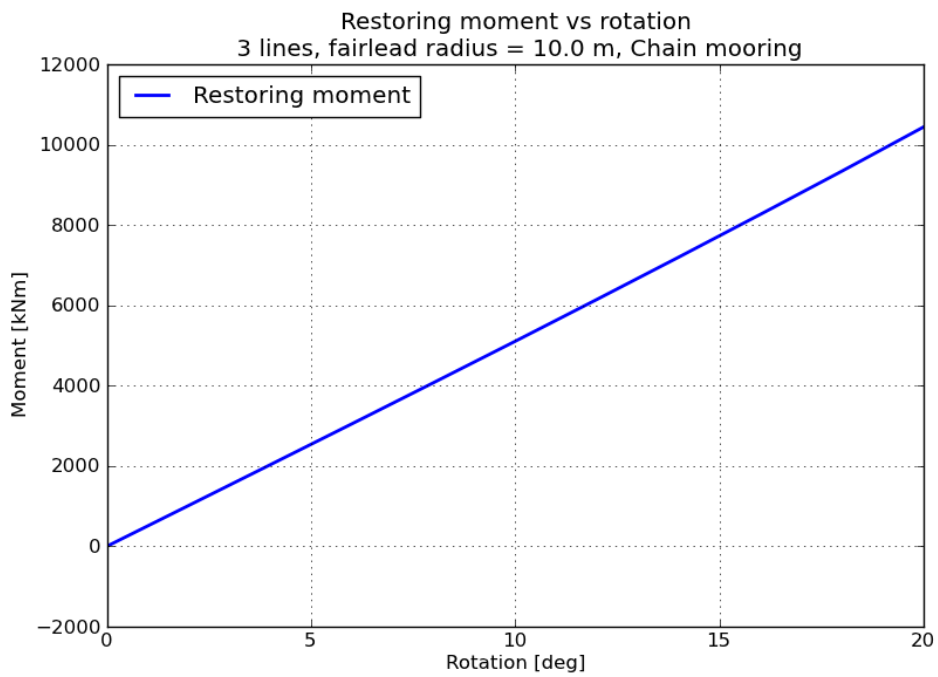


(b) Restoring moment

Figure B.10: Mooring system restoring properties for 3 line system; Case 2; fairlead radius, $R_f = 8.0$ m

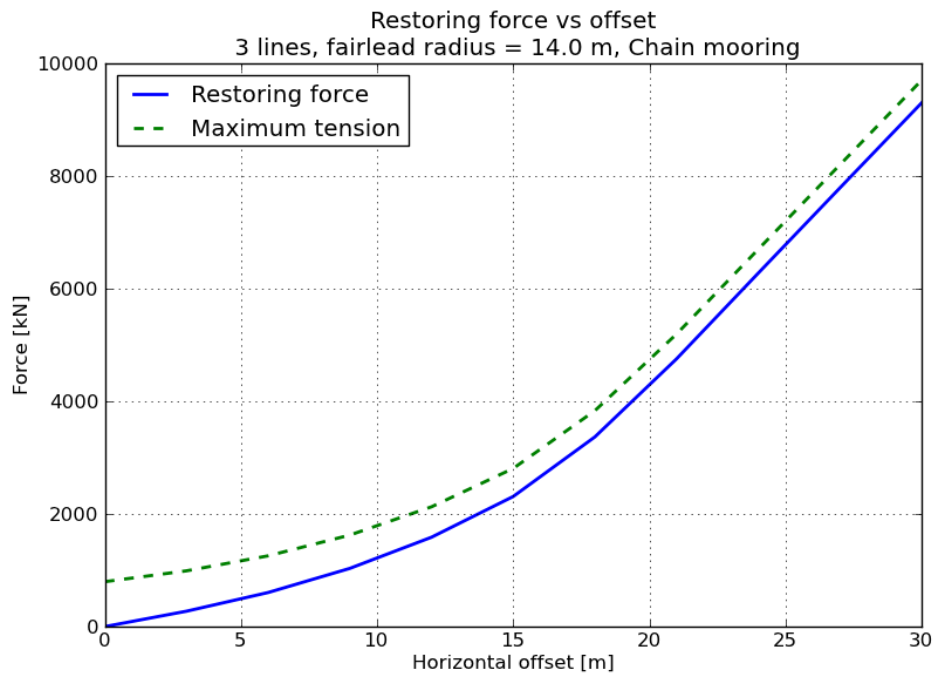


(a) Restoring force

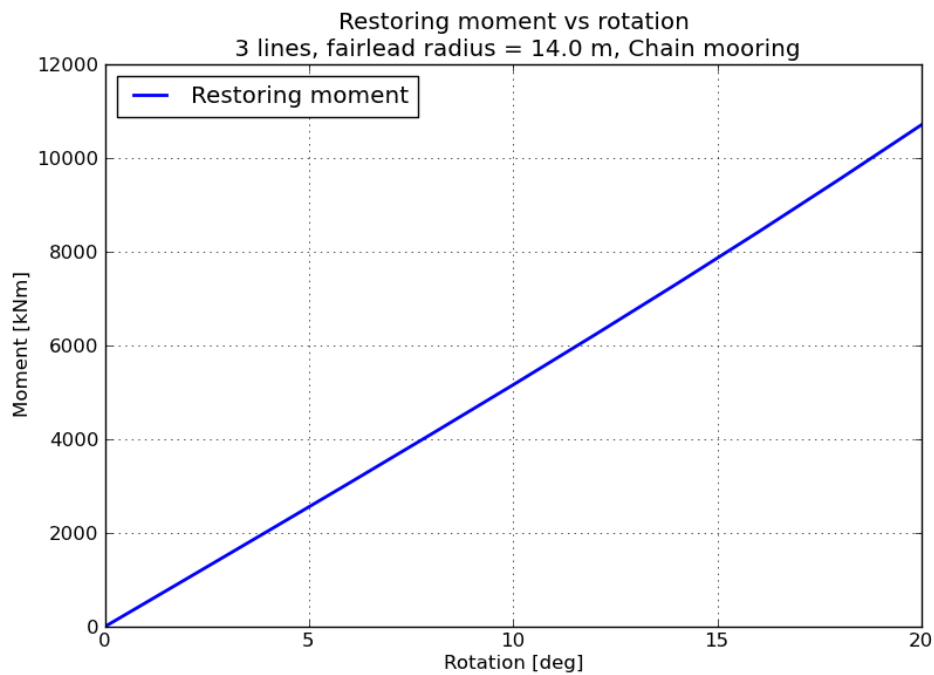


(b) Restoring moment

Figure B.11: Mooring system restoring properties for 3 line system; Case 2; fairlead radius, $R_f = 10.0$ m

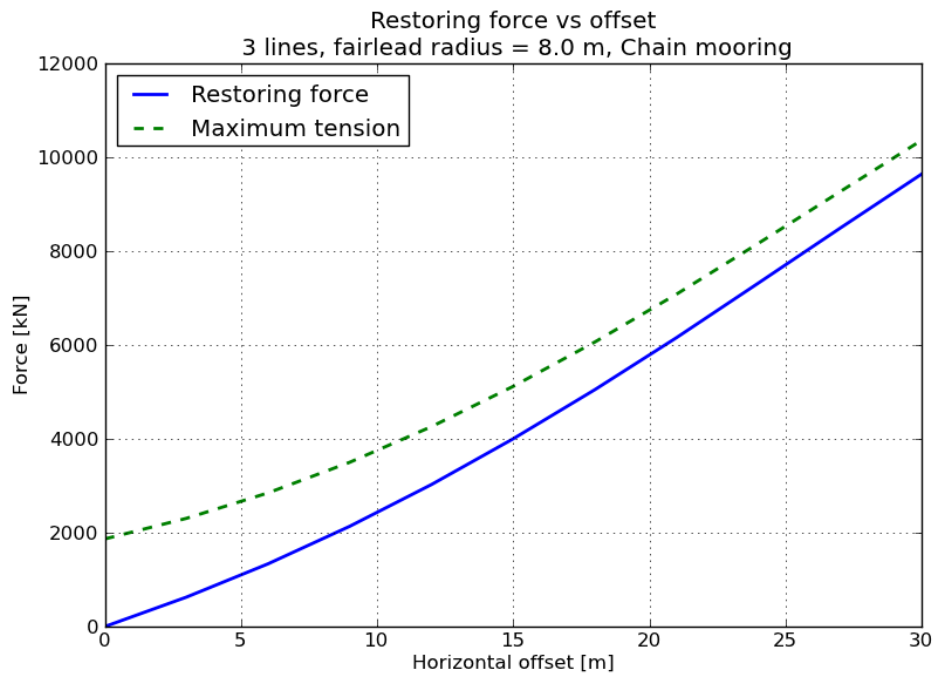


(a) Restoring force

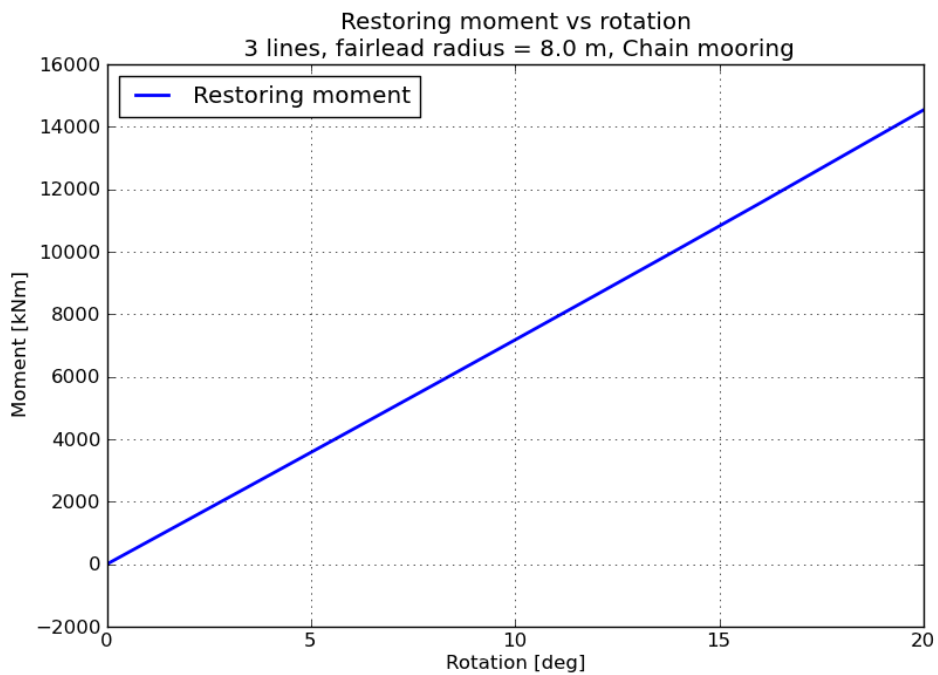


(b) Restoring moment

Figure B.12: Mooring system restoring properties for 3 line system; Case 2; fairlead radius, $R_f = 14.0$ m

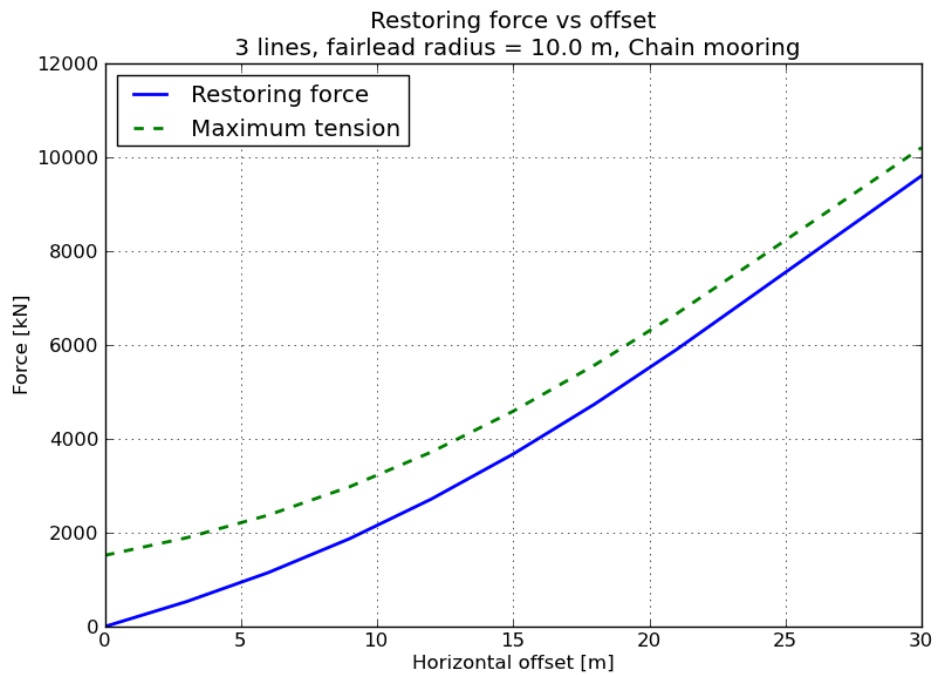


(a) Restoring force

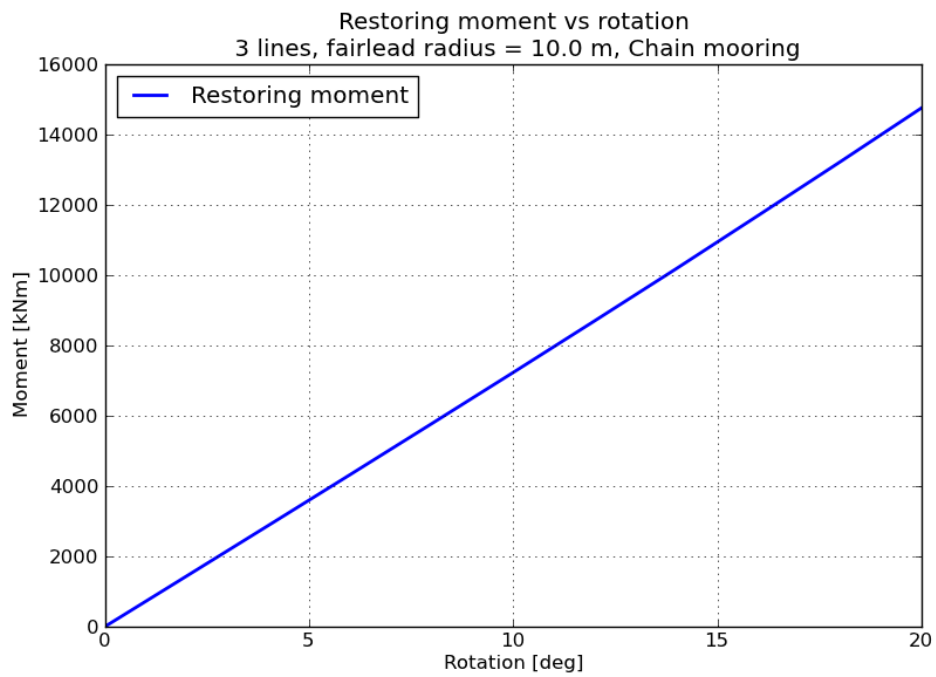


(b) Restoring moment

Figure B.13: Mooring system restoring properties for 3 line system; Case 3; fairlead radius, $R_f = 8.0$ m

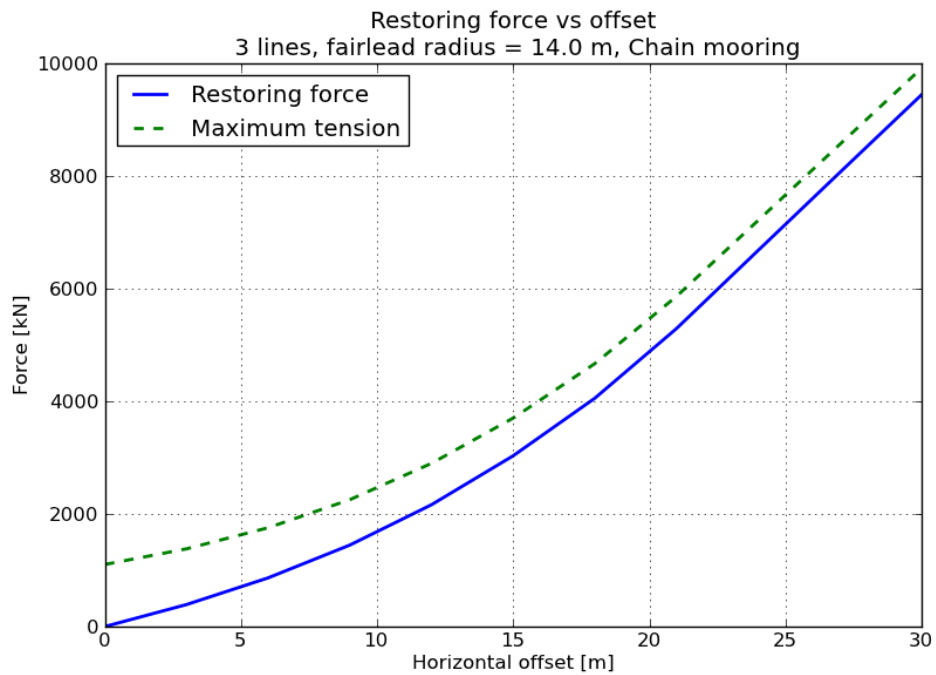


(a) Restoring force



(b) Restoring moment

Figure B.14: Mooring system restoring properties for 3 line system; Case 3; fairlead radius, $R_f = 10.0$ m

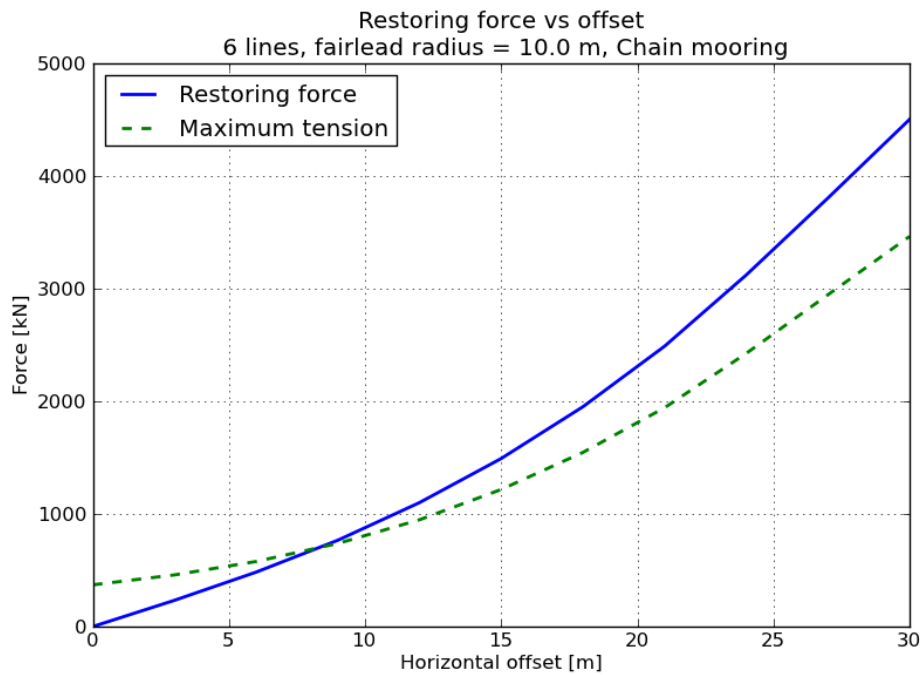


(a) Restoring force

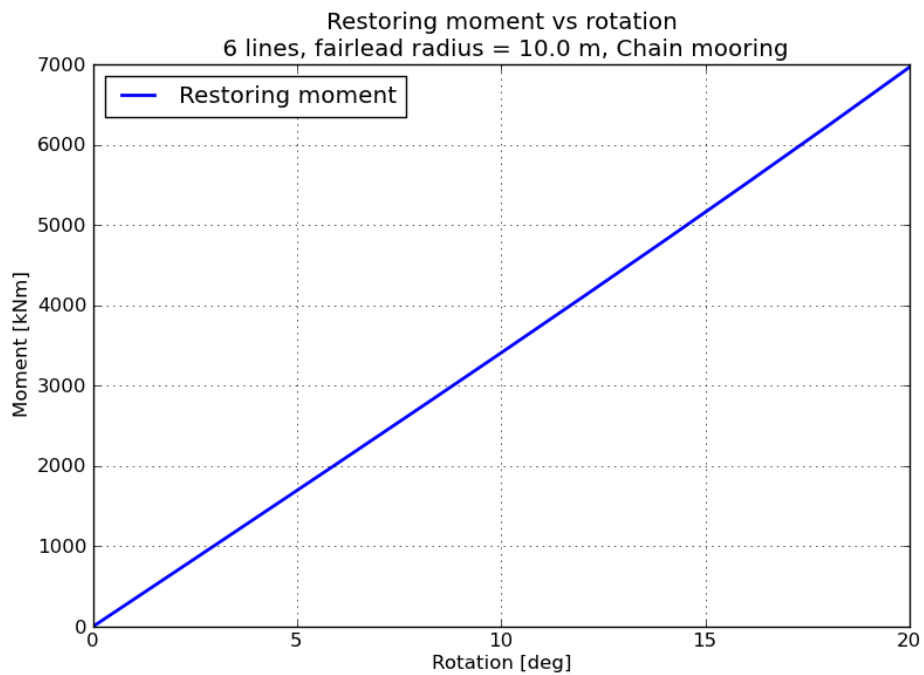


(b) Restoring moment

Figure B.15: Mooring system restoring properties for 3 line system; Case 3; fairlead radius, $R_f = 14.0$ m

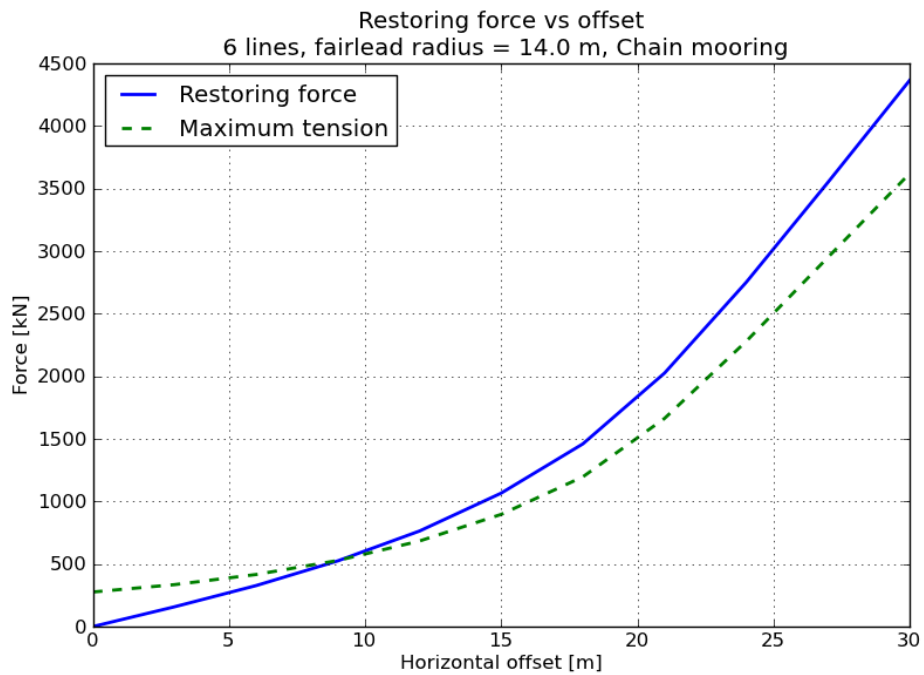


(a) Restoring force

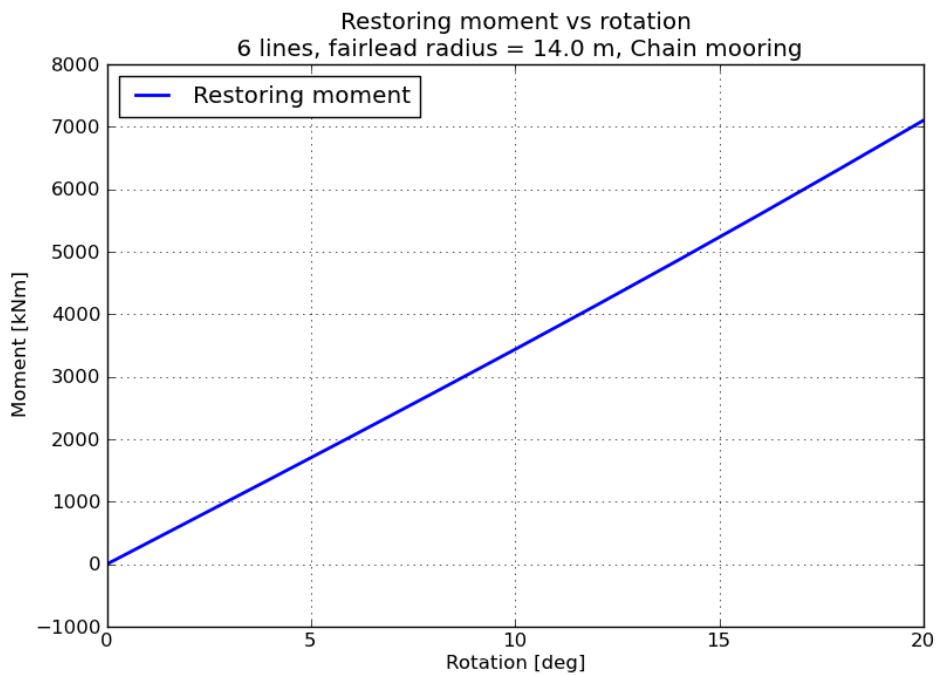


(b) Restoring moment

Figure B.16: Mooring system restoring properties for 6 line system; Case 1; fairlead radius, $R_f = 10.0$ m

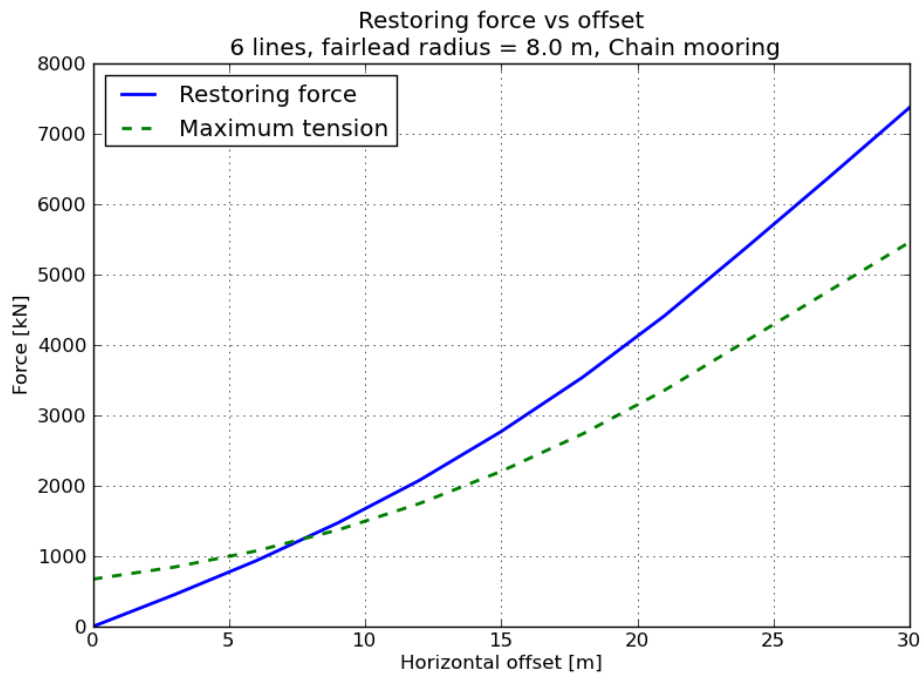


(a) Restoring force

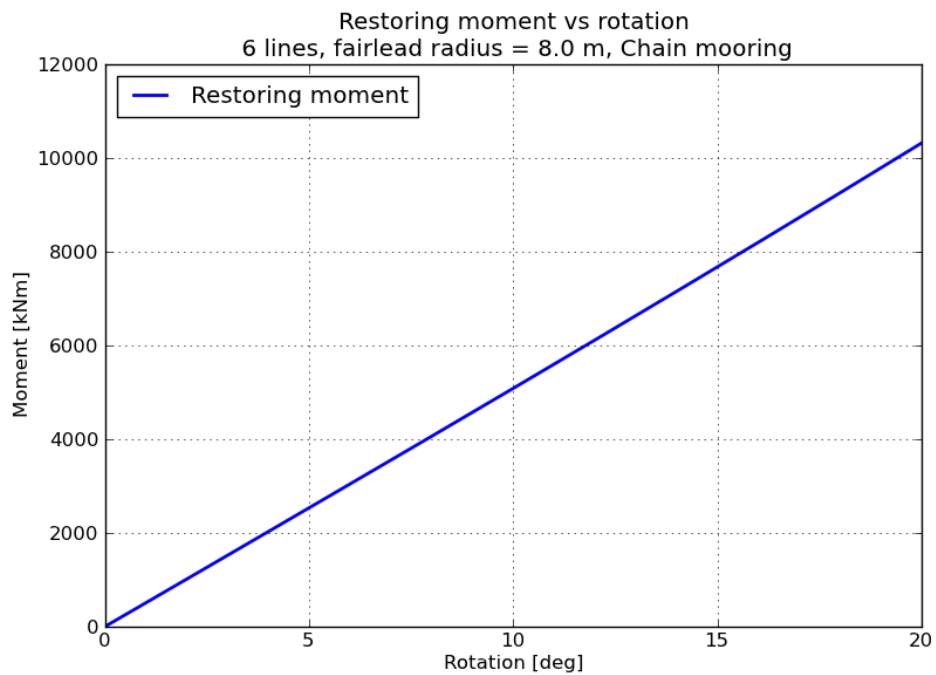


(b) Restoring moment

Figure B.17: Mooring system restoring properties for 6 line system; Case 1; fairlead radius, $R_f = 14.0$ m

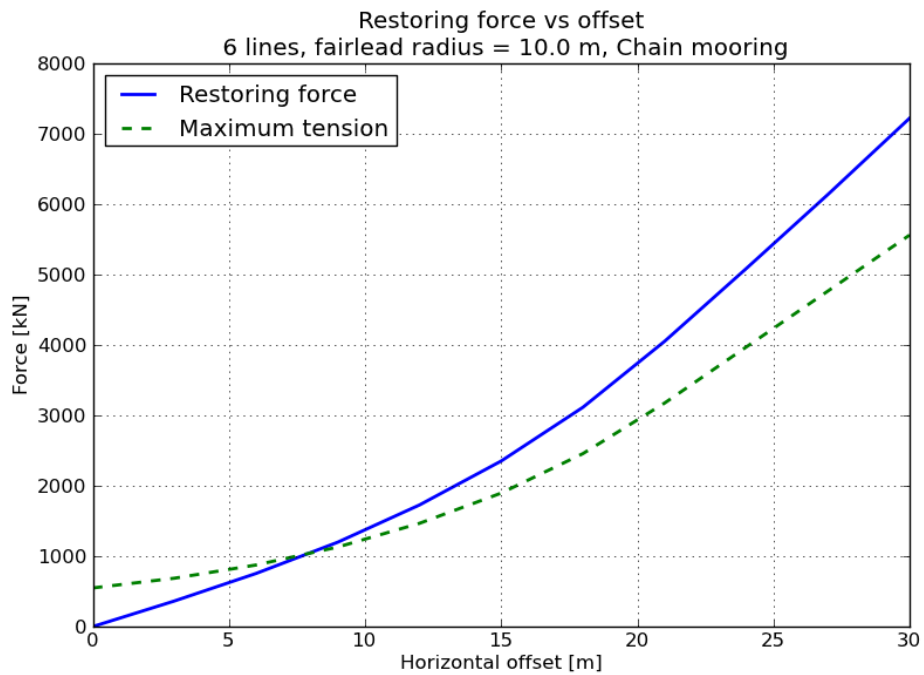


(a) Restoring force

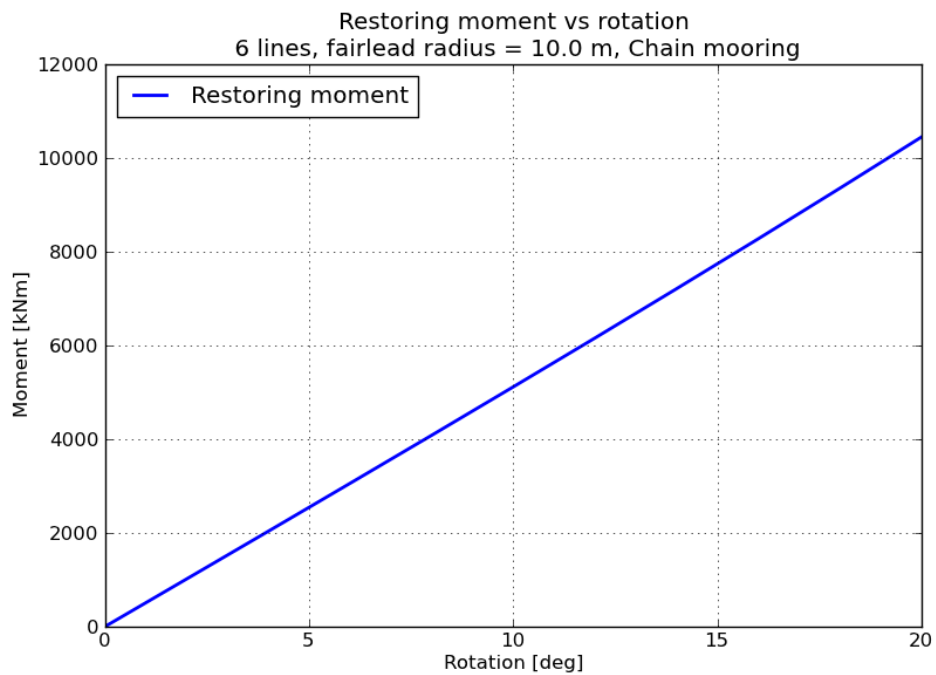


(b) Restoring moment

Figure B.18: Mooring system restoring properties for 6 line system; Case 2; fairlead radius, $R_f = 8.0$ m

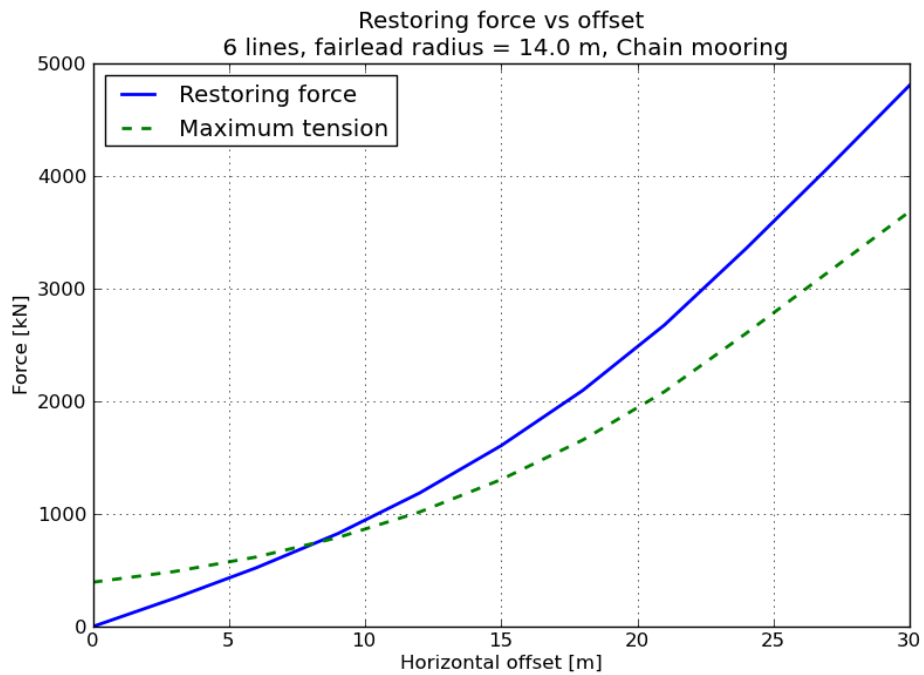


(a) Restoring force

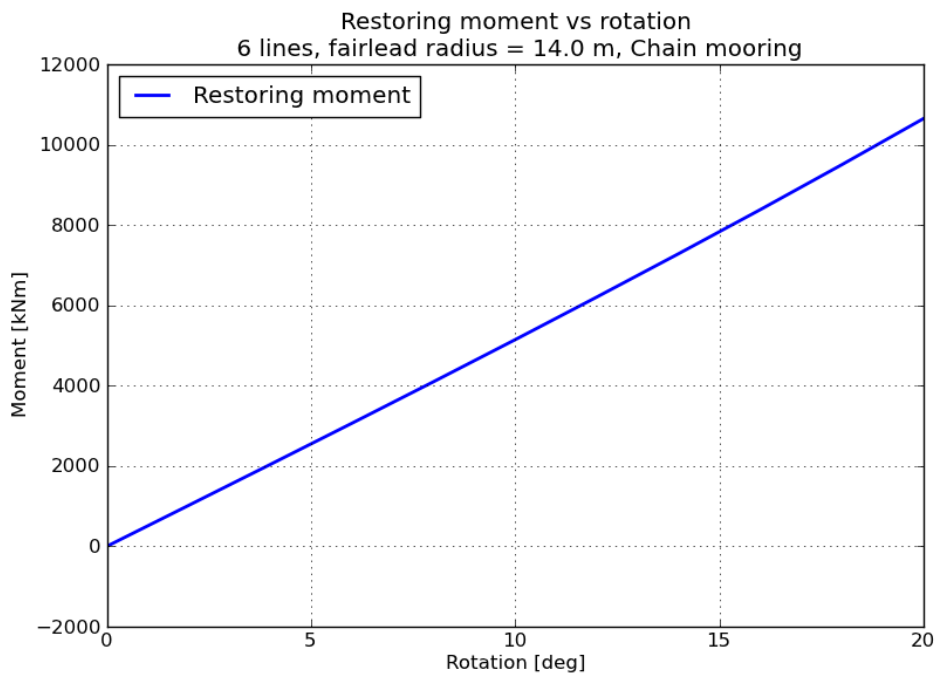


(b) Restoring moment

Figure B.19: Mooring system restoring properties for 6 line system; Case 2; fairlead radius, $R_f = 10.0$ m

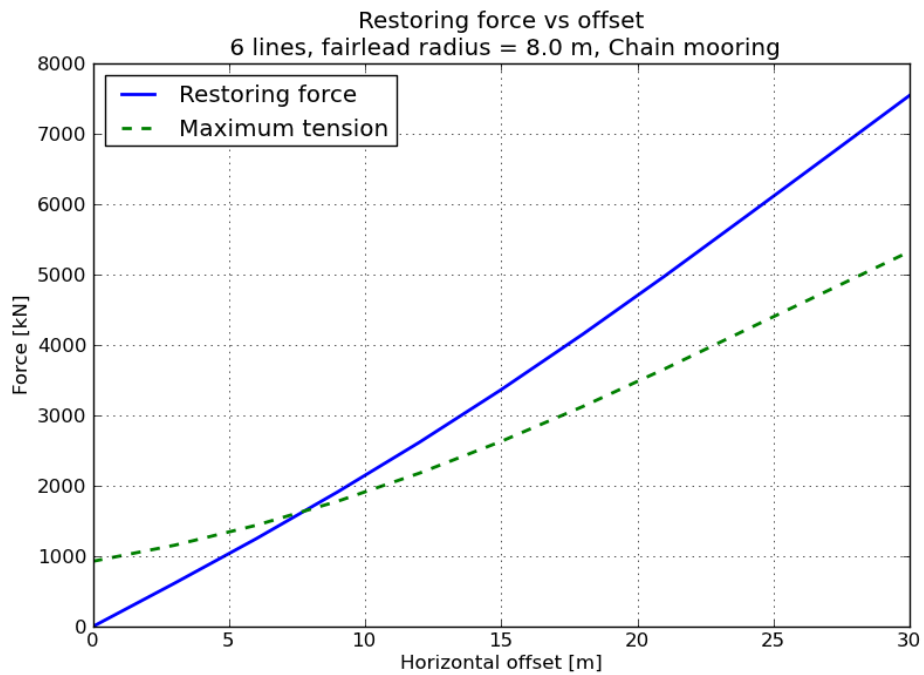


(a) Restoring force

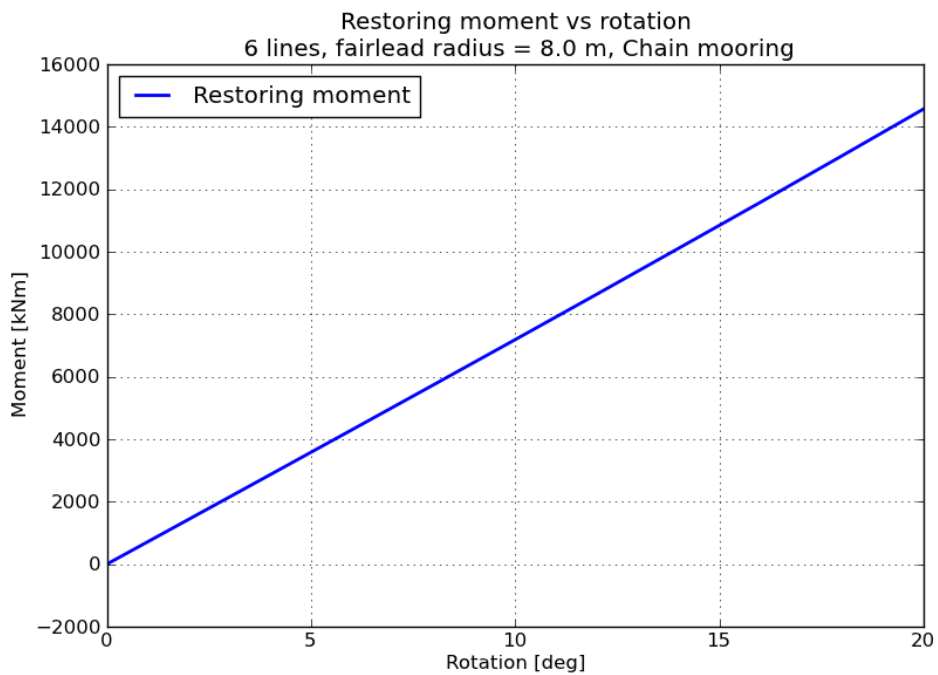


(b) Restoring moment

Figure B.20: Mooring system restoring properties for 6 line system; Case 2; fairlead radius, $R_f = 14.0$ m

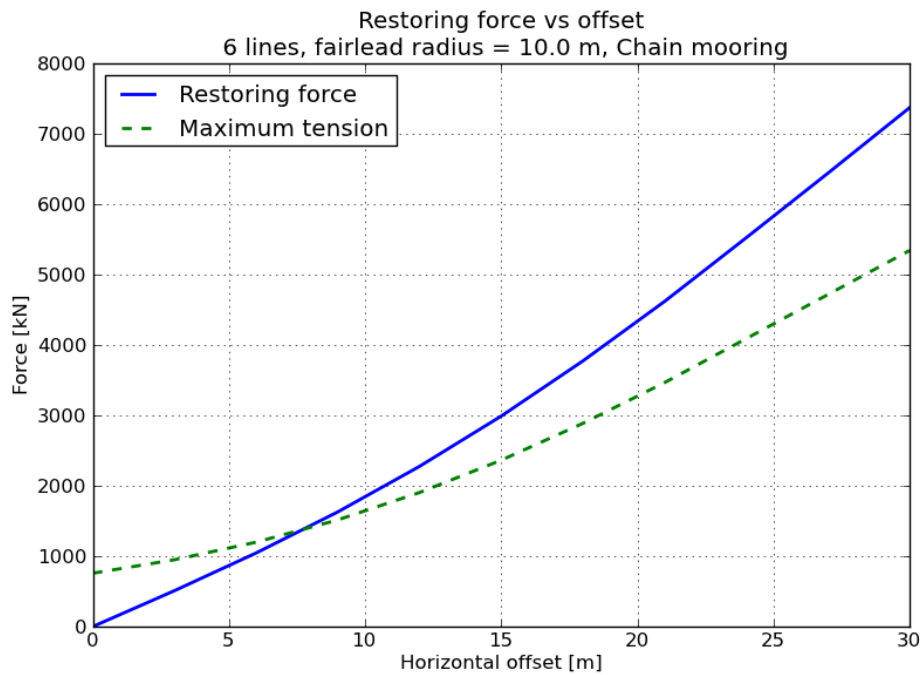


(a) Restoring force

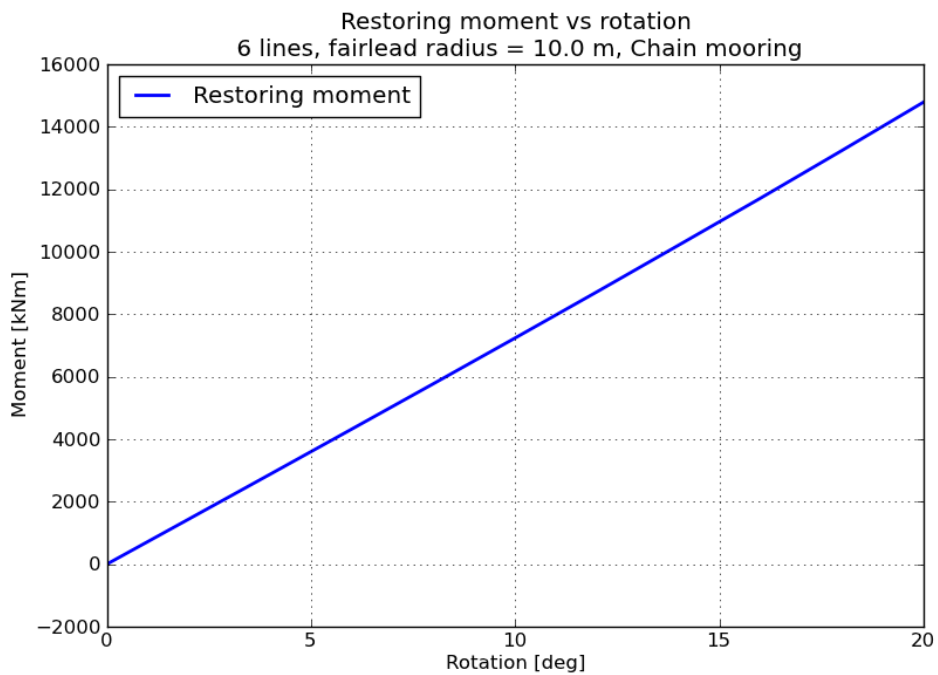


(b) Restoring moment

Figure B.21: Mooring system restoring properties for 6 line system; Case 3; fairlead radius, $R_f = 8.0$ m

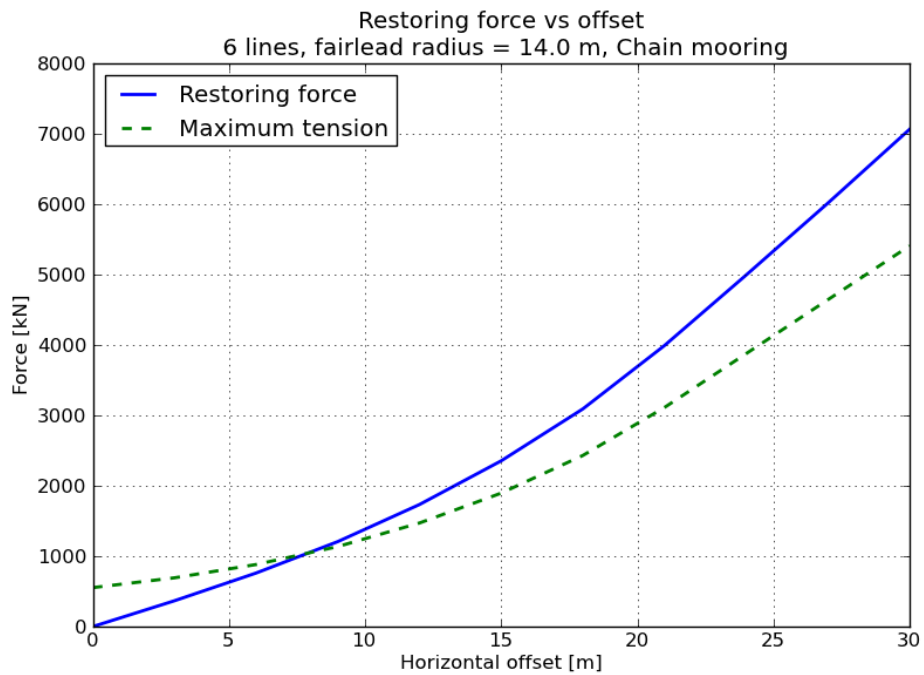


(a) Restoring force

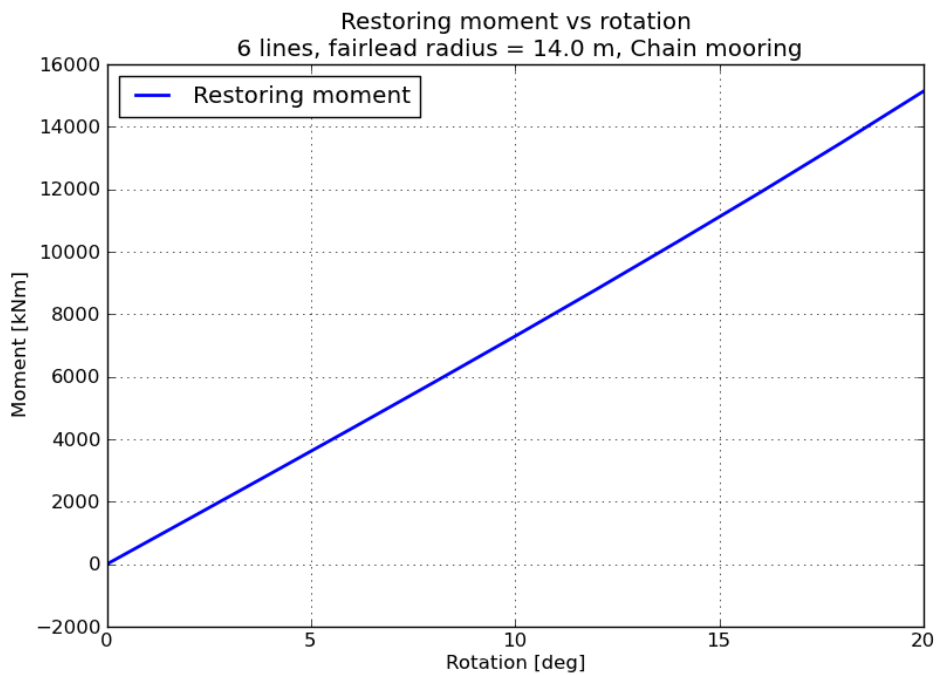


(b) Restoring moment

Figure B.22: Mooring system restoring properties for 6 line system; Case 3; fairlead radius, $R_f = 10.0$ m



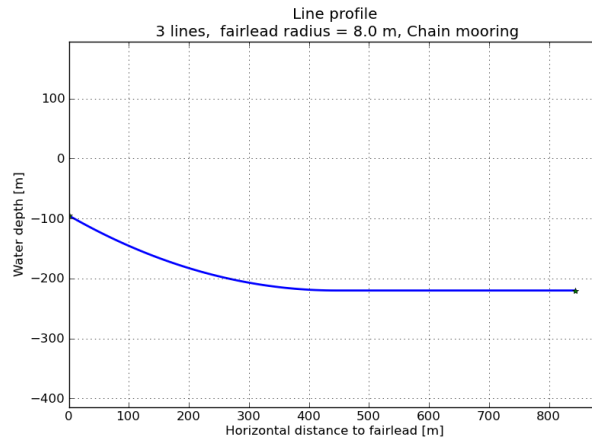
(a) Restoring force



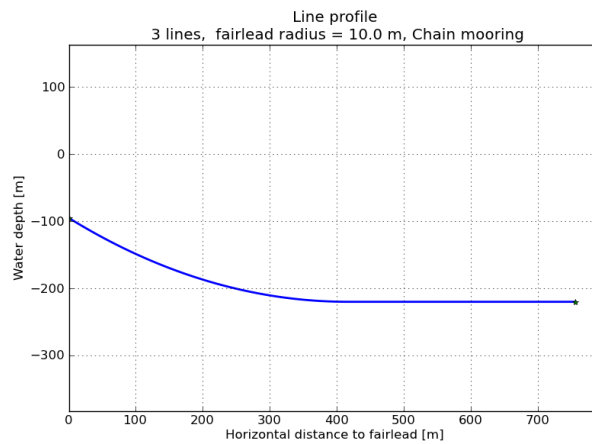
(b) Restoring moment

Figure B.23: Mooring system restoring properties for 6 line system; Case 3; fairlead radius, $R_f = 14.0$ m

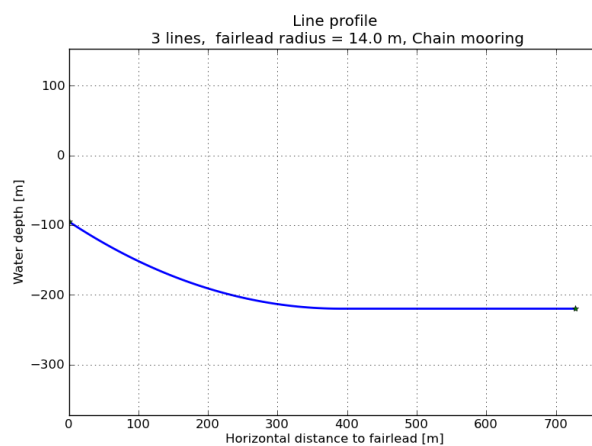
B.3 Line profiles



(a) Fairlead radius, $R_f = 8.0$ m

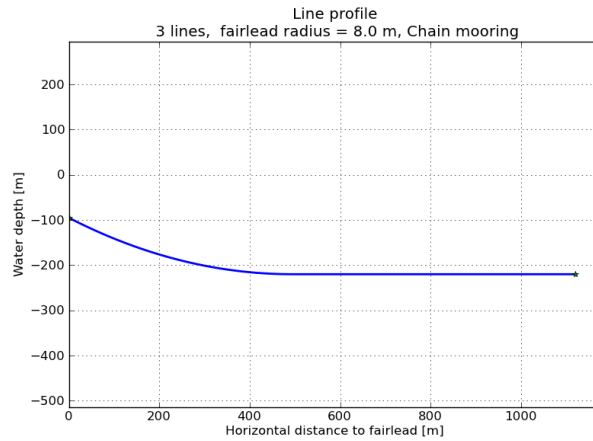


(b) Fairlead radius, $R_f = 10.0$ m

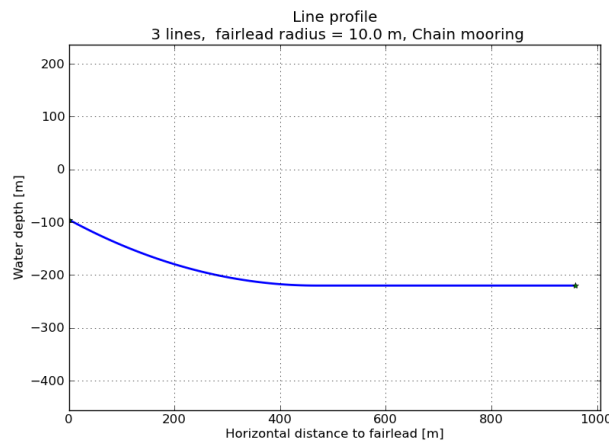


(c) Fairlead radius, $R_f = 14.0$ m

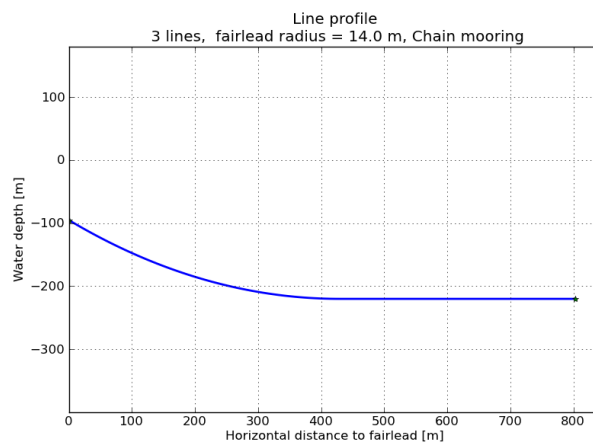
Figure B.24: Line profile for 3 line system, Case 1.



(a) Fairlead radius, $R_f = 8.0$ m

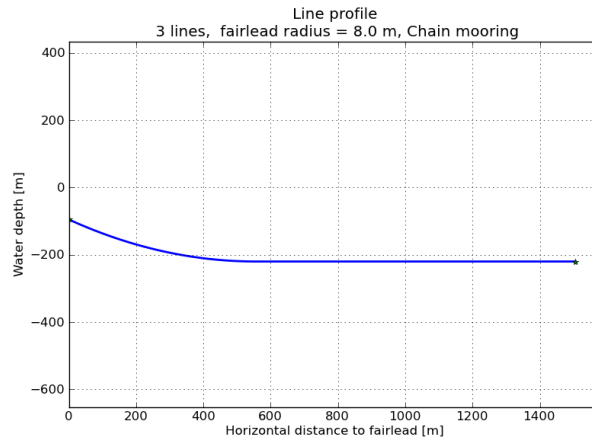


(b) Fairlead radius, $R_f = 10.0$ m

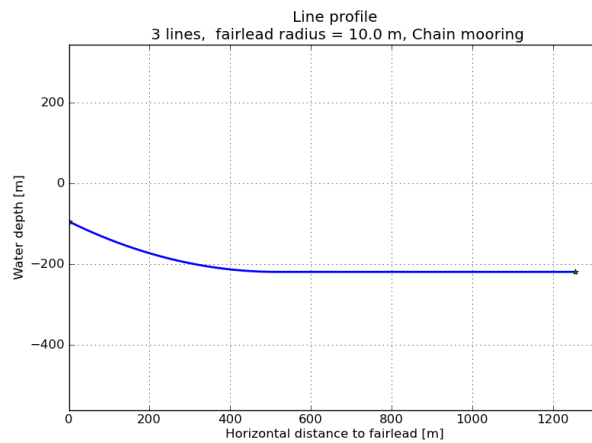


(c) Fairlead radius, $R_f = 14.0$ m

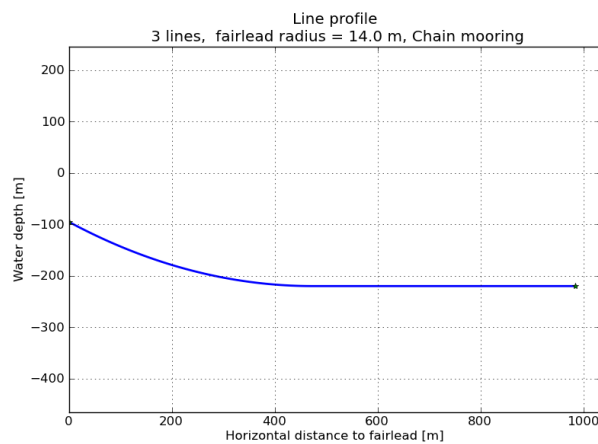
Figure B.25: Line profile for 3 line system, Case 2.



(a) Fairlead radius, $R_f = 8.0$ m

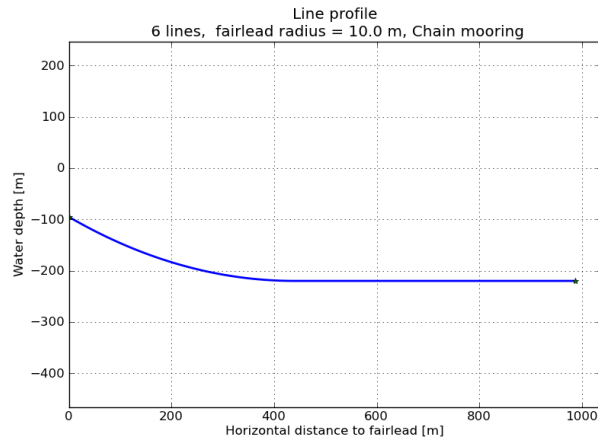


(b) Fairlead radius, $R_f = 10.0$ m

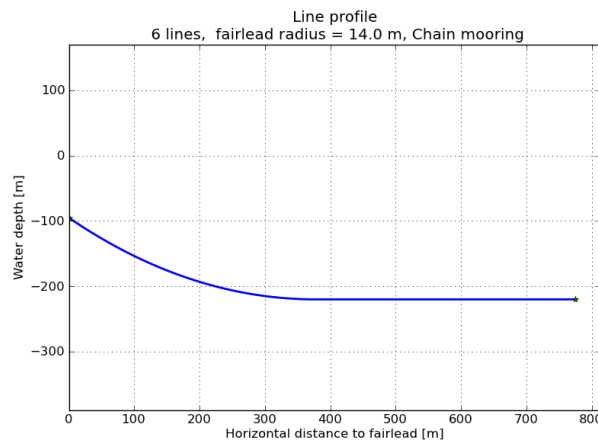


(c) Fairlead radius, $R_f = 14.0$ m

Figure B.26: Line profile for 3 line system, Case 3.

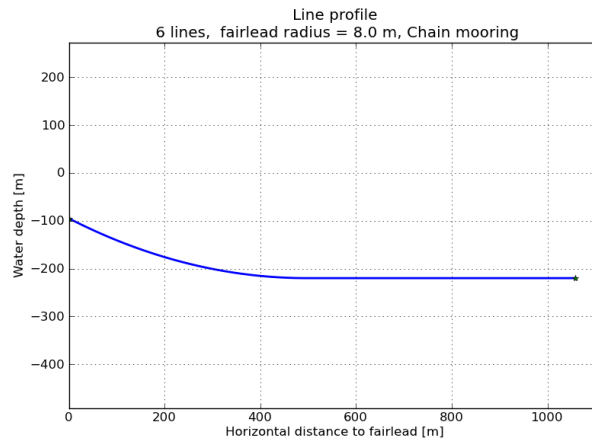


(a) Fairlead radius, $R_f = 10.0$ m

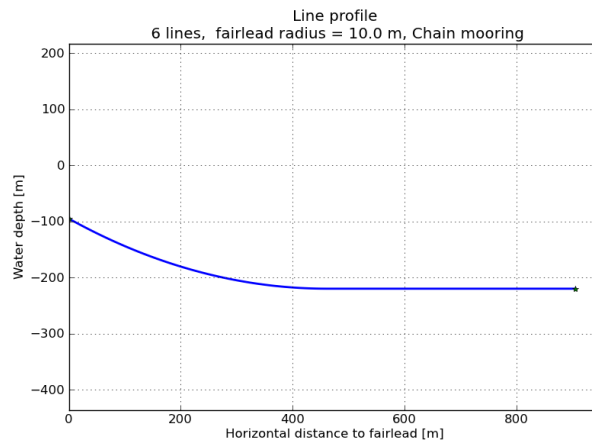


(b) Fairlead radius, $R_f = 14.0$ m

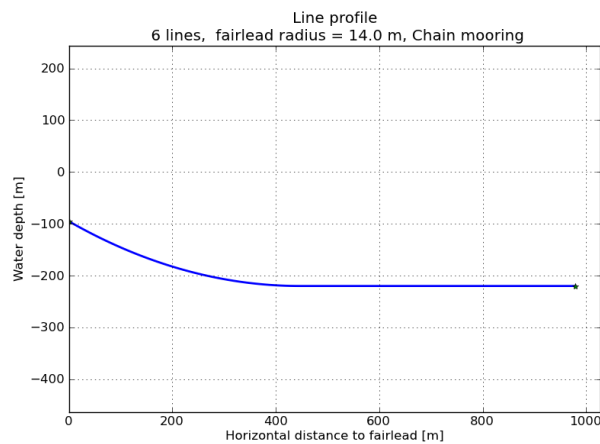
Figure B.27: Line profile for 6 line system, Case 1.



(a) Fairlead radius, $R_f = 8.0$ m

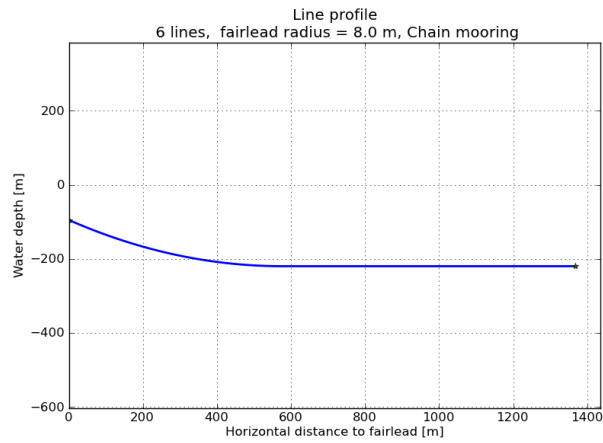


(b) Fairlead radius, $R_f = 10.0$ m

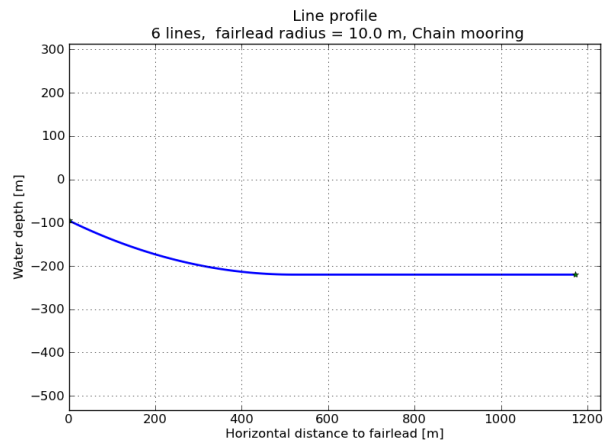


(c) Fairlead radius, $R_f = 14.0$ m

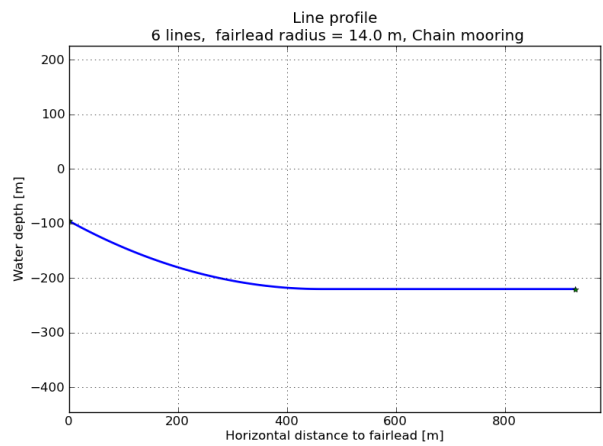
Figure B.28: Line profile for 6 line system, Case 2.



(a) Fairlead radius, $R_f = 8.0$ m



(b) Fairlead radius, $R_f = 10.0$ m



(c) Fairlead radius, $R_f = 14.0$ m

Figure B.29: Line profile for 6 line system, Case 3.



C ADDITIONAL TABLES

C.1 Line data

Table C.1: Line properties for 3 line system.

Fairlead radius [m]	Top tension [kN]	Horizontal tension [kN]	Horizontal distance [m]	Top angle [deg]	Length on seabed [m]	Min. safety factor [-]	Segment no. 1					
							Length [m]	Diameter [m]	weight in water [kN/m]	EA [kN/m ²]	MBL [kN]	Mass [kg/m]
Case 1												
8.0	923.7	800.7	843.5	60.10	397.9	1.85	864.83	0.0760	0.9851	5.1988e+05	6072	115.6
10.0	755.6	643.1	755.9	58.33	339.2	1.91	778.90	0.0730	0.9014	4.7965e+05	5556	105.7
14.0	547.2	456.7	727.4	56.57	336.6	1.91	752.03	0.0650	0.7252	3.8028e+05	4470	85.1
Case 2												
8.0	1352.8	1202.0	1119.4	62.69	625.5	1.88	1138.10	0.0840	1.2090	6.3509e+05	7451	141.8
10.0	1096.2	962.4	958.4	61.40	489.5	1.89	978.41	0.0790	1.0720	5.6173e+05	6607	125.7
14.0	800.9	687.3	802.5	59.11	373.4	1.91	824.82	0.0730	0.9099	4.7965e+05	5608	106.7
Case 3												
8.0	1870.1	1700.8	1504.3	65.43	948.6	1.84	1519.80	0.0890	1.3580	7.1294e+05	8370	159.3
10.0	1518.8	1361.7	1254.0	63.71	738.6	1.87	1271.60	0.0860	1.2600	6.6569e+05	7764	147.8
14.0	1107.1	974.5	983.6	61.67	509.8	1.89	1003.40	0.0790	1.0630	5.6173e+05	6553	124.7

Table C.2: Line properties for 6 line system.

Fairlead radius [m]	Top tension [kN]	Horizontal tension [kN]	Horizontal distance [m]	Top angle [deg]	Length on seabed [m]	Min. safety factor [-]	Segment no. 1					
							Length [m]	Diameter [m]	weight in water [kN/m]	EA [kN/m ²]	MBL [kN]	Mass [kg/m]
Case 1												
10.0	371.7	321.1	986.5	59.77	546.7	1.90	1008.10	0.0490	0.4051	2.1611e+05	2549	47.5
14.0	277.4	228.8	774.3	55.57	397.2	1.88	799.90	0.0480	0.3892	2.0738e+05	2449	45.7
Case 2												
8.0	676.0	601.4	1057.5	62.82	560.7	1.88	1076.10	0.0590	0.5982	3.1331e+05	3763	70.2
10.0	550.2	481.1	904.2	60.97	443.3	1.89	924.73	0.0570	0.5539	2.9243e+05	3485	65.0
14.0	394.5	342.4	978.7	60.20	531.5	1.89	999.86	0.0490	0.4182	2.1611e+05	2631	49.1
Case 3												
8.0	927.9	849.5	1367.0	66.27	789.7	1.78	1381.70	0.0610	0.6292	3.3491e+05	3959	73.8
10.0	758.2	681.1	1171.3	63.94	650.8	1.87	1188.70	0.0600	0.6182	3.2402e+05	3889	72.5
14.0	555.1	486.3	928.7	61.16	464.3	1.89	948.96	0.0570	0.5519	2.9243e+05	3473	64.7

C.2 Restoring properties of mooring system

C.2.1 Case 1, 3 lines

Table C.3: Mooring system restoring properties for 3 line system; Case 1; fairlead radius, $R_f = 8.0$ m

* RESTORING FORCE *

Offset in Direction 0. deg. rel. North

Offset (m)	Force in given direction (kN)	Force in transverse direction (kN)	Moment (kNm)	Maximum Tension (kN)	Line number
0.0	0.0	0.0	0.1870E-02	923.2	1
3.0	-324.4	0.0	0.2896E-02	1151.6	1
6.0	-718.8	0.0	0.4617E-02	1466.2	1
9.0	-1217.1	0.0	0.5523E-02	1896.9	1
12.0	-1859.8	0.0	0.7363E-02	2478.4	1
15.0	-2675.0	0.0	0.9141E-02	3242.3	1
18.0	-3803.1	0.0	0.1197E-01	4332.2	1
21.0	-5242.9	0.0	0.1551E-01	5740.6	1
24.0	-6794.1	0.0	0.1946E-01	7267.0	1
27.0	-8336.3	0.0	0.2295E-01	8789.4	1
30.0	-9873.6	0.0	0.2655E-01	10311.8	1

* RESTORING MOMENT *

Rotation (deg)	Force (kN)	in Direction rel. North (deg)	Moment (kNm)	Max. Tension (kN)	Line number
0.0	0.0	249.4	0.1870E-02	923.2	1
2.0	0.0	88.4	-677.0	923.5	3
4.0	0.0	59.0	-1355.	924.5	3
6.0	0.0	99.8	-2034.	926.1	3
8.0	0.0	90.1	-2716.	928.4	3
10.0	0.0	78.9	-3401.	931.4	3
12.0	0.0	79.3	-4089.	934.7	3
14.0	0.0	73.4	-4781.	938.8	3
16.0	0.0	81.1	-5478.	943.5	3
18.0	0.0	73.1	-6181.	948.8	3
20.0	0.0	82.9	-6890.	954.9	3



Table C.4: Mooring system restoring properties for 3 line system; Case 1; fairlead radius, $R_f = 10.0$ m

* RESTORING FORCE *

Offset in Direction 0. deg. rel. North

Offset (m)	Force in given direction (kN)	Force in transverse direction (kN)	Moment (kNm)	Maximum Tension (kN)	Line number
0.0	0.0	0.0	0.1808E-02	750.5	1
3.0	-251.6	0.0	0.3787E-02	929.2	1
6.0	-561.4	0.0	0.3762E-02	1176.5	1
9.0	-961.2	0.0	0.4316E-02	1520.7	1
12.0	-1481.5	0.0	0.7664E-02	1994.5	1
15.0	-2203.7	0.0	0.1005E-01	2679.8	1
18.0	-3329.2	0.0	0.1204E-01	3774.9	1
21.0	-4820.8	0.0	0.1696E-01	5247.8	1
24.0	-6397.7	0.0	0.2262E-01	6813.0	1
27.0	-7970.1	0.0	0.2753E-01	8378.3	1
30.0	-9538.7	0.0	0.3174E-01	9943.6	1

* RESTORING MOMENT *

Rotation (deg)	Force (kN)	in Direction rel. North (deg)	Moment (kNm)	Max. Tension (kN)	Line number
0.0	0.0	243.4	0.1808E-02	750.5	1
2.0	0.0	47.0	-677.1	750.8	1
4.0	0.0	94.0	-1355.	751.8	1
6.0	0.0	180.8	-2036.	753.4	1
8.0	0.0	337.0	-2720.	755.6	1
10.0	0.0	179.6	-3409.	758.5	1
12.0	0.0	238.5	-4103.	762.0	1
14.0	0.0	239.8	-4805.	766.2	1
16.0	0.0	240.2	-5515.	771.1	1
18.0	0.0	271.1	-6234.	776.7	2
20.0	0.0	240.2	-6965.	783.0	1



Table C.5: Mooring system restoring properties for 3 line system; Case 1; fairlead radius, $R_f = 14.0$ m

* RESTORING FORCE *

Offset in Direction 0. deg. rel. North

Offset (m)	Force in given direction (kN)	Force in transverse direction (kN)	Moment (kNm)	Maximum Tension (kN)	Line number
0.0	0.0	0.0	0.1665E-02	544.9	1
3.0	-173.7	0.0	0.4395E-02	667.7	1
6.0	-386.5	0.0	0.3777E-02	835.7	1
9.0	-658.7	0.0	0.6047E-02	1070.6	1
12.0	-1016.1	0.0	0.6148E-02	1397.3	1
15.0	-1509.2	0.0	0.8281E-02	1860.6	1
18.0	-2305.2	0.0	0.1217E-01	2635.0	1
21.0	-3457.1	0.0	0.1684E-01	3775.8	1
24.0	-4782.1	0.0	0.2261E-01	5097.3	1
27.0	-6115.3	0.0	0.2949E-01	6429.7	1
30.0	-7449.5	0.0	0.3463E-01	7762.2	1

* RESTORING MOMENT *

Rotation (deg)	Force (kN)	in Direction rel. North (deg)	Moment (kNm)	Max. Tension (kN)	Line number
0.0	0.0	256.0	0.1665E-02	544.9	1
2.0	0.0	240.2	-679.1	545.2	1
4.0	0.0	264.1	-1360.	546.1	2
6.0	0.0	264.9	-2044.	547.5	2
8.0	0.0	269.9	-2734.	549.6	2
10.0	0.0	262.4	-3430.	552.2	2
12.0	0.0	267.7	-4136.	555.5	2
14.0	0.0	266.0	-4852.	559.4	2
16.0	0.0	259.9	-5582.	564.0	2
18.0	0.0	260.8	-6326.	569.3	2
20.0	0.0	258.7	-7089.	575.4	2

Table C.6: Mooring system restoring properties for 3 line system; Case 2; fairlead radius, $R_f = 8.0$ m

* RESTORING FORCE *

 Offset in Direction 0. deg. rel. North

Offset (m)	Force in given direction (kN)	Force in transverse direction (kN)	Moment (kNm)	Maximum Tension (kN)	Line number
0.0	0.0	0.0	0.2008E-02	1349.2	1
3.0	-477.7	0.0	0.3320E-02	1686.7	1
6.0	-1043.1	0.0	0.8297E-02	2132.2	1
9.0	-1724.6	0.0	0.9367E-02	2707.9	1
12.0	-2536.6	0.0	0.8332E-02	3430.7	1
15.0	-3488.0	0.0	0.1061E-01	4303.4	1
18.0	-4573.1	0.0	0.1394E-01	5318.1	1
21.0	-5771.7	0.0	0.1721E-01	6456.6	1
24.0	-7095.4	0.0	0.2042E-01	7731.1	1
27.0	-8430.5	0.0	0.2413E-01	9019.0	1
30.0	-9759.5	0.0	0.2623E-01	10306.8	1

* RESTORING MOMENT *

Rotation (deg)	Force (kN)	in Direction rel. North (deg)	Moment (kNm)	Max. Tension (kN)	Line number
0.0	0.0	254.1	0.2008E-02	1349.2	1
2.0	0.0	58.9	-1011.	1349.7	3
4.0	0.0	89.3	-2024.	1351.2	3
6.0	0.0	117.7	-3039.	1353.6	1
8.0	0.0	90.2	-4058.	1357.0	3
10.0	0.0	78.6	-5081.	1361.3	3
12.0	0.0	59.7	-6110.	1366.7	3
14.0	0.0	89.5	-7146.	1373.0	3
16.0	0.0	89.1	-8191.	1380.4	3
18.0	0.0	73.4	-9244.	1388.8	3
20.0	0.1	68.4	-.1031E+05	1398.2	3

C.2.2 Case 2, 3 lines
C.2.3 Case 3, 3 lines

 PROJECT NO
302000201

 REPORT NO
MT2014 A-155

 VERSION
0

Page C-7

C.2.4 Case 1, 6 lines
C.2.5 Case 2, 6 lines



Table C.7: Mooring system restoring properties for 3 line system; Case 2; fairlead radius, $R_f = 10.0$ m

* RESTORING FORCE *

Offset in Direction 0. deg. rel. North

Offset (m)	Force in given direction (kN)	Force in transverse direction (kN)	Moment (kNm)	Maximum Tension (kN)	Line number
0.0	0.0	0.0	0.2851E-02	1091.8	2
3.0	-386.5	0.0	0.5412E-02	1366.6	1
6.0	-856.4	0.0	0.6621E-02	1738.2	1
9.0	-1435.6	0.0	0.7969E-02	2235.2	1
12.0	-2155.0	0.0	0.9547E-02	2883.3	1
15.0	-3032.3	0.0	0.1343E-01	3696.7	1
18.0	-4082.4	0.0	0.1515E-01	4693.1	1
21.0	-5376.8	0.0	0.1920E-01	5946.5	1
24.0	-6817.3	0.0	0.2362E-01	7349.4	1
27.0	-8252.2	0.0	0.2900E-01	8752.2	1
30.0	-9681.7	0.0	0.3273E-01	10155.0	1

* RESTORING MOMENT *

Rotation (deg)	Force (kN)	in Direction rel. North (deg)	Moment (kNm)	Max. Tension (kN)	Line number
0.0	0.0	356.2	0.2851E-02	1091.8	2
2.0	0.0	10.7	-1014.	1092.2	1
4.0	0.0	0.3	-2030.	1093.7	2
6.0	0.0	69.4	-3049.	1096.1	1
8.0	0.0	251.4	-4074.	1099.5	1
10.0	0.0	55.0	-5105.	1103.8	1
12.0	0.0	300.9	-6146.	1109.2	2
14.0	0.0	239.5	-7197.	1115.5	1
16.0	0.0	37.8	-8262.	1122.9	1
18.0	0.0	271.0	-9340.	1131.4	2
20.0	0.0	271.7	-.1044E+05	1140.9	2



Table C.8: Mooring system restoring properties for 3 line system; Case 2; fairlead radius, $R_f = 14.0$ m

* RESTORING FORCE *

Offset in Direction 0. deg. rel. North

Offset (m)	Force in given direction (kN)	Force in transverse direction (kN)	Moment (kNm)	Maximum Tension (kN)	Line number
0.0	0.0	0.0	-.1824E-02	797.2	1
3.0	-273.0	0.0	-.1475E-02	990.0	1
6.0	-604.9	0.0	-.2414E-02	1256.3	1
9.0	-1033.4	0.0	-.2813E-02	1624.6	1
12.0	-1586.6	0.0	-.3281E-02	2126.7	1
15.0	-2309.5	0.0	-.4914E-02	2807.9	1
18.0	-3367.7	0.0	-.7070E-02	3833.3	1
21.0	-4753.7	0.0	-.8945E-02	5194.5	1
24.0	-6275.2	0.0	-.1209E-01	6698.6	1
27.0	-7789.0	0.0	-.1720E-01	8199.6	1
30.0	-9298.4	0.0	-.1947E-01	9700.7	1

* RESTORING MOMENT *

Rotation (deg)	Force (kN)	in Direction rel. North (deg)	Moment (kNm)	Max. Tension (kN)	Line number
0.0	0.0	126.9	-.1824E-02	797.2	1
2.0	0.0	272.3	-1020.	797.7	2
4.0	0.0	258.7	-2043.	799.1	2
6.0	0.0	265.8	-3072.	801.6	2
8.0	0.0	266.3	-4111.	805.0	2
10.0	0.0	264.6	-5161.	809.5	2
12.0	0.0	267.6	-6228.	814.9	2
14.0	0.1	263.8	-7313.	821.5	2
16.0	0.1	260.1	-8420.	829.0	2
18.0	0.1	260.8	-9553.	837.7	2
20.0	0.1	258.7	-.1071E+05	847.6	2



Table C.9: Mooring system restoring properties for 3 line system; Case 3; fairlead radius, $R_f = 8.0$ m

* RESTORING FORCE *

Offset in Direction 0. deg. rel. North

Offset (m)	Force in given direction (kN)	Force in transverse direction (kN)	Moment (kNm)	Maximum Tension (kN)	Line number
0.0	0.0	0.0	0.3493E-02	1867.1	1
3.0	-627.8	0.0	0.9170E-02	2306.4	1
6.0	-1337.8	0.0	0.8289E-02	2849.4	1
9.0	-2137.9	0.0	0.1135E-01	3501.4	1
12.0	-3026.8	0.0	0.9984E-02	4260.6	1
15.0	-4001.4	0.0	0.1514E-01	5118.4	1
18.0	-5048.2	0.0	0.1695E-01	6063.6	1
21.0	-6156.8	0.0	0.1892E-01	7082.9	1
24.0	-7317.2	0.0	0.2243E-01	8163.6	1
27.0	-8486.4	0.0	0.2371E-01	9264.5	1
30.0	-9641.5	0.0	0.2624E-01	10362.4	1

* RESTORING MOMENT *

Rotation (deg)	Force (kN)	in Direction rel. North (deg)	Moment (kNm)	Max. Tension (kN)	Line number
0.0	0.0	253.3	0.3493E-02	1867.1	1
2.0	0.0	2.0	-1430.	1867.8	1
4.0	0.0	120.8	-2862.	1869.7	1
6.0	0.0	60.3	-4297.	1872.9	3
8.0	0.0	79.1	-5736.	1877.4	3
10.0	0.0	78.5	-7181.	1883.2	3
12.0	0.0	78.5	-8633.	1890.3	3
14.0	0.0	78.9	-.1009E+05	1898.7	3
16.0	0.1	73.6	-.1156E+05	1908.4	3
18.0	0.1	89.9	-.1305E+05	1919.4	3
20.0	0.1	70.7	-.1454E+05	1931.8	3



Table C.10: Mooring system restoring properties for 3 line system; Case 3; fairlead radius, $R_f = 10.0$ m

* RESTORING FORCE *

Offset in Direction 0. deg. rel. North

Offset (m)	Force in given direction (kN)	Force in transverse direction (kN)	Moment (kNm)	Maximum Tension (kN)	Line number
0.0	0.0	0.0	-.3221E-02	1518.1	1
3.0	-531.9	0.0	-.3160E-02	1891.9	1
6.0	-1149.6	0.0	-.1102E-02	2374.1	1
9.0	-1875.2	0.0	-.3996E-02	2981.1	1
12.0	-2719.0	0.0	-.4844E-02	3720.2	1
15.0	-3676.7	0.0	-.6969E-02	4589.2	1
18.0	-4743.6	0.0	-.5930E-02	5575.7	1
21.0	-5903.5	0.0	-.9242E-02	6665.0	1
24.0	-7136.6	0.0	-.9086E-02	7838.1	1
27.0	-8372.3	0.0	-.1382E-01	9021.9	1
30.0	-9605.2	0.0	-.1434E-01	10205.7	1

* RESTORING MOMENT *

Rotation (deg)	Force (kN)	in Direction rel. North (deg)	Moment (kNm)	Max. Tension (kN)	Line number
0.0	0.0	146.3	-.3221E-02	1518.1	1
2.0	0.0	2.5	-1437.	1518.8	2
4.0	0.0	178.0	-2876.	1520.8	1
6.0	0.0	178.4	-4320.	1524.1	1
8.0	0.0	359.6	-5772.	1528.7	2
10.0	0.0	239.9	-7232.	1534.7	1
12.0	0.0	298.7	-8705.	1542.0	2
14.0	0.0	301.3	-.1019E+05	1550.7	2
16.0	0.0	300.8	-.1170E+05	1560.8	2
18.0	0.0	300.8	-.1322E+05	1572.4	2
20.0	0.0	2.4	-.1476E+05	1585.4	2



Table C.11: Mooring system restoring properties for 3 line system; Case 3; fairlead radius, $R_f = 14.0$ m

* RESTORING FORCE *

Offset in Direction 0. deg. rel. North

Offset (m)	Force in given direction (kN)	Force in transverse direction (kN)	Moment (kNm)	Maximum Tension (kN)	Line number
0.0	0.0	0.0	0.3608E-02	1102.5	1
3.0	-390.7	0.0	0.5313E-02	1380.5	1
6.0	-865.1	0.0	0.1055E-01	1755.1	1
9.0	-1447.2	0.0	0.1049E-01	2253.4	1
12.0	-2163.8	0.0	0.1614E-01	2898.5	1
15.0	-3032.8	0.0	0.1764E-01	3702.5	1
18.0	-4055.4	0.0	0.2287E-01	4669.9	1
21.0	-5292.8	0.0	0.2577E-01	5864.1	1
24.0	-6680.5	0.0	0.3168E-01	7213.6	1
27.0	-8064.9	0.0	0.4077E-01	8564.2	1
30.0	-9443.9	0.0	0.4590E-01	9914.9	1

* RESTORING MOMENT *

Rotation (deg)	Force (kN)	in Direction rel. North (deg)	Moment (kNm)	Max. Tension (kN)	Line number
0.0	0.0	256.0	0.3608E-02	1102.5	1
2.0	0.0	241.2	-1443.	1103.2	1
4.0	0.0	259.1	-2889.	1105.3	2
6.0	0.0	256.4	-4345.	1108.7	2
8.0	0.0	263.4	-5813.	1113.6	2
10.0	0.1	262.6	-7299.	1119.8	2
12.0	0.1	263.2	-8807.	1127.6	2
14.0	0.1	266.2	-.1034E+05	1136.8	2
16.0	0.1	260.2	-.1191E+05	1147.5	2
18.0	0.1	260.9	-.1351E+05	1159.9	2
20.0	0.1	258.9	-.1515E+05	1173.9	2

Table C.12: Mooring system restoring properties for 6 line system; Case 1; fairlead radius, $R_f = 10.0$ m

* RESTORING FORCE *

 Offset in Direction 0. deg. rel. North

Offset (m)	Force in given direction (kN)	Force in transverse direction (kN)	Moment (kNm)	Maximum Tension (kN)	Line number
0.0	0.0	0.0	-.2126E-03	370.6	1
3.0	-233.1	0.0	0.6426E-03	458.7	1
6.0	-483.4	0.0	-.2363E-03	577.9	1
9.0	-766.6	0.0	0.1602E-03	737.9	1
12.0	-1100.6	0.0	0.1801E-02	948.3	1
15.0	-1492.0	0.0	-.7812E-04	1217.1	1
18.0	-1951.3	0.0	0.6719E-03	1546.0	1
21.0	-2488.8	0.0	-.1047E-02	1942.8	1
24.0	-3121.4	0.0	-.1500E-02	2425.4	1
27.0	-3804.4	0.0	0.3437E-03	2945.8	1
30.0	-4503.0	0.0	-.9375E-04	3464.1	1

* RESTORING MOMENT *

Rotation (deg)	Force (kN)	in Direction rel. North (deg)	Moment (kNm)	Max. Tension (kN)	Line number
0.0	0.0	116.6	-.2126E-03	370.6	1
2.0	0.0	58.3	-677.2	370.7	1
4.0	0.0	304.9	-1356.	371.2	3
6.0	0.0	62.0	-2036.	372.0	1
8.0	0.0	246.0	-2720.	373.1	1
10.0	0.0	51.6	-3409.	374.5	1
12.0	0.0	48.0	-4104.	376.3	1
14.0	0.0	114.6	-4806.	378.4	1
16.0	0.0	66.1	-5516.	380.9	1
18.0	0.0	140.0	-6235.	383.6	3
20.0	0.0	307.4	-6965.	386.8	3



Table C.13: Mooring system restoring properties for 6 line system; Case 1; fairlead radius, $R_f = 14.0$ m

* RESTORING FORCE *

Offset in Direction 0. deg. rel. North

Offset (m)	Force in given direction (kN)	Force in transverse direction (kN)	Moment (kNm)	Maximum Tension (kN)	Line number
0.0	0.0	0.0	0.1542E-02	276.4	1
3.0	-158.1	0.0	0.2095E-02	335.2	1
6.0	-327.7	0.0	0.2148E-02	416.2	1
9.0	-525.0	0.0	0.2688E-02	528.2	1
12.0	-763.5	0.0	0.5805E-02	683.7	1
15.0	-1066.4	0.0	0.5211E-02	896.5	1
18.0	-1459.9	0.0	0.5578E-02	1196.6	1
21.0	-2025.6	0.0	0.9437E-02	1663.5	1
24.0	-2751.1	0.0	0.9828E-02	2279.4	1
27.0	-3549.2	0.0	0.1497E-01	2950.1	1
30.0	-4364.0	0.0	0.1819E-01	3619.7	1

* RESTORING MOMENT *

Rotation (deg)	Force (kN)	in Direction rel. North (deg)	Moment (kNm)	Max. Tension (kN)	Line number
0.0	0.0	254.1	0.1542E-02	276.4	1
2.0	0.0	245.9	-680.3	276.6	1
4.0	0.0	240.7	-1362.	277.0	3
6.0	0.0	178.5	-2048.	277.8	6
8.0	0.0	118.9	-2740.	278.9	6
10.0	0.0	183.2	-3439.	280.3	6
12.0	0.0	182.2	-4148.	282.0	6
14.0	0.0	117.8	-4868.	284.0	6
16.0	0.0	175.4	-5601.	286.4	6
18.0	0.0	176.4	-6347.	289.0	6
20.0	0.0	169.9	-7104.	291.8	6



Table C.14: Mooring system restoring properties for 6 line system; Case 2; fairlead radius, $R_f = 8.0$ m

* RESTORING FORCE *

Offset in Direction 0. deg. rel. North

Offset (m)	Force in given direction (kN)	Force in transverse direction (kN)	Moment (kNm)	Maximum Tension (kN)	Line number
0.0	0.0	0.0	-.2574E-03	674.0	1
3.0	-453.7	0.0	0.5264E-03	845.8	1
6.0	-935.2	0.0	-.1893E-02	1074.3	1
9.0	-1472.6	0.0	-.1023E-02	1372.0	1
12.0	-2078.6	0.0	0.1219E-02	1748.3	1
15.0	-2771.0	0.0	-.3203E-03	2205.4	1
18.0	-3544.0	0.0	-.1312E-02	2738.6	1
21.0	-4415.5	0.0	0.1812E-02	3357.0	1
24.0	-5382.9	0.0	-.5844E-02	4057.5	1
27.0	-6369.2	0.0	-.5437E-02	4759.2	1
30.0	-7373.4	0.0	-.3688E-02	5461.0	1

* RESTORING MOMENT *

Rotation (deg)	Force (kN)	in Direction rel. North (deg)	Moment (kNm)	Max. Tension (kN)	Line number
0.0	0.0	161.6	-.2574E-03	674.0	1
2.0	0.0	242.6	-1012.	674.3	2
4.0	0.0	241.7	-2026.	675.0	2
6.0	0.0	27.8	-3042.	676.2	1
8.0	0.0	298.6	-4061.	677.9	2
10.0	0.0	352.9	-5085.	680.2	2
12.0	0.0	315.7	-6116.	682.9	2
14.0	0.0	238.8	-7154.	686.1	2
16.0	0.0	24.7	-8200.	689.8	2
18.0	0.0	33.4	-9255.	694.1	2
20.0	0.0	34.9	-.1032E+05	698.9	2



Table C.15: Mooring system restoring properties for 6 line system; Case 2; fairlead radius, $R_f = 10.0$ m

* RESTORING FORCE *

Offset in Direction 0. deg. rel. North

Offset (m)	Force in given direction (kN)	Force in transverse direction (kN)	Moment (kNm)	Maximum Tension (kN)	Line number
0.0	0.0	0.0	-.2696E-04	548.9	1
3.0	-363.7	0.0	0.1689E-03	687.1	1
6.0	-755.1	0.0	-.1109E-02	875.1	1
9.0	-1199.1	0.0	-.7422E-04	1129.9	1
12.0	-1727.6	0.0	0.5469E-03	1467.0	1
15.0	-2351.6	0.0	-.1016E-02	1896.1	1
18.0	-3114.4	0.0	0.9531E-03	2456.7	1
21.0	-4051.6	0.0	0.8281E-03	3174.8	1
24.0	-5085.6	0.0	0.5937E-03	3971.0	1
27.0	-6138.0	0.0	0.3750E-03	4766.2	1
30.0	-7221.5	0.0	-.1250E-03	5561.4	1

* RESTORING MOMENT *

Rotation (deg)	Force (kN)	in Direction rel. North (deg)	Moment (kNm)	Max. Tension (kN)	Line number
0.0	0.0	158.2	-.2696E-04	548.9	1
2.0	0.0	237.3	-1016.	549.1	1
4.0	0.0	241.9	-2034.	549.8	2
6.0	0.0	176.1	-3056.	551.0	1
8.0	0.0	180.6	-4082.	552.7	1
10.0	0.0	113.8	-5116.	554.8	6
12.0	0.0	119.1	-6158.	557.5	6
14.0	0.0	114.8	-7211.	560.6	1
16.0	0.0	78.0	-8276.	564.3	1
18.0	0.0	52.6	-9356.	568.5	3
20.0	0.0	169.0	-.1045E+05	573.2	6

Table C.16: Mooring system restoring properties for 6 line system; Case 2; fairlead radius, $R_f = 14.0$ m

* RESTORING FORCE *

Offset in Direction 0. deg. rel. North

Offset (m)	Force in given direction (kN)	Force in transverse direction (kN)	Moment (kNm)	Maximum Tension (kN)	Line number
0.0	0.0	0.0	0.2157E-02	394.0	1
3.0	-251.6	0.0	0.4165E-02	489.0	1
6.0	-521.7	0.0	0.6104E-02	617.7	1
9.0	-825.5	0.0	0.5727E-02	790.2	1
12.0	-1185.7	0.0	0.6844E-02	1016.9	1
15.0	-1606.6	0.0	0.5141E-02	1305.3	1
18.0	-2097.4	0.0	0.9875E-02	1656.9	1
21.0	-2678.3	0.0	0.1133E-01	2086.3	1
24.0	-3357.7	0.0	0.1744E-01	2604.5	1
27.0	-4072.5	0.0	0.1697E-01	3145.0	1
30.0	-4805.6	0.0	0.2428E-01	3684.8	1

* RESTORING MOMENT *

Rotation (deg)	Force (kN)	in Direction rel. North (deg)	Moment (kNm)	Max. Tension (kN)	Line number
0.0	0.0	270.0	0.2157E-02	394.0	1
2.0	0.0	33.6	-1017.	394.3	1
4.0	0.0	237.1	-2037.	395.0	3
6.0	0.0	6.0	-3063.	396.2	3
8.0	0.0	294.7	-4098.	397.9	3
10.0	0.0	29.2	-5145.	400.1	3
12.0	0.0	165.4	-6207.	402.8	3
14.0	0.0	291.1	-7284.	405.8	3
16.0	0.0	16.0	-8381.	409.3	3
18.0	0.0	153.0	-9502.	413.4	3
20.0	0.0	106.4	-.1065E+05	418.0	3



Table C.17: Mooring system restoring properties for 6 line system; Case 3; fairlead radius, $R_f = 8.0$ m

* RESTORING FORCE *

Offset in Direction 0. deg. rel. North

Offset (m)	Force in given direction (kN)	Force in transverse direction (kN)	Moment (kNm)	Maximum Tension (kN)	Line number
0.0	0.0	0.0	0.3113E-02	927.4	1
3.0	-615.4	0.0	0.2124E-02	1155.5	1
6.0	-1247.7	0.0	0.6242E-02	1439.1	1
9.0	-1914.5	0.0	0.6883E-02	1781.2	1
12.0	-2618.8	0.0	0.8391E-02	2180.0	1
15.0	-3365.4	0.0	0.1001E-01	2631.0	1
18.0	-4153.8	0.0	0.1125E-01	3126.4	1
21.0	-4977.4	0.0	0.8219E-02	3660.0	1
24.0	-5828.4	0.0	0.1359E-01	4216.9	1
27.0	-6685.0	0.0	0.1631E-01	4772.2	1
30.0	-7545.2	0.0	0.1744E-01	5327.6	1

* RESTORING MOMENT *

Rotation (deg)	Force (kN)	in Direction rel. North (deg)	Moment (kNm)	Max. Tension (kN)	Line number
0.0	0.0	182.1	0.3113E-02	927.4	1
2.0	0.0	242.7	-1431.	927.7	1
4.0	0.0	19.9	-2864.	928.7	1
6.0	0.0	177.3	-4300.	930.4	2
8.0	0.0	334.3	-5741.	932.7	2
10.0	0.0	107.1	-7187.	935.7	2
12.0	0.0	128.6	-8642.	939.4	2
14.0	0.0	181.0	-.1011E+05	943.7	2
16.0	0.0	25.3	-.1158E+05	948.8	2
18.0	0.0	239.7	-.1307E+05	954.4	2
20.0	0.0	116.3	-.1457E+05	960.8	2



Table C.18: Mooring system restoring properties for 6 line system; Case 3; fairlead radius, $R_f = 10.0$ m

* RESTORING FORCE *

Offset in Direction 0. deg. rel. North

Offset (m)	Force in given direction (kN)	Force in transverse direction (kN)	Moment (kNm)	Maximum Tension (kN)	Line number
0.0	0.0	0.0	0.2760E-02	757.9	1
3.0	-509.7	0.0	0.3383E-02	949.4	1
6.0	-1045.7	0.0	0.5629E-02	1198.9	1
9.0	-1629.1	0.0	0.5102E-02	1515.7	1
12.0	-2275.5	0.0	0.9469E-02	1904.3	1
15.0	-2989.4	0.0	0.1102E-01	2363.3	1
18.0	-3773.0	0.0	0.8203E-02	2886.8	1
21.0	-4618.5	0.0	0.1002E-01	3465.5	1
24.0	-5523.3	0.0	0.1719E-01	4090.5	1
27.0	-6440.4	0.0	0.2525E-01	4716.5	1
30.0	-7370.8	0.0	0.2244E-01	5342.6	1

* RESTORING MOMENT *

Rotation (deg)	Force (kN)	in Direction rel. North (deg)	Moment (kNm)	Max. Tension (kN)	Line number
0.0	0.0	251.6	0.2760E-02	757.9	1
2.0	0.0	242.5	-1438.	758.2	2
4.0	0.0	117.2	-2879.	759.2	1
6.0	0.0	238.4	-4325.	760.9	1
8.0	0.0	224.0	-5778.	763.3	1
10.0	0.0	312.7	-7241.	766.3	1
12.0	0.0	121.9	-8716.	770.1	6
14.0	0.0	67.1	-.1021E+05	774.5	2
16.0	0.0	85.4	-.1171E+05	779.7	1
18.0	0.0	43.2	-.1324E+05	785.6	3
20.0	0.0	63.6	-.1479E+05	792.2	3



Table C.19: Mooring system restoring properties for 6 line system; Case 3; fairlead radius, $R_f = 14.0$ m

* RESTORING FORCE *

Offset in Direction 0. deg. rel. North

Offset (m)	Force in given direction (kN)	Force in transverse direction (kN)	Moment (kNm)	Maximum Tension (kN)	Line number
0.0	0.0	0.0	0.3187E-02	553.5	1
3.0	-366.8	0.0	0.5801E-02	692.8	1
6.0	-760.9	0.0	0.8215E-02	881.9	1
9.0	-1207.4	0.0	0.9406E-02	1136.8	1
12.0	-1734.0	0.0	0.6750E-02	1471.6	1
15.0	-2354.2	0.0	0.8734E-02	1895.8	1
18.0	-3092.1	0.0	0.1858E-01	2431.0	1
21.0	-3993.0	0.0	0.1719E-01	3113.2	1
24.0	-4994.6	0.0	0.2213E-01	3878.0	1
27.0	-6015.6	0.0	0.3144E-01	4643.3	1
30.0	-7063.7	0.0	0.2281E-01	5408.5	1

* RESTORING MOMENT *

Rotation (deg)	Force (kN)	in Direction rel. North (deg)	Moment (kNm)	Max. Tension (kN)	Line number
0.0	0.0	265.9	0.3187E-02	553.5	1
2.0	0.0	45.7	-1443.	553.8	3
4.0	0.0	67.4	-2890.	554.8	3
6.0	0.0	24.4	-4345.	556.5	3
8.0	0.0	56.9	-5813.	558.9	3
10.0	0.0	81.6	-7298.	562.0	3
12.0	0.0	151.4	-8805.	565.8	3
14.0	0.0	77.4	-.1034E+05	570.3	3
16.0	0.0	39.4	-.1190E+05	575.7	3
18.0	0.0	246.8	-.1350E+05	581.8	3
20.0	0.0	59.5	-.1514E+05	588.7	3



Time domain analysis of the floater and mooring lines

Prepared by: David Verelst.

Checked by: Uwe S .Paulsen

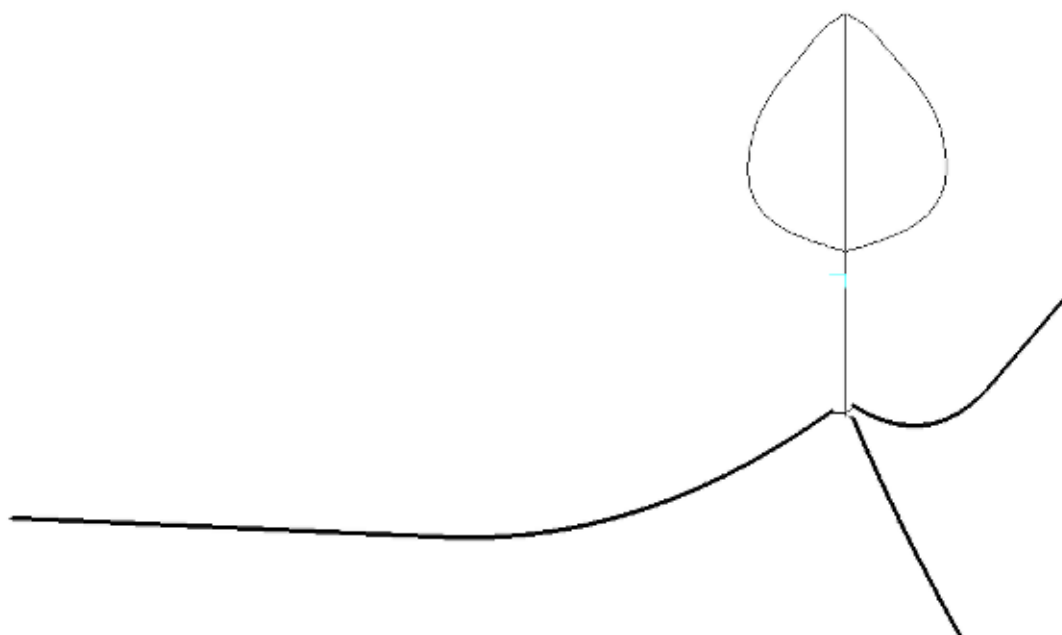
Uwe Schmidt Paulsen

24-09-2014

Task 5.4 Selection of floating support structure and mooring system configurations (MAT)
 For selected locations, characterized by water depth and wave- and current severity, floater and mooring system configurations are selected. For this activity we will use the mooring system analysis and design programs MIMOSA and WINDOPT (MAT). A time domain analysis for design verification is performed (RIS).

Time domain analysis of the floater and mooring lines

For the time domain analysis, the aeroelastic simulation program HAWC2 is used. In work package 1 these simulations are documented in more detail. In the figure below a visual representation of the corresponding beam model used in HAWC2 is given.



In order to illustrate the dynamic behaviour of the floater in the time domain simulations, the plots below show the floater position (around the mean sea level position) in the x-y plane (which is the horizontal plane in this case). Notice that the thrust force pushes the floater in the y direction approximately 16.5m away from its initial position.

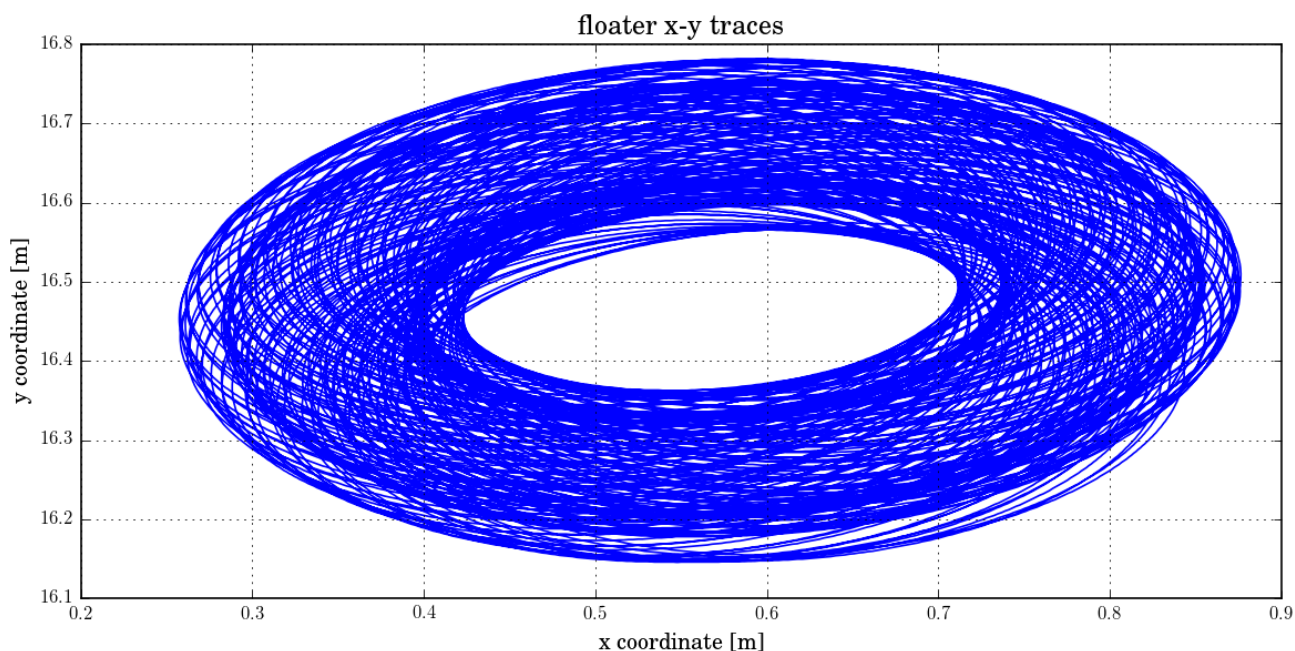
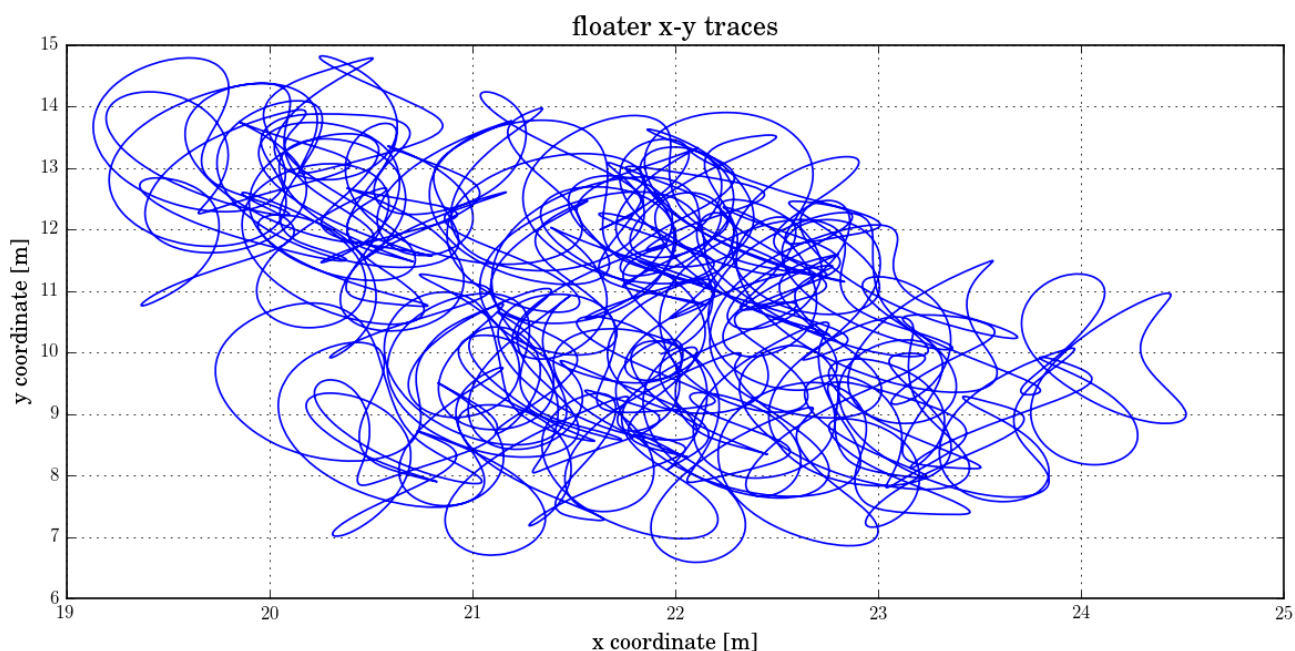


figure: for 10 m/s, deterministic wind conditions, no waves and no current we can see that the floater is describing small circles that originate from the cyclic aerodynamic loads over a single rotation.

When looking at turbulent wind conditions and with the influence of the sea current, the floater xy trace has, as expected, not such a regular pattern. Also note that due to current and the corresponding magnus effect, the floater now also moves into the x direction, which is perpendicular to the current direction (current has the same direction as the wind in this case).



For a more detailed analysis of the response of the floater under various conditions the reader is referred to the detailed hydro- servo- aeroelastic load analysis of work package 1.